Stony Brook University

Osteoporosis Drugs Prevent Bone Loss, Normalize Metabolic Parameters and Negatively Correlate Bone and Fat

A Thesis Presented

by

Andrea Trinward

To The Graduate School in Partial Fulfillment of the Requirements for the Degree of

Master of Science
in
Biomedical Engineering

Stony Brook University

2010

Stony Brook University
The Graduate School

Andrea Trinward

We, the thesis committee for the above candidate for the

Master of Science degree,

Hereby recommend acceptance of this thesis.

Stefan Judex, Doctor of Philosophy
Advisor, Biomedical Engineering

Lisa Miller, Doctor of Philosophy
Committee Chair, Biomedical Engineering

Clinton Rubin, Doctor of Philosophy
Department Chair, Biomedical Engineering

This thesis is accepted by the Graduate School

Lawrence Martin
Dean of the Graduate School

ABSTRACT OF THE THESIS

Osteoporosis Drugs Prevent Bone Loss, Normalize Metabolic Parameters and Negatively Correlate Bone and Fat

by

Andrea Trinward

Master of Science

in

Biomedical Engineering

Stony Brook University

2010

Post-menopausal osteoporosis is associated with bone loss but menopause can also increase body mass and abdominal adiposity, factors that can pose a secondary risk to skeletal health. Drugs such as alendronate (ALN), parathyroid hormone (PTH) and sodium fluoride (NaF) target bone loss but their effects on adiposity, metabolism, and the interrelationship between bone and fat are largely unknown. To this end, we subjected OVX rats to short-term (2 months) and long-term (6 months) treatments of different doses of ALN, PTH and NaF and analyzed body weight, vertebral bone, abdominal fat volume, liver fatty acids, and serum leptin and IGF-I. Six-month old Sprague-Dawley rats were assigned to age-matched controls, untreated OVX, OVX treated with high (H), medium (M), or low (L) doses of hPTH (60, 15, or 0.3μg/kg/d), or OVX treated with H, M, or L-ALN (100, 10, or 1μg/kg/2xwk) or OVX treated with H or L-NaF (500ppm or 100ppm in drinking water). Rats were sacrificed at 6, 8, and 12 months of age (n=10/group/age).

Body mass and fat accumulation was strongly influenced by age. Age-matched controls gained 12.7% more weight throughout the course of the study than OVX controls and weighed 10% less, while treated animals gained 28.1% less weight than OVX controls and weighed 4.9% less. At 12 months of age, H-ALN treatment had 37.8% less subcutaneous fat than OVX controls. ($p<0.01$) By 12 months all treated animals had smaller fat pads than OVX controls.($p<0.05$) Liver esterfied free fatty acid (NEFA)

concentrations were smaller at 8 months in H-PTH and L-ALN rats compared to OVX controls.($p<0.05$) At 12 months, all groups except M-ALN had lower liver triglyceride (TG) and NEFA concentrations than OVX controls.($p<0.05$)

At 8 months, H-, M- and L-ALN as well as H- and M-PTH showed higher vertebral bone apparent density (*in vivo* μCT) than OVX controls.($p<0.05$). Both H- and M-PTH had higher trabecular thickness (*ex vivo* μCT) while only H-PTH had higher bone volume fraction than OVX controls.($p<0.05$) At 12 months and compared to OVX controls, apparent vertebral densities (*in vivo* μCT), trabecular number and trabecular apparent densities (*ex vivo* μCT) were significantly higher in H-, M-, and L-ALN, H-, and M-PTH groups as well as H-NaF, while trabecular spacing was decreased.($p<0.05$) However, high doses of ALN and PTH suppressed IGF-I levels.($p<0.01$)

Body mass was positively correlated to bone volume and density for age-matched controls with high dose treatment groups ($r^2= 0.36$, $p<0.01$), but was not correlated in the OVX controls with low dose treatments. Liver TG content was not correlated to bone volume fraction in OVX controls ($r^2=0.001$, $p<0.93$), but ALN, PTH and NaF treatment normalized this relationship to that seen in age-matched controls. ALN and PTH treatment reduced the elevation of the total fat to body mass relationship compared to age matched controls, indicating a reduction due to treatment. OVX controls showed no correlation between bone density and liver TG, while AM controls and NaF showed a positive relationship. All ALN treatment groups combined and H and M- PTH treatment groups combined both showed negative correlations between density and liver TG content; the highest responders to treatment had the lowest TG concentrations.

These data demonstrate that treatment with moderate to high doses of ALN, PTH and NaF can normalize bone morphology and indices of fat metabolism to those of normal age-matched controls. Treatments slowed the rate of weight gain throughout the course of the study while decreasing fat accumulation. ALN and PTH were able to reverse the association between fat and apparent mineral density; demonstrating a secondary positive effect of treatment on fat metabolism. Drug therapies can reduce the severity of post-menopausal osteoporosis but they also reduce fat accumulation and could lower the incidence of menopause related obesity.

TABLE OF CONTENTS

LIST OF SYMBOLS

ALN:	alendronate
App.MD:	apparent mineral density
BMD:	bone mineral density
BV/TV:	bone volume fraction
Conn.D	connectivity density
IACUC:	Institutional Animal Care and Use Committee
IGF-1:	insulin-like growth factor 1
NaF:	sodium fluoride
ppm:	parts per million
PTH:	parathyroid hormone
NEFA:	non-esterfied free fatty acid
S.D.:	standard deviation
Tb.Th:	trabecular thickness
Tb.#:	trabecular number
TG:	triglyceride
TMD:	tissue mineral density
Tb.Sp.:	trabecular space
ug:	micrograms
uL:	microliters
µCT:	micro computed tomography
ǂ:	significance, $p<0.001$
*:	significance, $p<0.01$
**:	significance, $p<0.05$

LIST OF FIGURES

Figure 11. Apparent mineral density was determined via *in vivo* microCT of L1-L5 vertebrae at 156 um resolution for all animals from the 12 month time point. Animals were scanned at 6, 8 and 12 months with *in vivo* microCT. Data is represented as means + SD for age matched controls (AM), ovariectomy controls (OVX), OVX with high dose alendronate (ALN) treatment (OVX + H-ALN), OVX with medium ALN treatment (OVX + M-ALN), OVX with low ALN treatment (OVX + L-ALN), OVX with high parathyroid hormone (PTH) treatment (OVX + H-PTH), OVX with medium PTH treatment (OVX + M-PTH), OVX with low PTH treatment (OVX + L-PTH), OVX with high sodium fluoride (NaF) treatment (OVX + H-NaF) and OVX with low NaF treatment (OVX + L-NaF). (ANOVA) *$p<0.01$- 8 month time point, ǂ $p<0.001$- 12 month time point.

Figure 12. % Change in apparent mineral density from 6 to 8 months (white) and from 6 to 12 months (black) was determined via *in vivo* microCT of L1-L5 vertebrae at 156 um resolution for all animals from the 12 month time group. Animals were scanned at 6, 8 and 12 months with *in vivo* microCT. Data is represented as means + SD for age matched controls (AM), ovariectomy controls (OVX), OVX with high dose alendronate (ALN) treatment (OVX + H-ALN), OVX with medium ALN treatment (OVX + M-ALN), OVX with low ALN treatment (OVX + L-ALN), OVX with high parathyroid hormone (PTH) treatment (OVX + H-PTH), OVX with medium PTH treatment (OVX + M-PTH), OVX with low PTH treatment (OVX + L-PTH), OVX with high sodium fluoride (NaF) treatment (OVX + H-NaF) and OVX with low NaF treatment (OVX + L-NaF). (ANOVA) +$p<0.01$ - 8 mo time point. ++$p<0.05$ – 8 mo. * $p<0.01$ - 12 mo time point.

Figure 13. A representative microCT 3D reconstruction image of the visceral (red) and subcutaneous fat (white).

Figure 14. Animals were scanned at 6, 8 and 12 months with *in vivo* microCT. A.)Total fat volume, B.) visceral fat volume, C.) subcutaneous fat volume at 6, 8 and 12 months of age and D.) subcutaneous fat volume at 12 months. Data is represented as means + SD for age matched controls (AM), ovariectomy controls (OVX), OVX with high dose alendronate (ALN) treatment (OVX + H-ALN), OVX with medium ALN treatment (OVX + M-ALN), OVX with low ALN treatment (OVX + L-ALN), OVX with high parathyroid hormone (PTH) treatment (OVX + H-PTH), OVX with medium PTH treatment (OVX + M-PTH), OVX with low PTH treatment (OVX + L-PTH), OVX with high sodium fluoride (NaF) treatment (OVX + H-NaF) and OVX with low NaF treatment (OVX + L-NaF). (ANOVA) *$p<0.01$

Figure 15. Fat volume at 6, 8 and 12 months for age matched controls (black-AM), ovariectomy controls (dark gray – OVX) and all high dose animals pooled (light gray – OVX + Treatment). Data is, represented as mean + SD. (ANOVA) *$p<0.01$,**$p<0.05$

Figure 16. Representative bone images from *ex vivo* micro CT. A.) Healthy and B.) OVX rat trabecular bone from the L-4 vertebral body.

Figure 17. Micro architectural parameters of the L-4 vertebrae for animals at 6 months of age were determined via microCT. Microarchitecture is characterized by: A.) Bone volume fraction, B.) apparent mineral density C.) Trabecular thickness, D.) trabecular number, E.) trabecular spacing and F.) connectivity density. Data is represented as mean + S.D. for age matched (AM) and ovariectomy (OVX) control. (Student t-test)

Figure 18. A.) Bone volume fraction and B.) apparent mineral density were determined for the trabecular region of the L-4 vertebral body at 8 months of age for age matched control (AM), ovariectomy control (OVX), OVX with high dose alendronate (ALN) treatment (OVX + H-ALN), OVX with medium ALN treatment (OVX + M-ALN), OVX with low ALN treatment (OVX + L-ALN), OVX with high parathyroid hormone (PTH) treatment (OVX + H-PTH), OVX with medium PTH treatment (OVX + M-PTH), OVX with low PTH treatment (OVX + L-PTH), OVX with high sodium fluoride (NaF) treatment (OVX + H-NaF) and OVX with low NaF treatment (OVX + L-NaF). (ANOVA) *$p<0.01$

Figure 19. Microarchitectural parameters of the L-4 vertebrae for animals at 8 months of age were determined via microCT. Data is represented as group mean + SD. A.) Trabecular thickness, B.) trabecular number, C.) trabecular spacing and D.) connectivity density. Data is represented as age matched control (AM), ovariectomy control (OVX), OVX with high dose alendronate (ALN) treatment (OVX + H-ALN), OVX with medium ALN treatment (OVX + M-ALN), OVX with low ALN treatment (OVX + L-ALN), OVX with high parathyroid hormone (PTH) treatment (OVX + H-PTH), OVX with medium PTH treatment (OVX + M-PTH), OVX with low PTH treatment (OVX + L-PTH), OVX with high sodium fluoride (NaF) treatment (OVX + H-NaF) and OVX with low NaF treatment (OVX + L-NaF). (ANOVA) * $p<0.001$, **$p<0.05$

Figure 20. A.) Bone volume fraction and B.) apparent mineral density were determined for the trabecular region of the L-4 vertebral body at 12 months of age for age matched control (AM), ovariectomy control (OVX), OVX with high dose alendronate (ALN) treatment (OVX + H-ALN), OVX with medium ALN treatment (OVX + M-ALN), OVX with low ALN treatment (OVX + L-ALN), OVX with high parathyroid hormone (PTH) treatment (OVX + H-PTH), OVX with medium PTH treatment (OVX + M-PTH), OVX with low PTH treatment (OVX + L-PTH), OVX with high sodium fluoride (NaF) treatment (OVX + H-NaF) and OVX with low NaF treatment (OVX + L-NaF). (ANOVA) ǂp<0.001, *p<0.01, **p<0.05

Figure 21. Microarchitectural parameters of the L-4 vertebrae for animals at 12 months of age were determined via microCT. Data is represented as group mean + SD. A.) Trabecular thickness, B.) trabecular number, C.) trabecular spacing and D.) connectivity density. Data is represented as age matched control (AM), ovariectomy control (OVX), OVX with high dose alendronate (ALN) treatment (OVX + H-ALN), OVX with medium ALN treatment (OVX + M-ALN), OVX with low ALN treatment (OVX + L-ALN), OVX with high parathyroid hormone (PTH) treatment (OVX + H-PTH), OVX with medium PTH treatment (OVX + M-PTH), OVX with low PTH treatment (OVX + L-PTH), OVX with high sodium fluoride (NaF) treatment (OVX + H-NaF) and OVX with low NaF treatment (OVX + L-NaF). (ANOVA) * p<0.001, *p<0.01, **p<0.05

Figure 22. Bone volume fraction at 6, 8 and 12 months for age matched control (black-AM), ovariectomy control (dark gray – OVX) and all high dose treatments pooled (light gray – OVX + Treatment). Data is, represented as mean + SD. (ANOVA) *p<0.01,**p<0.05

Figure 23. Tissue mineral density fraction at 6, 8 and 12 months for age for all data from each time point pooled. Data is, represented as age mean + SD. (ANOVA) ǂp<0.001,*p<0.01

Figure 24. A.) Liver, B.) fat pad and C.) brown fat masses at sacrifice at 6 months of age in baseline controls (AM) and baseline OVX controls (OVX). Data is represented as group mean + S.D. (Student t-test) *p<0.01, **p<0.05

Figure 25. A.) Liver, B.) fat pad and C.) brown fat masses at 8 months of age for age matched control (AM), ovariectomy control (OVX), OVX with high dose alendronate (ALN) treatment (OVX + H-ALN), OVX with medium ALN treatment (OVX + M-ALN), OVX with low ALN treatment (OVX + L-ALN), OVX with high parathyroid hormone (PTH) treatment (OVX + H-PTH), OVX with medium PTH treatment (OVX + M-PTH), OVX with low PTH treatment (OVX + L-PTH), OVX with high sodium fluoride (NaF) treatment (OVX + H-NaF) and OVX with low NaF treatment (OVX + L-NaF). (ANOVA) * p<0.001, *p<0.01, **p<0.05

Figure 26. A.) Liver, B.) fat pad and C.) brown fat masses at sacrifice at 12 months of age for age matched control (AM), ovariectomy control (OVX), OVX with high dose alendronate (ALN) treatment (OVX + H-ALN), OVX with medium ALN treatment (OVX + M-ALN), OVX with low ALN treatment (OVX + L-ALN), OVX with high parathyroid hormone (PTH) treatment (OVX + H-PTH), OVX with medium PTH treatment (OVX + M-PTH), OVX with low PTH treatment (OVX + L-PTH), OVX with high sodium fluoride (NaF) treatment (OVX + H-NaF) and OVX with low NaF treatment (OVX + L-NaF). (ANOVA) * p<0.001, *p<0.01, **p<0.05

Figure 27. Triglyceride content of the liver for A.) 6 month, (Student t-test) B.) 8 month (ANOVA) and C.) 12 month old animals (ANOVA) . Data is represented as mean +S.D for age matched control (AM), ovariectomy control (OVX), OVX with high dose alendronate (ALN) treatment (OVX + H-ALN), OVX with medium ALN treatment (OVX + M-ALN), OVX with low ALN treatment (OVX + L-ALN), OVX with high parathyroid hormone (PTH) treatment (OVX + H-PTH), OVX with medium PTH treatment (OVX + M-PTH), OVX with low PTH treatment (OVX + L-PTH), OVX with high sodium fluoride (NaF) treatment (OVX + H-NaF) and OVX with low NaF treatment (OVX + L-NaF). (Student t-test, ANOVA) ǂ p<0.001, *p<0.01, **p<0.05

Figure 28. TG content of the serum for A.) 6 mo animals, B.) 8 mo animals and C.) 12 mo animals. Data is represented as group mean + SD for age matched control (AM), ovariectomy control (OVX), OVX with high dose alendronate (ALN) treatment (OVX + H-ALN), OVX with medium ALN treatment (OVX + M-ALN), OVX with low ALN treatment (OVX + L-ALN), OVX with high parathyroid hormone (PTH) treatment (OVX + H-PTH), OVX with medium PTH treatment (OVX + M-PTH), OVX with low PTH treatment (OVX + L-PTH), OVX with high sodium fluoride (NaF) treatment (OVX + H-NaF) and OVX with low NaF treatment (OVX + L-NaF). (Student t-test, ANOVA) ǂ p<0.001, *p<0.01, **p<0.05

Figure 29. Serum triglyceride content at 6, 8 and 12 months of age for age matched controls (AM), ovariectomy controls (OVX) and ovariectomy controls that underwent treatment (OVX + Treat) (ANOVA) *p<0.01

Figure 30. NEFA concentrations in the liver at A.) 6 months, B.) 8 months and C.) 12 months. Data is represented as mean + SD for age matched control (AM), ovariectomy control (OVX), OVX with high dose alendronate (ALN) treatment (OVX + H-ALN), OVX with medium ALN treatment (OVX + M-ALN), OVX with low ALN treatment (OVX + L-ALN), OVX with high parathyroid hormone (PTH) treatment (OVX + H-PTH), OVX with medium PTH treatment (OVX + M-PTH), OVX with low PTH treatment (OVX + L-PTH), OVX with high sodium fluoride (NaF) treatment (OVX + H-NaF) and OVX with low NaF treatment (OVX + L-NaF). (Student t-test, ANOVA) ǂ p<0.001,*p<0.01, **p<0.05

Figure 31. NEFA concentrations in the liver at A.) 6 months, B.) 8 months and C.) 12 months. Data is represented as mean + SD for age matched control (AM), ovariectomy control (OVX), OVX with high dose alendronate (ALN) treatment (OVX + H-ALN), OVX with medium ALN treatment (OVX + M-ALN), OVX with low ALN treatment (OVX + L-ALN), OVX with high parathyroid hormone (PTH) treatment (OVX + H-PTH), OVX with medium PTH treatment (OVX + M-PTH), OVX with low PTH treatment (OVX + L-PTH), OVX with high sodium fluoride (NaF) treatment (OVX + H-NaF) and OVX with low NaF treatment (OVX + L-NaF). (Student t-test, ANOVA)

Figure 32. NEFA concentrations in the liver at 6, 8 and 12 months. Data is represented as mean + SD for age matched controls (AM - black), ovariectomy controls (OVX-dark gray) and the combined data set of all ovariectomy treated animals (OVX + Treatment - light gray) (ANOVA) ǂ p<0.001, **p<0.05

Figure 33. Leptin serum concentrations at A.) 6 months, B.) 8 months and C.) 12 months of age. Data is represented as mean + SD for age matched control (AM), ovariectomy control (OVX), OVX with high dose alendronate (ALN) treatment (OVX + H-ALN), OVX with medium ALN treatment (OVX + M-ALN), OVX with low ALN treatment (OVX + L-ALN), OVX with high parathyroid hormone (PTH) treatment (OVX + H-PTH), OVX with medium PTH treatment (OVX + M-PTH), OVX with low PTH treatment (OVX + L-PTH), OVX with high sodium fluoride (NaF) treatment (OVX + H-NaF) and OVX with low NaF treatment (OVX + L-NaF). (Student t-test, ANOVA) *p<0.01

Figure 34. Leptin concentrations at 6, 8 and 12 months in age matched control (AM - black) and ovariectomy control (OVX - gray) animals. Leptin concentrations were lower in 6 month controls and 8 month OVX controls compared to 12 month controls. (ANOVA) **p<0.05

Figure 35. IGF-1 serum concentrations at A.) 6 months, B.) 8 months, C.) 12 months. Data is represented as means +SD for age matched control (AM), ovariectomy control (OVX), OVX with high dose alendronate (ALN) treatment (OVX + H-ALN), OVX with medium ALN treatment (OVX + M-ALN), OVX with low ALN treatment (OVX + L-ALN), OVX with high parathyroid hormone (PTH) treatment (OVX + H-PTH), OVX with medium PTH treatment (OVX + M-PTH), OVX with low PTH treatment (OVX + L-PTH), OVX with high sodium fluoride (NaF) treatment (OVX + H-NaF) and OVX with low NaF treatment (OVX + L-NaF (Student t-test, ANOVA) ϕ p<0.02 *p<0.01, **p<0.05

Figure 36. Body mass was positively correlated to A.) fat pad weights and B.) *in vivo* microCT fat volume. Data are represented as individual animals for all time points throughout the study. (Linear regression) (r^2=0.36, p<0.0001, r^2=0.29, p<0.0001)

Figure 37. Body mass was positively correlated to fat volume at 12 months of age, in age matched control (AM), high dose alendronate (H-ALN) and high dose parathyroid hormone (H-PTH) groups. The slopes are similar but the treated animals have lower body mass to fat relationship. (Linear Regression, ANCOVA) p<0.0001

Figure 38. AM controls and high treatment groups were pooled and OVX controls and low treatment groups were pooled for all 12 month data. Body mass was positively correlated to bone volume in AM and treated animals and the correlation was strengthened with just AM, H-ALN and H-PTH groups . Body mass was not correlated to body weight in OVX and low dose treatment. (Linear Regression) (r^2=0.12, p<0.05) (r^2=0.36, p<0.01) (r^2=0.018, p>0.05)

Figure 39. AM controls and high treatment groups were pooled, OVX controls and low treatment groups were pooled for all 12 month data. Body mass was positively correlated to *in vivo* apparent mineral density in AM and high dose treatment but was not correlated in OVX and low dose treatment. (Linear Regression) (r^2=0.25, p<0.02)(r^2=0.01, p=0.50)

Figure 40. Body mass was not correlated to bone density at 12 months of age in the combined data set of OVX controls pooled with L-PTH and L-NaF. (Left) It was positively correlated in the combined data set of AM controls with ALN treatments and H and M-PTH and H-NaF. (Middle) The high dose treated animals had a higher slope than AM controls pooled with M and L-ALN and M-PTH. (Left) (Linear Regression, ANCOVA) $p<0.01$

Figure 41. Metabolic parameters: liver triglyceride concentration (Liver –TG (mg)), liver non-esterfied free fatty acid concentration (Liver – NEFA (mEq/L)), serum leptin concentration (Leptin (ng/ml)), serum triglyceride concentration (Serum-TG (mg/dL)) and serum non-esterfied free fatty acid concentration (Serum – NEFA (mgEq/L)) were each correlated to body mass (top row), fat pad mass (middle row) and total adipose volume (from *in vivo* microCT) (bottom row). There was a significant positive relationship in all correlations except serum NEFA concentration to body mass, fat pad mass and total adipose tissue.

Figure 42. Fat pad mass was negatively correlated to bone volume fraction in all animals pooled for 6 (black -squares), 8 (black-diamonds), and 12 months (gray -circles). 12 month had a higher elevation than 8 months which was higher than 6 months. (ANCOVA) $p<0.0001$

Figure 43. A) There was a negative correlation between liver TG content A.) *in vivo* apparent mineral density, B.) *ex vivo* apparent mineral density and C.) *ex vivo* BV/TV. (Linear regression) (r^2=0.18 or 0.21, $p<0.0001$)

Figure 44. There was a negative relationship between BV/TV and Liver TG in AM Controls (Black squares, black line), ALN treated animals (Black –triangles, blue line) , PTH treated animals (black – diamonds, green line) or OVX pooled with L-PTH and L-NaF had low bone volume fraction with a large array of liver triglyceride content (Dark gray-diamonds, black line).

Figure 45. Apparent mineral density correlated to liver triglyceride content for all animals at 12 months of age. Animals were grouped as age matched controls pooled with high sodium fluoride (black - square), ovariectomy controls pooled with low sodium fluoride and low PTH (grey- triangle), H and M-PTH groups pooled (green - circle) and all alendronate treatments pooled (blue- triangle).

ACKNOWLEDGEMENTS

I would like to thank Dr. Judex for his help with my research and for his commitment to teaching me the best research practices, the value of diligence in making the right academic decisions and for being the master of statistics.

Special thanks to Steven Tommasini, for bestowing upon me the wisdom of his own experiences and previous learning as well as working on this study as my teacher and friend.

Thank you to Lisa Miller and Alvin Acerbo for their continued efforts and support at Brookhaven National Labs and for always making themselves available to assist with the project.

Clint Rubin, thank you to for inspiring me to become a “bone-head.” More importantly, thank you for demanding answers to the tough questions and always keeping me on my toes.

Thank you to my lab mates for their help in preparing for this dissertation as well as always offering advice and support.

A special thanks to my wonderful family for being a support system and tolerating my need for nerdy engineering conversations and editing help. Kyle and Pam, you never lose faith in my abilities, your confidence helps me through.

CHAPTER 1

INTRODUCTION

1.1 OVERVIEW

The skeletal system is an organ of the body that provides structural support and locomotion, protection to internal organs and acts as a calcium reservoir (Loveridge, 1999). Bone is comprised of cells that are sensitive to chemical, mechanical and hormonal signals (Winer, 2009). Response to these signals activates a process called bone remodeling where the skeleton is broken down and replaced with new tissue. During menopause, women experience a significant decrease in circulating levels of estrogen. Reduced estrogen levels initiates an overall decrease in bone volume and bone density caused by increased rates of resorption compared to formation (Manolagas, 1995). This has been termed post-menopausal osteoporosis. Decreases in estrogen can also have negative effects on body composition, including weight gain, visceral fat accumulation as well as negative effects on fat metabolism (Sowers, 2008, Petzel, 2007). Osteoporosis is treated clinically with drugs that act as anabolic agents to increase bone formation rates (i.e. parathyroid hormone) or anti-catabolic agents to decrease the rate of resorption (i.e. alendronate) (Crannery, 2002). Sodium fluoride is an anabolic drug used in research, but is not prescribed clinically due to its inability to prevent osteoporotic-related fractures (Lafage, 1995). The goals of this study were to determine the short (2 months) and long term (6 months) effects of various doses of alendronate, parathyroid hormone and sodium fluoride on body composition, vertebral bone quantity and microarchitecture as well as drug effects on indices of fat metabolism.

1.2 SKELETAL TISSUE

The skeletal system provides the basic shape and form of the body. The purpose of the skeleton is to protect internal organs, facilitate movement and act as a calcium reservoir for the rest of the body (Loveridge, 1999). Bone is a dynamic tissue that has active cellular mechanisms causing constant turnover. Bone cells degrade the bone matrix and replace it with new tissue in a pair of coupled processes called bone remodeling (Parfitt, 1996). This occurs for a variety of reasons: in order to release calcium into the blood stream for systemic distribution, to adapt to changes in mechanical

demand, or to repair itself after incidences of microdamage in order to maintain skeletal integrity (Mori, 1993).

Bone Composition

Bone is composed of four main cell types, osteocytes, osteoblasts, osteoclasts and bone lining cells. It is also made up of its extracellular matrix which consists of 20% water, 35% organic material (proteins and cells) and 45% inorganic mineral (mineral). The organic phase is composed predominantly of a protein called Type I collagen which gives bone its flexibility and tensile strength. The inorganic phase is composed of a mineral called hydroxyapetite which incorporates into the collagen fibrils and increases bone's compressive strength (Constantz, 1995).

Bone is composed of two types of tissue called cortical and trabecular bone. Cortical bone is densely packed tissue that provides the shell on the exterior of all bones. The cortical bone is 5-10% porous, the pores are made up of Haversian and Volkmann's canals which are a network of small channels where blood vessels carry nutrients to the dense tissue. Cortical bone accounts for 80% of the skeletal mass (Seeman, 2010).

Trabecular bone is found within cortical shells of certain regions of bones. It is made up of a series of interconnected plates and rods that network together to form a tissue that has the appearance of a sponge with a high porosity between 75-95% (Eriksen, 1990). The empty space is filled with a gelatinous medium called bone marrow, compromised of bone cells, mesenchymal stem cells, hematapocytes, blood and nutrients (Manolagas, 1995). Since trabecular bone has a high surface volume exposed to bone marrow, it is the site of active tissue turnover in a process called bone remodeling.

Bone Remodeling

Twenty five percent of trabecular bone is remodeled every year, while only 3% of cortical bone is remodeled (Manolagas, 1995). 70-85% of trabecular bone surfaces are in contact with bone marrow. Bone marrow contains the cells responsible for the bone remodeling process (Malaval, 1994). This makes trabecular bone more susceptible to bone turnover due to the constant interaction of remodeling cells in contact with the tissue surfaces. In diseased states, such as osteoporosis, this is where the greatest changes in bone density and bone volume occur (Benhamou, 2007).

Bone remodeling is the process of bone tissue degradation and replacement with new tissue. It occurs to remove calcium from the tissue reservoir in order to release it into the blood stream for use by the rest of the body. It also remodels in adaption to mechanical loading to ensure adequate bone mass for structural support (Parfitt, 1996, Loveridge, 1999). Bone mass and bone microarchitecture have been shown to be regulated by mechanical loading (Rubin 1987, Lanyon, 1996). Bone can remodel in response to tissue injury. The accumulation of microcracks within skeletal tissue can initiate remodeling in order to remove damaged tissue and replace it with new tissue (Mori, 1987). Bone remodeling occurs when tissue is removed by cells called osteoclasts through resorption followed by the creation of new tissue by cells called osteoblasts through formation.

Osteoclasts are multinucleated cells responsible for bone resorption. Osteoclastogenesis is initiated through a series of cytokines including colony stimulating factor and interleukin-1, 3, 6 and 11 (Horowitz, 2003, Manolagas, 1995). Signaling leads to the fusion of monocytes from hematapooetic cells that reside within the bone marrow (Suda, 1992). Osteoclasts are recruited to bone surfaces and actively erode away pockets of exposed bone. This occurs by first creating a seal along the bone surface with a ruffled cell edge (Loveridge, 1999). The cells demineralize the exposed bone with acids and proceed by excreting enzymes which degrade extracellular matrix. (Loveridge, 1999) This process creates resorption pits across a bone surface. Resorption occurs along trabecular bone edges as well as along the endosteal surfaces of cortical bone. It can also occur around the cortical blood vessels called Haversian canals. Cortical bone is removed by a basic multicellular unit (BMU) called a cutting cone which tunnels into the dense tissue starting from a Haversian canal (Parfitt, 2001). During resorption, osteoclasts actively secrete cytokines which signal for osteoblast recruitment in order to initiate bone formation (Harowitz, 1992, Allan, 2008).

Osteoblasts are mononucleated cells that are differentiated from mesenchymal stem cells or bone lining cells (Parfitt, 1990, Malaval, 1994). Osteoblastogenesis occurs in response to a variety of cell signaling including insulin-like growth factor 1, and other cytokines. Bone remodeling is a coupled process. Osteoclasts and osteoblasts are stimulated by some of the same cytokines such as interleukin-6 and 11, demonstrating

that activation of one process is coupled to the activation of the other (Manolagas, 1995).Once activating, osteoblasts migrate to sites of remodeling and secrete extracullar matrix called osteoid, into resorption pits. Osteoid is composed predominantly of collagen (Parafitt, 1990). The new matrix is poorly mineralized but will become stiffer over time to match the material properties of its surrounding tissue. Occasionally an osteoblast will become embedded into the extracellular matrix it is laying down. When this occurs, the osteoblast becomes a part of a network of bone cells within the extracellular matrix called osteocytes.

Osteocytes are bone cells responsible for major cellular signaling. Cell signaling occurs between osteocytes as well as from osteocytes to other types of bone cells (Bonewald, 2008). Signaling occurs through long cellular processes called canaliculi which create gap junctions across the bone matrix (Burger, 1999). Cell to cell signaling is conducted through the gap junctions via secretion of secondary messengers, they are transmitted as hormones and paracrine factors which activate bone cells through a complex series of signaling pathways (Duncan, 1995) Osteocytes are critical for initiating both resorption and formation in response to changes in the mechanical strain environments. During incidences of high strain osteocytes can recruit osteoblasts to increase bone formation rates to increase tissue volume (Bonewald, 2008). Scientists also believe that in low strain environments, osteocytes can undergo apoptosis which attracts osteoclasts and initiates bone resorption (Burger, 2003). Osteocytes also communicate directly with bone lining cells and can stimulate their differentiation into osteoblasts for new bone formation.

Bone lining cells are attached to the surfaces of bone tissue. They are flattened, inactive osteoblasts that remain quiescent until cellular communication initiates their differentiation (Malaval, 1994). Bone lining cells are thought to be sensitive to mechanical stimulation and can differentiate into osteoblasts during cyclic mechanical loading, especially fluid shear flow across their surfaces (Duncan, 1995). They have cell surface receptors for both estrogen and parathyroid hormone, indicating their sensitivity to a variety of chemical, hormonal and mechanical signaling (Rickard, 2006). During resorption, osteoclasts release chemicals which activate bone lining cells causing differentiation into osteoblasts. When activated, differentiatiated bone lining cells will

form new bone directly at their site of attachment (Parfitt, 2001). Bone remodeling is controlled by a series of chemical, hormonal and mechanical signals; however insulin-like growth factor-1 plays a critical role in skeletal growth as well as bone mass maintenance throughout adulthood by up-regulation of bone formation.

IGF-1

Insulin-like growth factor 1 (IGF-1) is an endocrine hormone responsible for regulation of growth and development (Yakar, 2002). It is a peptide consisting of 70 amino acids that is synthesized primarily in the liver. It is an important hormone for the regulation of bone mass through its stimulatory effects on bone formation (Rosen, 1994).

In adults, IGF-1 is anabolic to bone, it increases the activation of healthy osteoblasts through binding to IGF-1 receptors on the osteoblast surface. This helps to maintain proper skeletal architecture due to its direct effects on osteoblasts (Canalis 1989, 1993, Birnbaum, 1995). It does not have an effect on the differentiation of mesenchymal stem cells towards osteoblastic lineages (Canalis, 2010). Studies have shown that it plays an important role in bone integrity by increasing mineralization and trabecular bone volume (Zang, 2002). There is a decline in IGF-1 levels during aging which contributes to decreases in bone mineral density that occurs throughout adulthood (Guistina, 2008). Bone mineral density is correlated to serum levels of IGF-1 in post-menopausal women (Canalis, 2010). Overstimulation of IGF-1 in a mouse model led to increased bone formation rates and increased trabecular and cortical bone volume. This was contributed to the increased overproduction of osteoblast activity without the differentiation of new osteoblasts (Zhao, 2000). Another regulator of bone formation is mechanical strain. Mechanical strain is sensed by osteocytes who respond by secreting cytokines that activate osteoblast differentiation, causing bone formation.

Biological Response to Mechanical Signals

The skeletal system adapts to mechanical stimuli, making body weight an important role in bone health. There is a direct relationship between body mass and bone volume due to skeletal adaption in response to mechanical loads (Rubin, 1987). Obesity has a positive effect, as a protection against osteoporosis. Obese post-menopausal women have higher bone mass and reduced rates of resorption compared to healthy weight

individuals (Cifuentes, 2004, Petzel, 2007). The significantly higher mechanical demand placed on the skeletal system due to large mass results in larger skeletal frames and increased bone volume and bone mineral density with decreased risk of developing hip fractures (Usi-Rasi, 2009, Nordin, 1992). Inversely, underweight individuals tend to have smaller skeletal systems and are at a higher risk of developing osteoporosis (Ravn, 1999). There has been a large amount of evidence linking patients diagnosed with anorexia with severe osteoporosis due to reduced weight bearing (Seeman, 1992). More evidence of the negative effects on skeletal health due to reduced load bearing is seen for those who have lost a significant amount of weight after menopause. (Garnero, 2000, Shapses, 2003). Anorexia reduces levels of circulating IGF-1, a key hormone in the regulation of bone formation which contributes to the decline in bone mass (Klibanki, 2010).

Although load bearing is an important contributor to skeletal tissue mass and density, there is recent evidence that suggests negative consequences of fat accumulation and increased fat mass on skeletal health. Patients with type 1 and 2 diabetes mellitus have lower bone mineral density with a higher fracture risk than their healthy weight counterparts (Tuominen, 1999). It has also been shown that post-menopausal obese women have lower rates of bone formation and suppressed collagen formation than healthy weight women (Papakitsou, 20004). This data suggests that the bone-body relationships are complex and bone health relies on more than just mechanical load bearing of the skeleton. Skeletal mass is regulated by a complex array of factors including genetics, growth factors and hormones (Luu, 2009). An important hormone that plays a key role in the maintenance of skeletal tissue is estrogen. It is an important regulator of bone mass because it can act directly on mesenchymal stem cells and bone lining cells to activate bone formation as well as prevent osteoclast mediated resorption (Ogita, 2008, Hughes, 1996). In its presence bone formation rates are matched to rates of formation, but when levels of estrogen decrease, there are serious consequences to bone health due to reduced bone formation.

Estrogen's Role in the Regulation of Bone Tissue

Estrogen is a sex steroid present in the body. It is produced predominantly in the ovaries by developing egg follicles throughout reproductive life, beginning at the onset of menstruation until menopause (Compston, 2001). There are three types of hormones: estrone, estradiol and estriol. Estrogen also has an important function in maintaining metabolism and regulating fat accumulation within the body. Reduced circulating estrogen levels leads to visceral fat accumulation (Tchernof, 2000 Deshaies, 1997, Wade, 1985) and increased serum leptin and cholesterol concentrations (Zoth, 2010, Ke, 1997). In a study of aromatase knockout mice (estrogen deficient), where the estrogen receptor was deactivated, the mice presented with obesity and hepatic steatosis (Hewitt, 2003). Estrogen replacement therapy in an obese animal model reduced visceral fat accumulation and leptin concentrations (Zoth, 2010).

Estrogen is a key regulator in bone metabolism due to its inhibitory effects on bone resorption as well as its activation of bone formation. Estrogen stimulates bone formation through activation of osteoblasts via estrogen receptors (Compston, 2001). Scientists have shown that estrogen replacement therapy increases the differentiation of pre-osteoblasts as well as osteoblast proliferation (Ogita, 2008). Estrogen can also stimulate osteoclast apoptosis, and reduce resorption rates (Hughes,1996). Scientists have shown that decrease in systemic estrogen increases the incidence in osteocyte apoptosis in humans with endometriosis; the increase in incidence of osteocyte apoptosis was strongly correlated with increases in bone resorption (Tomkinson, 1997). Estrogen replacement therapy is effective at reversing the effects of bone loss, and lean body mass as well as decreasing the effects of menopause related obesity. (Sorenson, 2001, Tchernoff, 2000). The decreased levels of estrogen results in changes to bone cell activity ultimately leading to a severe loss of bone mass and bone density, which has been named post-menopausal osteoporosis.

1.3 POST-MENOPAUSAL OSTEOPOROSIS

Post-menopausal osteoporosis occurs in women after the onset of menopause, when drastic reduction in circulating levels of estrogen leads to an imbalance of bone resorption to bone formation rates (Compston, 2001). Osteoporosis is characterized as a reduction in bone mass and bone mineral density, causing the bone to become brittle.

This predisposes those affected by osteoporosis to skeletal fragility and fracture (Fox, 2006, Recker, 2005, Neer, 2001, Marshall, 1996). The most serious consequences of osteoporosis are fractures, commonly associated with the hips, spine and wrists, with an incidence of 1.5 million fractures each year (NIAMS, 2009) 30% of women over the age of 75, and 50% of women over the age of 85 will experience a spinal fracture within their lives (NIAMS, 2009). The direct costs in the U.S. for osteoporotic related fractures are up to $18 billion dollars a year (Carmona, 2004).

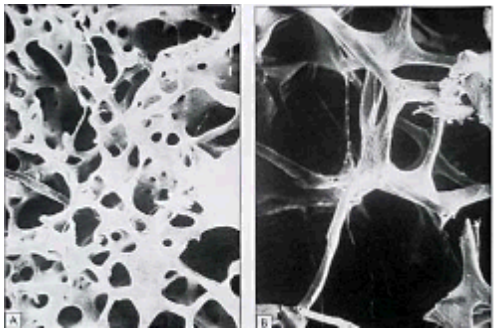

Figure 1. Scanning electron microscope image of A. healthy trabecular bone and B. osteoporotic trabecular bone. Osteoporotic bone has fewer trabecular struts and decrease in total trabecular volume.

Osteoporosis is clinically defined as a bone density reading 2.5 standard deviations below the national average. Ten million people over the age of 50 are living with osteoporosis while an additional 34 million have developed osteopenia, the early stage of osteoporosis, where bone density readings are 1 to 2.5 standard deviations below the national average (Delmas, 2007). Determination of bone mineral density is measured clinically through X-ray absorptiometry (DXA). However, this technique has encountered criticism because it is not a good predictor of osteoporotic related fractures (Marshall, 1996). In addition to reductions in bone mass and density, osteoporosis severely degrades trabecular microarchitecture. This includes a decrease in trabecular number and thickness as well as increase in the spacing between struts and reduced connectivity density (Benhamou, 2007). (Fig. 1) Important information regarding bone quality can be obtained through computed tomography imaging (Benhamou, 2007). Indices of trabecular architecture are good determinants of bone quality and strength (Tommasini, 2005, Turner, 2002).

Osteoporosis Pharmaceuticals and Drugs

Osteoporosis occurs when the rate of formation is reduced compared to the rate of resorption (Recker, 2004). Current pharmaceutical interventions focus on correcting this interruption in the remodeling cycle. Anabolic treatments such as parathyroid hormone

(PTH) and sodium fluoride (NaF) increase the rate of bone formation while anti-catabolic drugs such as alendronate (ALN) prevent bone resorption (Canalis, 2010, Crannery, 2002, Behamou, 2006, Bodenner, 2007).

Alendronate

Alendronate (ALN), clinically known as FOSOMAX, is a bisphosphonate used to treat osteoporosis. The drug is an anti-catabolic that works as a specific inhibitor of osteoclast-mediated bone-resorption by binding to the hydroxyapetite found in bone (Nancollas, 2005). Bisphosphonates are a class of drugs most commonly used to treat metabolic bone diseases including Paget's disease, osteogenesis imperfecta, hypercalcemia, osteopenia and osteoporosis (Watts, 2010).

The structure of a bisphosphonate is composed of two phosphonates and two side chains called R^1 and R^2 that are both joined to carbon. The phosphonates are chelating agents that bond strongly to metal ions such as calcium, and magnesium. This creates a high affinity for the drug to bind to the hydroxyapetite crystals found on the bone surface. The R^1 side chain is responsible for aiding in the binding affinity; they have a high affinity to bone sites where active remodeling occurs (Nancollas, 2005).

After the drug has bound itself to bone tissue it will interact with osteoclasts during remodeling. When an osteoclast attaches to the tissue surface it secretes enzymes that digest the bone. The R^2 side chain is released and enters the osteoclast (Watts, 2010). This causes the osteoclast to lose its resorptive properties and will trigger osteoclastic apoptosis (Hughes, 1996). Osteoclastic apoptosis will block the remodeling cycle and prevent further resorption.

Alendronate is one of a class of four commonly used bisphosphonates that all contain nitrogen. The nitrogen is found in the R^2 chain and gives the compound its binding strength. A drug with better binding strength will have longer residual within the bone but they will not be distributed as deeply into the tissue due to slower infusion. Lower binding strengths will not last as long but there is potential for them to interact with the osteocyte network within the bone due to faster spreading time and access to internal tissue (Nancollas, 2005).

Bisphosphonates are taken orally in the morning on an empty stomach, after the 8 hour fasting that occurs during sleep. Patients are recommended not to eat for 30-60

minutes after taking the drug in order to maximize absorption into the blood stream. Under these optimal conditions only 1% of the drug is absorbed and only 50% of the absorbed drug binds to bone. The remainder of the drug is excreted by the kidneys (Body, 2005).

Alendronate has been shown to prevent bone resorption and can increase bone density. It is clinically proven to reduce the incidence of hip fractures (Black, 1996), vertebral fractures (Black, 2000, Cummings, 2002) and non-vertebral fractures in post menopausal women (Black, 1996, Pols, 1999). A ten year clinical study in women with post-menopausal osteoporosis demonstrated that alendronate taken at 10 mg for 10 years increased bone mineral density in the lumbar spine by 13.7% and in the proximal femur by 6.7% (Bone, 2004). It also improved the microarchitecture of bone compared to placebo treatment in post-menopausal women Over the course of two or three years, bone volume fraction was 17% greater in alendronate treated women, trabecular thickness was 13.4% greater and trabecular spacing was significantly smaller than untreated women (Recker, 2005).

Anti-catabolic drugs suppress natural bone turnover so there is an increase in tissue mineralization that may be detrimental to tissue health. Long term alendronate use has been shown to increase microdamage by accumulation of microcracks in dogs (Allen 2007, 2006). Microdamage is associated with increased risk of fracture and is prevalent in post-menopausal women (Stepan, 2007). Because the drug remains as a reservoir in the skeletal system long after treatment ends, it is important to consider the treatment duration. A duration that maximizes the benefits of treatment while minimizing the potential for oversuppresion of bone turnover would be most beneficial (Watts, 2010).

Parathyroid Hormone

Parathyroid hormone (PTH) is a hormone naturally secreted by the parathyroid gland. It has an 84-amino acid sequence and is responsible for increasing calcium concentration in the blood (Akerstrom, 2005). Parathyroid hormone is critical for the regulation of calcium and phosphate of bones by increasing resorption and increasing calcium reabsorption by the kidney's proximal tubule (Paula, 2010). PTH can respond quickly to subtle changes in circulating calcium levels. Synthetic PTH is called

Teriparatide, which is used as a pharmaceutical treatment for bone disease (Benhamou, 2007, Bodenner, 2007).

A synthetic analog of PTH called hPTH(1-34) has been shown to have similar anabolic effects to naturally secreted PTH. PTH encourages bone lining cell differentiation into osteoblasts which increases bone formation (Turner, 1995). PTH receptors are more abundant on bone cells that are not adjacent to osteoid indicating its key role in osteoblast recruitment to sites of active remodeling. PTH enhances osteoblast productivity, cell differentiation of bone lining cells into osteoblasts and prevents osteoblast apoptosis (Kulkarni, 2007). It has been shown to enhance precursor cells toward osteoblastic lineage, but it directly targets bone lining cells and mature osteoblasts (Rickard, 2006). PTH binds specifically to osteoblast cells which then secrete an enzyme that also deactivates the osteoclastic action (Rodan, 1982). Therefore PTH can directly increase bone formation while indirectly decreasing resorption (Canalis, 2010, Lindsay, 1997).

Teriparatide is the only FDA approved version of synthesized parathyroid hormone. It is only used in patients with severe cases of osteoporosis who are unable to take other medications (Bodenner, 2007). This is due to high costs, the need for daily injections and the fact that long-term side effects are greatly unknown (Benhamou, 2007). In animal studies, there is an incidence of a bone cancer related with long term PTH treatment called osteosarcoma (Vahle, 2002).

A study showed that Teriparatide treatment at 20-µg or 40-µg were 35 or 40% less likely to have one or more non-vertebral fractures as compared to placebo controls. Decreases in bone mineral density were significantly lower than in placebo controls with 40-µg treatment having the greatest effect at preventing loss in bone density ($p<0.001$) (Neer, 2001). Another group studied the three year effect of PTH during estrogen replacement therapy in post-menopausal women. PTH in conjunction with estrogen continuously increased bone mineral density to values 13% greater in the vertebral body and 2.7% greater in the hip than placebo controls. The largest increases in bone mineral density were seen in the first year of treatment (Lindsay, 2000). Others have shown similar positive effects of PTH administration in post-menopausal women (Greenspan, 2007, Hodsman, 2003).

PTH administration creates bone of good quality with similar structural properties of healthy tissue. Teriparatide treatment increased the amount of trabecular bone with improved trabecular architecture as well as induced a 22% increase in cortical bone (Jiang 2003). In contrast, sodium fluoride is another anabolic drug that is effective at increasing bone volume and bone mineral density, however the quality of tissue formed during sodium fluoride treatment tissue quality is reduced and treatment cannot prevent against fracture.

Sodium Fluoride

Sodium fluoride (NaF) is an inorganic compound commonly used to prevent tooth cavities by strengthening tooth enamel. Sodium fluoride was originally thought to be an excellent treatment for osteoporosis because it has a strong anabolic effect on bone. It is incorporated within the crystal structure of the bone and can replace hydroxyapetite which alters the chemical structure of bone (Lindsay, 1990). The fluoride embedded within the bone promotes osteoblast attachment and proliferation (Qu, 2006). The presence of sodium fluoride stimulates bone formation leading to a net gain in the bone remodeling cycle (Eriksen, 1985). However, bone quality is reduced due to a defect that occurs when fluoride binds to the hydroxyapetite which causes a reduction in the material properties of tissue (Riggs, 1990). The reduction in bone strength has been attributed to either the non-uniformity in mineralization during formation, decreased bending strength in the crystal-matrix or decreased collagen crosslinking (Lafage, 1995).

Researchers have found that sodium fluoride treatment increases trabecular volume and connectivity density while increasing bone volume fraction (Eriksen, 1985, Vesterby, 1991). However, it does not prevent against osteoporosis related fracture in post-menopausal women (Riggs, 1980, 1982, Lindsay, 1990). Sogaard et. al found that five years of treatment in post-menopausal women who underwent sodium fluoride treatment had decreased mechanical strength of bone taken from iliac crest biopsies (Sogaard, 1994). Due to its inability to prevent against osteoporotic related fractures, sodium fluoride is not FDA approved for pharmaceutical use.

Drug Dosage in the OVX Rat Model

The ovariectomized rat model is commonly used in research to study osteoporosis because the model shows changes in bone parameters and responds to drug treatment in similar ways as post-menopausal patients (Kalu, 1991, Lelovas, 2008). In this model the ovaries are removed from the animal causing drastic reduction in circulating levels of estrogen and subsequent bone loss. Some of the limitations of the ovariectomized rat model are slow progression of bone loss after ovariectomy and smaller magnitudes of loss in comparison to post-menopausal bone loss (Egermann, 2005).

There are several important considerations when using the OVX rat model. Age of ovariectomy is important, for animals ovariectomized too early can severely slow healthy tissue development (Shinoda, 2002). The start point of initiation of drug treatment is also a major concern for osteoporosis research. It is important to understand whether treatment is preventing bone loss, before estrogen-withdrawal bone loss has set in, or reversing loss that has already occurred. (Egermann, 2005).

Selection of treatment dosage is an important consideration for achieving clinically relevant data (Sama, 2004, Rosen, 2004). There appears to be a relationship between increases in BMD and the amount of drug administered (Rosen, 2004). Doses can be determined based on other ovariectomized animal models (Balena, 1993, Ke, 1997, Heindel, 1996, Iwata, 2006, Lemeiux, 2003. Fox, 2006, Yao, 2005).

Therefore, during the current study, treatment doses were selected as a low dose or clinically relevant dose, a high dose determined by the highest studied dose that did not cause adverse side effects or toxicity in rats, a medium dose was chosen between high and low, in order to establish dose dependent changes in bone mass and quality. The high dose of PTH was below the dose that when given over two years, induced osteosarcoma in adult rats (Vahle, 2002). Sodium fluoride can cause fluoride poisoning which can cause stomach ulcers and gastric indigestion. (National Toxic. Program, 1990) Due to the distaste of the water it is difficult to induce adequate drinking to ensure proper dosage amounts during high dose NaF treatment. Sodium fluoride treatment has anabolic effects on rat bone when administered in the drinking water and does not affect palatability in adult rats in doses up to 300 ppm (Heindel, 1996). Sodium fluoride can be toxic to

humans and animals at a dose that exceeds 10 mg/L, our dose stayed well below this concentration. All treatments were administered below a toxic dose.

1.4 ADIPOSE TISSUE

Adipose tissue stores energy, cushions and insulates the body. It is composed of cells called adipocytes that accumulate together to create fat pads (Trayhurn, 2001). The buildup of excessive fat adipose tissue within the body is called obesity (Mantzoros, 1999). The cause of obesity can be attributed to an imbalance between energy intake and energy expenditure, resulting in excess adipose tissue storage. In 1991 in the United States, 65% of adults and 13% of children were considered overweight (National Center for Health Statistics). 72 million people in the U.S. are considered obese. It afflicts all races, ethnic groups and genders and is the cause of over 300,000 deaths each year in the U.S. Obesity is associated with heart disease, type 2 diabetes and some cancers (Kopelman, 2010). Obesity has an estimated economic cost of over $100 billion dollars each year in the U.S. (Wolf, 1998).

There are two types of adipose tissue: white and brown. Fat is an important hormone regulator and works by secreting leptin, adiponectin, resistin and other adipokines to increase the rate of fat storage or release fat for systemic energy use (Trayhurn, 2001). Adipose tissue accumulates in specific locations called ‘adipose depots’ (Casteilla, 2008). In rodents, fat accumulates into eight adipose depots. Accumulated fat underneath the skin is called subcutaneous fat and is used for insulation from heat and cold. The fat found in the abdominal cavity is predominantly visceral fat. The fat associated with the gonadal organs, attached to the uterus and ovaries in females, or the epididymis and testes in males, is called gonadal fat (Casteilla, 2008).

Increased visceral adipose tissue accumulation causes insulin resistance and can result in type 2 diabetes (Wajchenberg, 2000). Insulin resistance causes a reduction in the uptake of glucose which leads to increased release of free fatty acids and glycerol as well as a reduced rate of fatty acid re-esterification (Zierath, 1998). The increased levels of circulating free fatty acids cause overexposure to cells called lipotoxicity (Guo, 2007). Free fatty acids are metabolized by the liver, secreted into the blood stream, and

sequestered by fat cells within the adipose tissue, liver and skeletal muscle to prevent lipotoxicity (Sepe, 2010).

Aging and Fat Accumulation

There is a significant decline in lean body mass and an increase in fat body mass during aging (DeNino, 2001, Kyle, 2001). Fat is redistributed from subcutaneous fat into abdominal visceral fat depots. An increase in fat accumulation also occurs within the bone marrow, muscle and the liver (Sepe, 2010). In elderly male and female patients there is an increase in abdominal fat as compared to their healthy young counterparts (Kelley, 2000). Female sex hormones cause fat to be stored in the hips, thighs and buttocks of women which prepares the body for pregnancy and child bearing (O'Sullivan, 2001). However, during menopause fat gravitates from these regions and accumulates within the abdomen, as visceral fat (Mazariegos 1994). During menopause the reduction in ovarian hormones leads to a disruption in energy balance and a subsequent increase in adipose tissue accumulation (Richard, 1986).

Weight gain associated with aging increases abdominal fat which can lead to insulin resistance. This impairs the body's ability to store excess fat into adipose depots (Heilbronn, 2004, Kelley, 2000). Fat accumulation has been associated with increased incidences obesity, type 2 diabetes and a overall decline in metabolic health (Allison 1997, Heitmann 2000, Zamboni, 1997, DeNino 2001, Hughes, 2004, Goodpaster, 2005). Understanding the complex changes that occur during aging in fat and bone are critical for determining optimal ways of treating osteoporosis and metabolic disorders such as obesity and metabolic syndrome.

The Metabolic Functions of the Liver

The liver is the largest glandular organ in the body. It is responsible for synthesis and secretion of bile, synthesis of plasma proteins, regulation of metabolic functions, and systemic detoxification (Bjornsson, 2009). The liver receives blood supply via the portal vein and hepatic arteries. Hepatocytes are the cells found within the liver and they are responsible for maintaining homeostasis and regulating energy balances. Hepatocytes oxidize triglycerides to produce energy for the body.

A sign of poor metabolic health is elevated levels of triglyceride and free fatty acids, both within the liver and in blood circulation (Gastaldelli, 2002, Poehlman, 1995). Nonalcoholic liver disease is the accumulation of fat within the liver. It is the leading cause of chronic liver disease in adults and humans; it is associated with obesity and insulin resistance (Lewis, 2010). Nonalcoholic liver disease results in an enlarged liver with yellowish tint. A histological analysis of liver through a liver biopsy shows an increase in fat content, seen by increase in lipid droplet diameter and number (white circles). Nonalcoholic fatty liver disease can increase the risk of cardiovascular disease and metabolic syndrome (Tiniakos, 2010). (Fig. 2)

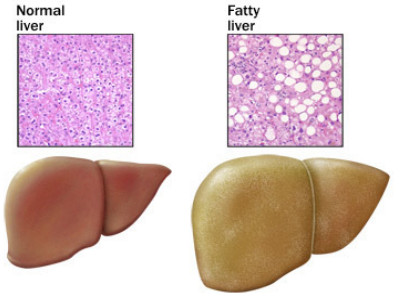

Figure 2. An artistic representation of A.) healthy liver and B.) liver with steatosis. The healthy liver has histological slides (above) with minimal fat accumulation. Steatosis causes cellular fat sequestration, seen as lipid droplets (white circles).

Triglycerides and Free Fatty Acids

Triglycerides are a key energy source involved in metabolism and transportation of dietary fat (Asiedu, 1995). The liver hydrolyzes triglycerides into free fatty acids and glycerol which are then carried out of the liver via the blood and are exported throughout the body to mitochondria for energy (Zierath, 1998). Free fatty acids can also be derived from excess carbohydrates and proteins. Excess free fatty acids are converted back into triglycerides and accumulated within adipocytes and stored in adipose tissue as energy storage (Bowen, 1995).

High levels of triglycerides have been linked to atherosclerosis, heart disease, stroke and obesity (Lewis, 2010). Saturated fatty acids are dangerous to adipose tissue function because pre-adipocytes, or undifferentiated fat cells, become susceptible to lipotoxicity (Wu, 2007). Adipocyte progenitor cells are capable of self replicating and can lead to an increase in fat cell number and increases in adipose tissue volume (Sepe, 1995).

Pre-adipocytes are sensitive to free fatty acid and insulin levels, as well as hormonal regulators such as estrogen and insulin like growth factor 1, they become susceptible to lipotoxicity with aging (Guo, 2007). Adipocytes can also secrete endocrine

and paracrine factors that can generate estradiol from testosterone which contributes to the increased body mass plays as a protective mechanism against bone loss during post-menopausal osteoporosis (Gimble, 1996). Adipocytes also secrete other hormones that are metabolic to bone, such as leptin.

Leptin

Leptin is synthesized by adipocytes as a 16kD molecule. Circulating levels of leptin are directly proportional to the total amount of fat in the body (Whitefield, 2001). Leptin regulates energy intake and energy expenditure and regulate appetite (Zhao, 2008). It is produced by both white and brown fat cells as well as within the ovaries, skeletal muscle, bone marrow, the pituitary gland and the liver (Whitefield, 2001).

Obesity is associated with elevated levels of circulating leptin concentration. Obesity is caused when there is an imbalance in the amount of stored adipose tissue compared to energy expenditure. In healthy and obese humans, Ohannesian et al, found that there was a strong positive correlation between serum leptin levels and the percentage of body fat (Ohannesian, 1996).Increased fat accumulation indicates more adipocytes and an overall increase in cellular secretions of leptin. Long term elevation of leptin levels can result in leptin desensitization which causes the inability to feel satiated after eating, leading to overeating and cyclic weight gain which aggravates the already devastating effects of obesity (Aydin, 1962).

Leptin has positive effects on bone health and is an important regulator of bone metabolism. Leptin promotes bone marrow stromal cell differentiation into osteoblasts (Thomas, 1999), and inhibits osteoclast formation (Holloway, 2002). After menopause, heavier women have been shown to conserve bone mass better than smaller statured women, and heavier women also have greater concentrations of leptin. Additionally, scientists have shown that leptin concentrations can either decrease (Rosenbaum, 1996) or increase (Sowers, 2008) in post-menopausal women. The increase in leptin seen after menopause could be a natural defense mechanism against bone loss and could explain why heavier women are more successful at conserving bone mass. The metabolic factors that contribute to bone health are complex, however there is an important relationship between estrogen, leptin and other hormonal regulators of bone mass. The relationships

between both and their effects on skeletal health are important concerns for post-menopausal women (Rosenbaum, 1996).

1.5 SPECIFIC AIMS

Osteoporosis and obesity are two diseases that affect millions of people in the United States. Current interventions for osteoporosis have been effective at improving bone quantity while reducing osteoporotic related fractures, but little is known of drug effects on fat accumulation and metabolism. We hypothesize that osteoporosis drugs will prevent bone loss, normalize metabolic parameters and negatively correlate bone and fat. Using the ovariectomized (OVX) rat model, we will determine how body composition and bone microarchitecture are affected by age, OVX, and osteoporosis drug treatment (SA1), determine changes in fat metabolism with age, OVX, and drug treatment (SA2), and determine how bone quantity and quality correlate to fat metabolism and fat accumulation during drug treatment (SA3).

Hypothesis 1: After ovariectomy the reduction in systemic estrogen results in substantial loss in bone mass as well as increases in body mass and abdominal fat. We hypothesize that osteoporosis treatments such as alendronate, parathyroid hormone, and sodium fluoride will not only improve bone mass, but also decrease fat accumulation and weight gain, especially at high doses during long-term treatment.

Specific Aim 1: To determine how body composition and trabecular bone microarchitecture are affected by age, ovariectomy (estrogen withdrawal), and osteoporosis treatments.

Changes in body composition in the ovariectomized rat will be determined through body mass monitoring, *in vivo* μCT to determine fat content, bone volume and apparent mineral density and *ex vivo* μCT to determine changes in trabecular architecture caused by ovariectomy and treatment. Sprague Dawley rats will be sacrificed at 6, 8 and 12 months to determine body compositional changes due to age, ovariectomy, and short (2 month) and long term (6 month) osteoporosis drug intervention, including alendronate, parathyroid hormone and sodium fluoride at various doses.

Hypothesis 2: We hypothesize that osteoporosis treatments such as alendronate, parathyroid hormone, and sodium fluoride treatments will prevent negative effects on fat metabolism (i.e. increased fat accumulation) that occur during ovariectomy. Long term, high dose treatments will have the most beneficial effects on fat metabolism and fat accumulation.

Specific Aim 2: To determine how osteoporosis treatments affect OVX-induced fat accumulation and metabolism.

Changes in fat metabolism during ovariectomy will be examined through the determination of tissue mass, and measurements of liver and serum triglyceride and free fatty acid concentrations as well as leptin and IGF-1 serum concentrations. Sprague Dawleys rats will be sacrificed at 6, 8 and 12 months of age to determine changes in fat due to age, ovariectomy and short (2 month) and long term (6 month) osteoporosis drug intervention, including alendronate, parathyroid hormone and sodium fluoride at various doses.

Hypothesis 3: We hypothesize that osteoporosis treatments will normalize the positive relationship of bone mass to body mass that is perturbed due to ovariectomy. We hypothesize that measures of bone quality will be negatively associated to fat content and osteoporosis treatments will strengthen this association.

Specific Aim 3: To determine and correlate bone quality, quantity, body mass and fat content as well as measures of fat metabolism after ovariectomy and during drug intervention.

Animal mass monitoring, *in vivo* and *ex vivo* μCT, determination of tissue weights and measurements of fat metabolism will be used to correlate changes in bone morphology and quality to changes in adiposity and tissue fat accumulation in order to determine if there is a positive bone-mass relationship as well as a negative bone quality to fat relationship due to age, ovariectomy and short (2 month) and long term (6 month) osteoporosis drug intervention, including alendronate, parathyroid hormone and sodium fluoride at various doses.

CHAPTER 2

BODY COMPOSITION CHANGES DURING OVARIECTOMY AND IS IMPROVED WITH DRUG INTERVENTIONS

2.1 ABSTRACT

Post-menopausal osteoporosis is associated with bone loss as well as increases in body mass and abdominal adiposity, factors that can pose a secondary risk to skeletal health. Drugs such as alendronate (ALN), parathyroid hormone (PTH) or sodium fluoride (NaF) target bone loss but their effects on body mass and abdominal fat accumulation are largely unknown. To this end, we subjected OVX rats to short-term (2 months) and long-term (6 months) treatments of different doses of ALN, PTH and NaF and analyzed body weight, vertebral bone, and abdominal fat volume. Six-month old Sprague-Dawley rats were assigned to age-matched controls, untreated OVX, OVX treated with high (H), medium (M), or low (L) doses of hPTH (60, 15, or 0.3μg/kg/d), or OVX treated with H, M, or L-ALN (100, 10, or 1μg/kg/2xwk) or OVX treated with H or L-NaF (500ppm or 100ppm in drinking water). Rats were sacrificed at 6, 8, and 12 months of age (n=10/group/age). All 12 month animals were scanned via *in vivo* μCT at 6, 8 and 12 months of age to determine longitudinal changes in bone volume and apparent mineral density as well as abdominal fat accumulation. After sacrifice, L-4 vertebrae were scanned via *ex vivo* μCT to determine differences in trabecular microarchitecture.

Body mass and fat accumulation was strongly affected by age. Age-matched controls gained 12.7% more weight throughout the course of the study than OVX controls but weighed 10% less, while treated animals gained 28.1% less weight than OVX controls and weighed 4.9% less at 12 months of age. There were no differences between the group's fat content within any time point except at 12 months of age, H-ALN treatment had 37.8% less subcutaneous fat than OVX controls. ($p<0.01$)

At 8 months, H-, M- and L-ALN as well as H- and M-PTH showed higher vertebral bone apparent density (*in vivo* μCT) than OVX controls.($p<0.05$). H-PTH showed higher bone volume fraction and both H- and M-PTH had higher trabecular thickness (*ex vivo* μCT) than OVX controls.($p<0.05$) At 12 months and compared to OVX controls, apparent vertebral density (*in vivo* μCT), trabecular number and trabecular

apparent density (*ex vivo* μCT) remained significantly higher in H-, M-, and L-ALN, H-, and M-PTH groups as well as H-NaF, while trabecular spacing was decreased.($p<0.05$) These data demonstrate that treatment with moderate to high doses of ALN, PTH and NaF can prevent deterioration of bone morphology and indices of bone quality caused by ovariectomy to values similar to age-matched controls. Treatment also had an effect on adiposity and slowed the rate of weight gain throughout the course of the study.

2.2 INTRODUCTION

Aging alters body composition by inducing weight gain, fat accumulation and reducing lean body mass (Kyle, 2001,Garthwaite, 1986). During menopause, women experience a drastic decrease in circulating estrogen levels which can exacerbate the age-related body compositional changes (Poehlman 1995, Gallhager, 1987, Goodpaster, 2005, Hughes, 2004, Tchernoff, 2000, Sorenson, 2001). One of the most serious consequences of menopause is severe decreases in bone quantity and quality, leading to increased risk of skeletal fracture. (Lemieux,2003, Uusi-Rasi 2009). Bone loss associated with menopause is called post-menopausal osteoporosis and is currently treated with pharmaceutical interventions such as anti-catabolic drugs (i.e. alendronate), or anabolic drugs (i.e. PTH). The effectiveness of pharmaceuticals on bone health has been well documented but there has been far less research done on drug effects on body mass and fat accumulation.

Bone density and trabecular bone volume have been shown to decrease linearly with age, starting sometime after the age of 25 to 30. (Marcus, 1983, Hansen, 1986) In a study on pre- and post-menopausal women the findings suggest that post-menopausal related changes on bone volume and density were 20% greater than the reductions seen as a function of age. The loss acquired in the first four years of menopause was similar to the total bone loss over 25 years of normal aging (Gallagher, 1987). Since bone loss is so significant after the onset of menopause it is usually treated with pharmacological interventions.

Treatments for osteoporosis target signaling pathways that block bone from resorbing (i.e. anti-catabolic) or promote bone formation (i.e. anabolic). Because these drugs target different pathways there are differences in bone quality and variations in

trabecular architecture (Banhamou, 2007). Alendronate and parathyroid hormone have both been used clinically to prevent bone loss (ALN) or reverse the loss (PTH). Bone mineral density increased in post-menopausal women during both treatments, while incidence of skeletal fractures decreased (Black, 2000, Lindsay, 2007, Neer, 2001, Recker 2005). The effects of these drugs on body composition including body mass and fat accumulation are widely unknown.

Age-related changes in lean mass and fat mass are associated with an increase in sedentary life style that results in a change in energy intake verses energy needs (Kyle, 2001). Age has been shown to cause causes a steady increase in trunk and appendicular fat accumulation throughout adulthood until 74 years of age in women (Kyle, 2001). In elderly male and female patients there is an increase in abdominal fat and waist circumference as compared to their healthy young counterparts (Kelley, 2000). There is also an increase in tissue fat accumulation within the bone marrow, muscle and the liver that is associated with aging (Sepe, 2010).

Using the ovariectomized rat model for osteoporosis, we hypothesized that body composition would be improved during alendronate, parathyroid hormone and sodium fluoride treatments. Indices of bone quantity and quality would be improved compared to OVX controls, and body mass and fat accumulation would be reduced during treatment. Long term, high dose treatment would have a greater effect on body composition than short term, low dose treatment.

2.3 MATERIALS AND METHODS

Experimental Design

Adult (5 months old) Sprague Dawley rats were ovariectomized and randomized into healthy age matched controls, ovariectomized controls or ovariectomized drug treated groups (n=10 per group) for short term (2 months) and long term (6 months) treatment duration. Drug treatments included alendronate at three doses: high (2 mg/kg), medium (100 µg/kg) and low (10 µg/kg); parathyroid hormone at three doses: high (75 µg/kg), medium (15 µg/kg) and low (0.3 µg/kg); and sodium fluoride at two doses: high (500 ppm) and low (100 ppm). Treatment dose was determined based on previous literature for the clinically relevant dose (low), the maximum tolerable dose without known evidence of cytotoxicity (high) and a moderate dose that fell within the two limits

(medium). Treatments began at six months of age. All rats were individually housed in standard cages and allowed free access to standard rodent chow and tap water. Weights for all animals were recorded weekly. All procedures were reviewed and approved by the Institutional Animals Care and Use Committee at the State University of New York at Stony Brook.

Animal Mass Monitoring

Animals were weighed weekly throughout the study to monitor growth rates Average group values were plotted in a line graph to observe rate of gain as well as in a bar graph to demonstrate average differences between groups at 6, 8 and 12 months of age.

In vivo Micro Computed Tomography (microCT)

All animals from the 12 mo time point were anesthetized with isofluorane and scanned by micro-computed tomography at 6, 8 and 12 months of age. (VivaCT 75, Scanco Medical Inc., SUI 45kV, 133 uA, 300-ms integration time, 512x512 pixel matrix) The abdomen of the animal was scanned from the pelvic region to the rib cage transversely at an isotropic voxel size of 156 micron. The abdominal volume of interest (VOI) was chosen between the proximal end of the L1 vertebra and the distal end of the L4 vertebra, using a microCT scout view. (Fig. 3) An automated script was used to analyze each scan, this provided longitudinal changes in individual animal's visceral and subcutaneous fat content, vertebral bone volume, and vertebral bone apparent mineral density (Lublinksi, 2009).

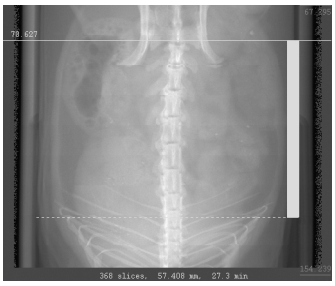

Figure 3. A representative scout view image from viva CT 75 showing the abdomen of a rat. The pelvis to the ribs are selected as the region of interest for scanning.

Vertebral Bone Determination

Total bone volume and apparent mineral density of the L1 to L4 vertebral region were analyzed for each animal at 6, 8 and 12 months of age. Bone tissue was segmented from soft tissue using thresholding. The defined edge of bone verses non-bone creates a double peak of gray scale intensities. A Gaussian distribution curve for the low peak with an associated average pixel value for soft tissue density and a Gaussian distribution curve for the high peak with an associated average pixel value for bone density. The standard

deviations of each peak are determined to find the midpoint between the two peaks in order to obtain the appropriate "threshold value." The large difference in density between hard and soft tissue makes it possible to separate bone from soft tissue using this method.

Apparent mineral density was determined by finding the average pixel intensity throughout the entire bone region with high pixel intensities associated with bone tissue. Higher density tissue correlates to brighter pixel values. A more porous bone will have larger regions of low pixel densities leading to decreased overall apparent mineral density. The scans were not performed at a high enough resolution to detect trabecular architecture; the output is therefore not considered bone mineral density but apparent mineral based on the average density within the entire volume of vertebral bone (including cortical bone).

Subcutaneous and Visceral Fat Determination

Total fat volume, visceral fat volume and subcutaneous fat volume was determined for each animal at 6, 8 and 12 months of age. Visceral and subcutaneous fat content were determined using an automated algorithm based on an automated algorithm (Lublinski, 2009). This method separates fat volume based on tissue density thresholding. The separation of visceral and subcutaneous fat content utilizes the barrier between tissue layers created by the thin muscular wall of the abdomen. Total fat content and visceral fat content is determined and the subcutaneous fat content is calculated by subtracting visceral fat from total fat volumes.

Ex vivo Micro Computed Tomography (microCT)

The L-4 vertebra was extracted from the spine of each animal and the soft tissue was removed. Samples were mounted in foam holders, secured into a microCT sample holder and immersed in 70% ethanol. All samples were scanned with the desktop μCT at 36 μm resolution with an integration time of 300 ms, energy of 55kV and intensity of 145 μA. The threshold value was set to 305. Vertebral bodies were analyzed through contour drawing around trabecular bone, separating it from the cortical shell. Regions of analysis were selected using the growth plates of the proximal and distal ends of the vertebra as land marks (Lublinski, 2007). The structural architecture of trabecular bone was

determined. Outputs include bone volume fraction, trabecular number, thickness and spacing, connectivity density, as well as tissue and apparent mineral density.

Statistical Analysis

All values are presented as group mean + standard deviation. At the 6 month time point, a Student t-test was performed to determine statistical significance between the two groups: baseline controls and ovariectomy controls. For 8 and 12 month time points, statistical significance was computed by performing a One-Way ANOVA followed by a Tukey post-hoc test when ANOVA detected a difference. Significant differences between groups were reported with their associated p-values.

A Two-way ANOVA was conducted to determine effects caused by both age and treatment and the interaction between each parameter.

2.4 RESULTS

Animal Mass Monitoring

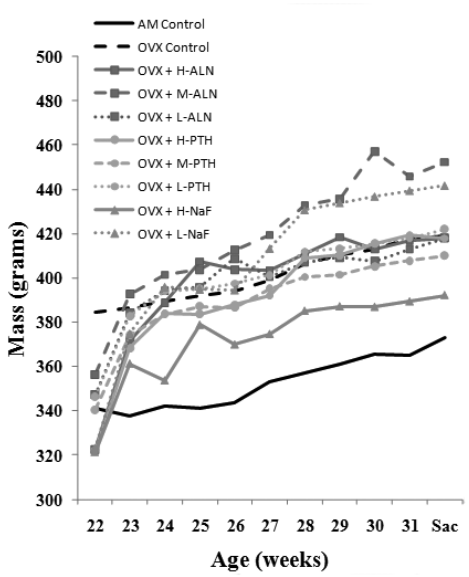

Average animal group weights for the 8 month treatment samples were not significantly different from each other. The rate of gain was similar for all treatment groups. At 8 months of age, AM control animals were 13.8% smaller than OVX controls but these differences were not significant. At 8 months, OVX + H-NaF were 11.8% lighter than OVX controls. (Fig. 4)

Figure 4. A line graph showing weekly average group body mass from 22 weeks to 32 weeks of age for age matched (AM) control, ovariectomy (OVX) control, OVX with high dose alendronate (ALN) - (OVX + H-ALN), OVX with medium ALN (OVX + M-ALN), OVX with low ALN (OVX + L-ALN), OVX with high parathyroid hormone (PTH) - (OVX + H-PTH), OVX with medium PTH (OVX + M-PTH), OVX with low PTH (OVX + L-PTH), OVX with high sodium fluoride (NaF) - (OVX + H-NaF) and OVX with low NaF (OVX + L-NaF).

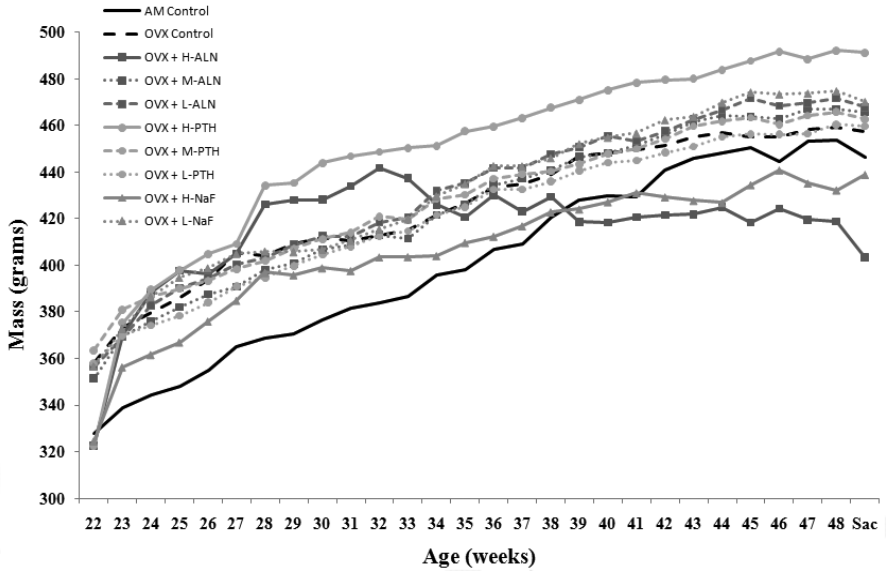

Figure 5. A line graph showing weekly average group body mass from 22 weeks to 49 weeks of age for age matched (AM) control, ovariectomy (OVX) control, OVX with high dose alendronate (ALN) - (OVX + H-ALN), OVX with medium ALN (OVX + M-ALN), OVX with low ALN (OVX + L-ALN), OVX with high parathyroid hormone(PTH) - (OVX + H-PTH), OVX with medium PTH (OVX + M-PTH), OVX with low PTH (OVX + L-PTH), OVX with high sodium fluoride (NaF) - (OVX + H-NaF) and OVX with low NaF (OVX + L-NaF).

Average animal group weights for the 12 month treatment samples were not significantly different. AM controls were 10% smaller than OVX controls. The rate of gain was similar for all treatment groups however the rate of gain for OVX + H-ALN and OVX + H-NaF slowed during the last two months of treatment. AM control animals weighed less than all treatment groups until 38 weeks but were higher than OVX + H-ALN and OVX + H- NaF from 38 weeks until the end of the study at 49 weeks. (Fig. 5)

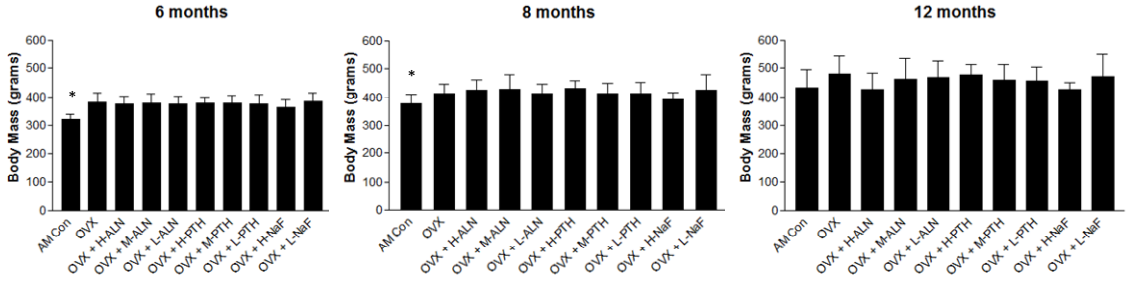

Figure 6. Average group body mass at A.) 6, B.) 8 and C.) 12 months of age for age matched controls (AM con), ovariectomy controls (OVX), OVX with high dose alendronate (ALN) treatment (OVX + H-ALN), OVX with medium ALN treatment (OVX + M-ALN), OVX with low ALN treatment (OVX + L-ALN), OVX with high parathyroid hormone (PTH) treatment (OVX + H-PTH), OVX with medium PTH treatment (OVX + M-PTH), OVX with low PTH treatment (OVX + L-PTH), OVX with high sodium fluoride (NaF) treatment (OVX + H-NaF) and OVX with low NaF treatment (OVX + L-NaF). Values are reported as group average mass + SD. The data represent all animals within a group within the study at each given point. (ANOVA) *p<0.01

At 6 months of age, AM controls were 18.9% lighter than OVX controls. ($p<0.01$) There were no significant differences between any OVX treatment groups compared to OVX controls. At 8 months of age, AM controls were 13.6% lighter than OVX controls. ($p<0.05$) There were no differences between any OVX treatment groups compared to OVX controls. At 12 months of age AM were 6% lighter but this difference was not significant. (Fig. 6)

Age Related Changes in Body Mass

Changes in body mass were strongly influenced by age. Weight gains from 6 to 8 to 12 months within groups were all significant, except from 6 to 8 months in OVX controls. ($p<0.01$) All groups at 6 months were significantly lower than all groups at 12 months. From 6 to 8 months and then 8 to 12 months: AM animals gained 15.2 and 12.5%, OVX gained 8.3 and 13.4% and treated animals gained 9.6 and 8.1%, respectively.

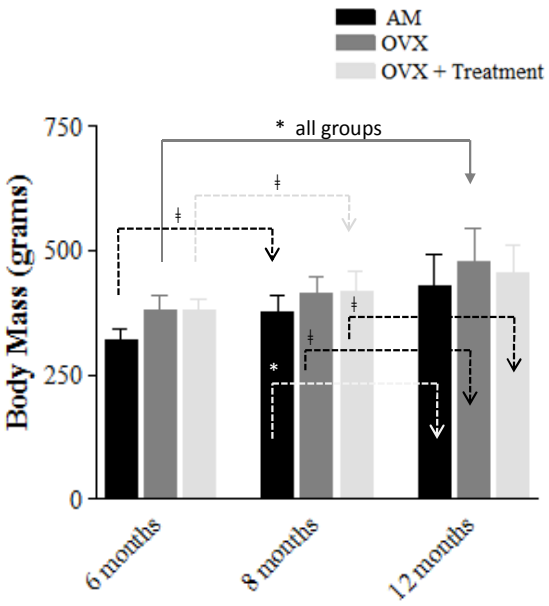

Figure 7. Body mass at 6, 8 and 12 months for age matched controls (black - AM) OVX controls (dark gray - OVX) and the combined data set of all ovariectomized animals that received treatment – (light gray - OVX + Treatment). Data is represented as mean + SD, arrows denote where the differences were seen. (ANOVA) ǂ p<0.001 *p<0.01

At six months of age, AM controls were 18.9% lighter than OVX controls ($p<0.001$). By 8 months, AM animals were 13.6% lighter ($p<0.001$) and by 12 months AM animals were only 6.0% lighter than OVX controls. Throughout the study, AM controls gained 12.7% more weight than OVX controls while the treated animals gained 28.1% less weight than OVX controls. (Fig. 7)

In vivo Vertebral Bone Analysis

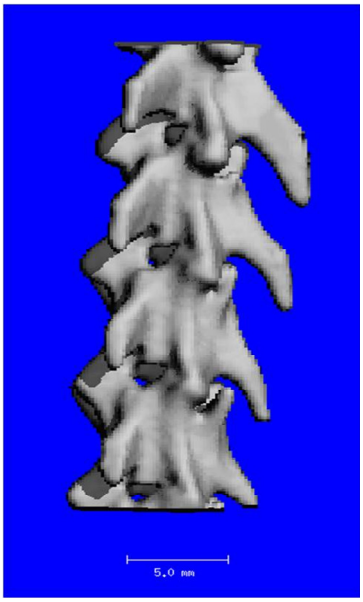

The lumbar vertebrae were analyzed for all animals at 6, 8 and 12 months of age from the 12 month treatment groups. Total bone volume and apparent mineral density was evaluated and longitudinal changes for each animal were calculated. Bone was separated from the abdominal cavity by thresholding based on the high density values of bone compared to soft tissue. (Fig. 8)

Figure 8. A µCT 3-D reconstruction, representative image of the vertebral bone after an animal was scanned using the *in vivo* µCT and analyzed using a separation script.

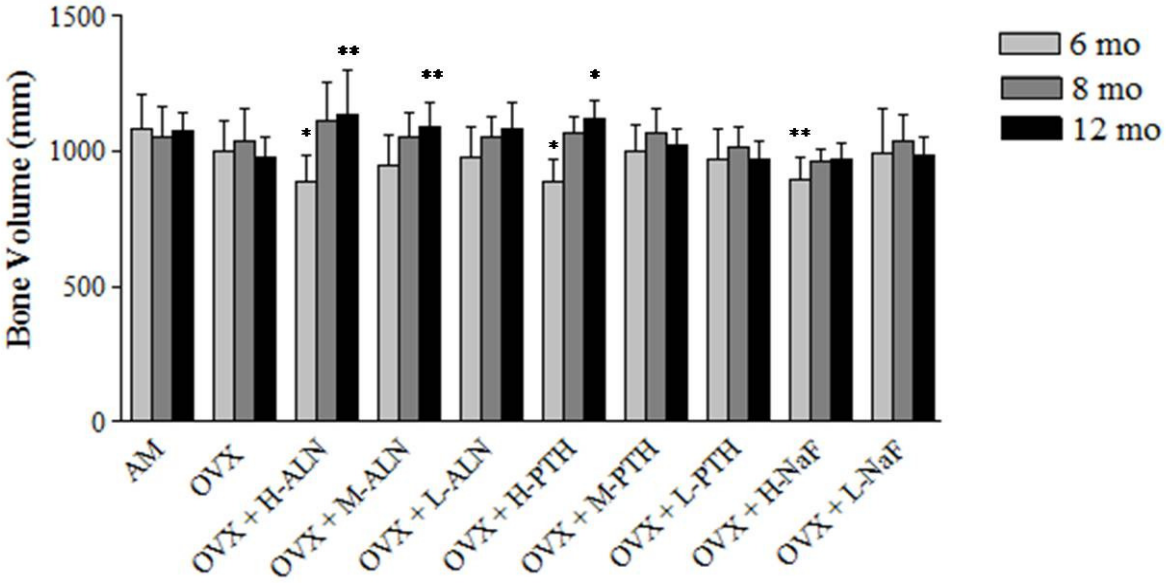

Figure 9. Bone Volume was determined via *in vivo* microCT at 156 um resolution for all animals from the 12 month time group. Animals were scanned at 6, 8 and 12 months with *in vivo* microCT. Data is represented as means + SD for age matched controls (AM), ovariectomy controls (OVX), OVX with high dose alendronate (ALN) treatment (OVX + H-ALN), OVX with medium ALN treatment (OVX + M-ALN), OVX with low ALN treatment (OVX + L-ALN), OVX with high parathyroid hormone (PTH) treatment (OVX + H-PTH), OVX with medium PTH treatment (OVX + M-PTH), OVX with low PTH treatment (OVX + L-PTH), OVX with high sodium fluoride (NaF) treatment (OVX + H-NaF) and OVX with low NaF treatment (OVX + L-NaF). (ANOVA) *p<0.01 **p<0.05

Longitudinal bone volume was increased at 8 months and even greater at 12 months in OVX + H, M and L-ALN and H-PTH treated animals. H-NaF gained at 8 months and maintained this gain until 12 months of age. M and L-PTH as well as L-NaF increased bone volume until 8 months but had decreased bone volume from 8 to 12 months. At six months of age, high dose animals had less bone volume than AM controls. ($p<0.01$) At 12 months of age H and M-ALN and H-PTH all had greater total bone volume than OVX controls. ($p<0.05$) (Fig. 9)

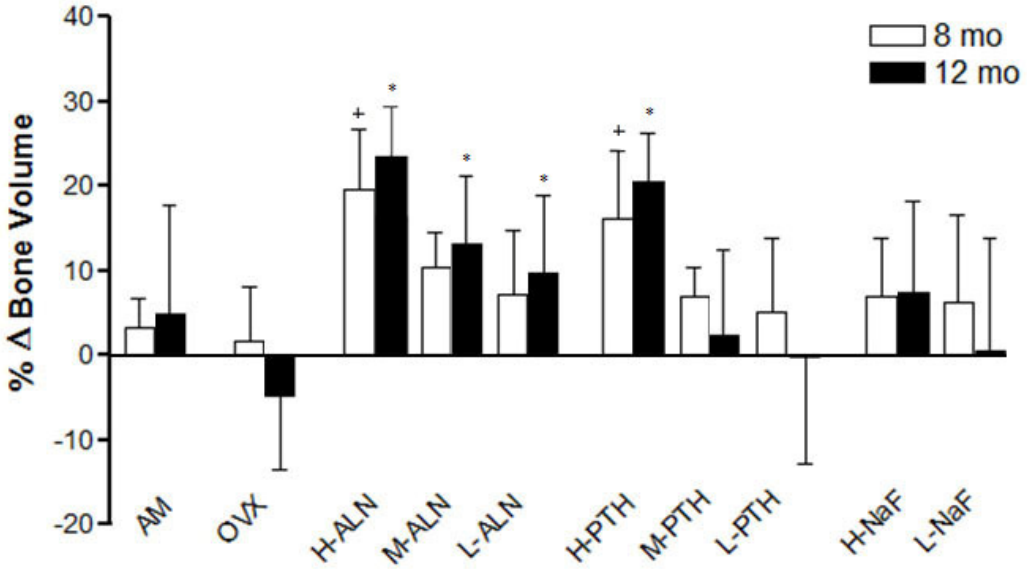

Figure 10. % Change in bone volume from 6 to 8 months (white) and from 6 to 12 months (black) were determined via *in vivo* microCT of L1-L5 vertebrae at 156 um resolution for all animals from the 12 month time point. Animals were scanned at 6, 8 and 12 months with *in vivo* microCT. Data is represented as means + SD for age matched controls (AM), ovariectomy controls (OVX), OVX with high dose alendronate (ALN) treatment (OVX + H-ALN), OVX with medium ALN treatment (OVX + M-ALN), OVX with low ALN treatment (OVX + L-ALN), OVX with high parathyroid hormone (PTH) treatment (OVX + H-PTH), OVX with medium PTH treatment (OVX + M-PTH), OVX with low PTH treatment (OVX + L-PTH), OVX with high sodium fluoride (NaF) treatment (OVX + H-NaF) and OVX with low NaF treatment (OVX + L-NaF). (ANOVA) +p<0.01 - 8 month time point, * p<0.01 - 12 month time point

Bone volume increased by 4.78% in the AM controls throughout the study. Bone volume was decreased by 4.76% at 12 months of age in the ovariectomized rat. ALN treatment increased bone volume by 21.81, 13.13 and 9.75% for high medium and low doses at 12 months, respectively. PTH treatment increased bone volume by 20.56 and 2.57% in high and medium doses. High dose sodium fluoride water increased bone volume by 7.34%. Low dose PTH injections and sodium fluoride water showed little change at -0.29 and 0.37%, respectively at 12 months of age. (Fig. 10)

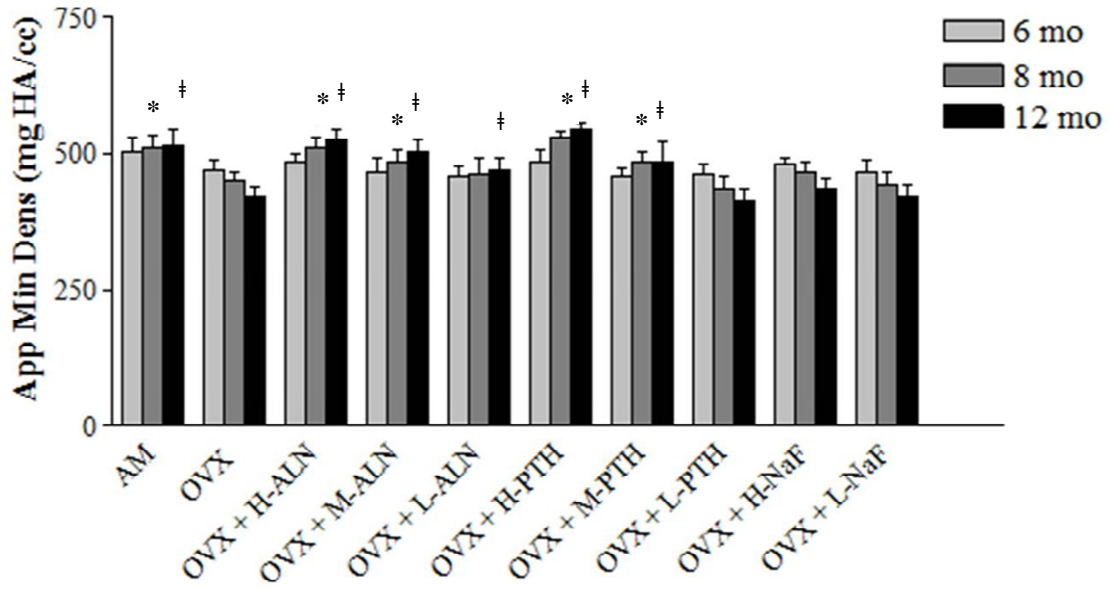

Figure 11. Apparent mineral density was determined via *in vivo* microCT of L1-L5 vertebrae at 156 um resolution for all animals from the 12 month time point. Animals were scanned at 6, 8 and 12 months with *in vivo* microCT. Data is represented as means + SD for age matched controls (AM), ovariectomy controls (OVX), OVX with high dose alendronate (ALN) treatment (OVX + H-ALN), OVX with medium ALN treatment (OVX + M-ALN), OVX with low ALN treatment (OVX + L-ALN), OVX with high parathyroid hormone (PTH) treatment (OVX + H-PTH), OVX with medium PTH treatment (OVX + M-PTH), OVX with low PTH treatment (OVX + L-PTH), OVX with high sodium fluoride (NaF) treatment (OVX + H-NaF) and OVX with low NaF treatment (OVX + L-NaF). (ANOVA) *p<0.01- 8 month time point, ǂ p<0.001- 12 month time point.

Apparent mineral density increased with age in AM controls, H, M and L-ALN, as well as H and M-PTH. Apparent mineral density was decreased by 12 months in OVX, L-PTH and H and L-NaF groups. At 8 months of age, apparent mineral density was significantly higher than OVX controls in AM, H and M-ALN and H and M-PTH treated animals and it remained higher at 12 months of age. ($p<0.001$) (Fig. 11)

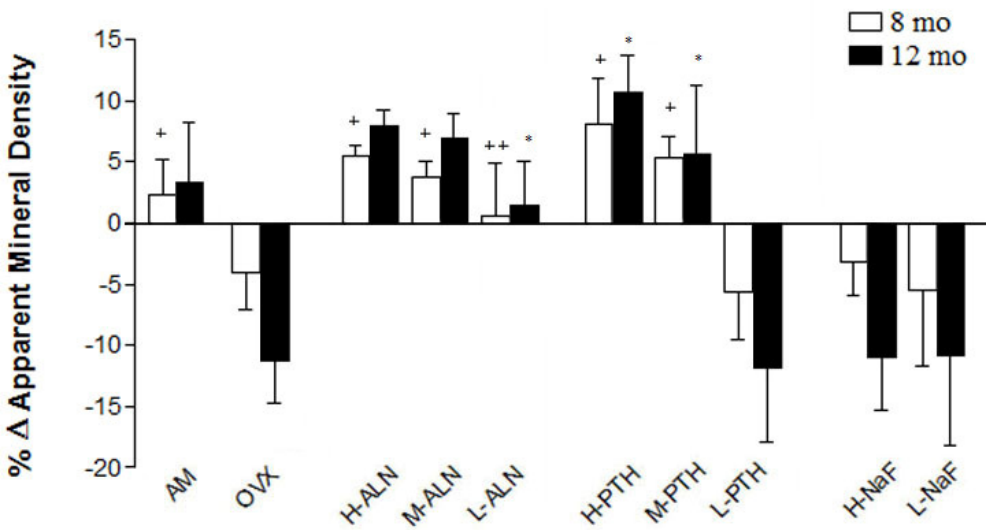

Figure 12. %Change in apparent mineral density from 6 to 8 months (white) and from 6 to 12 months (black) was determined via in vivo microCT of L1-L5 vertebrae at 156 um resolution for all animals from the 12 month time group. Animals were scanned at 6, 8 and 12 months with in vivo microCT. Data is represented as means + SD for age matched controls (AM), ovariectomy controls (OVX), OVX with high dose alendronate (ALN) treatment (OVX + H-ALN), OVX with medium ALN treatment (OVX + M-ALN), OVX with low ALN treatment (OVX + L-ALN), OVX with high parathyroid hormone (PTH) treatment (OVX + H-PTH), OVX with medium PTH treatment (OVX + M-PTH), OVX with low PTH treatment (OVX + L-PTH), OVX with high sodium fluoride (NaF) treatment (OVX + H-NaF) and OVX with low NaF treatment (OVX + L-NaF). (ANOVA) +p<0.01 - 8 mo time point. ++p<0.05 – 8 mo. * p<0.01 - 12 mo time point.

Apparent bone mineral density increased 3.23% in the AM control throughout the study but decreased by 11.24% in the ovariectomized rat. ALN treatment increased apparent mineral density by 7.94, 6.9 and 1.46% for high medium and low doses at 12 months of age, respectively. PTH treatment increased bone volume by 10.68 and 5.6% in high and medium doses. Low dose PTH treatment as well as high and low dose sodium fluoride water did not prevent the decrease in apparent mineral density, caused by OVX, with net losses of 11.92, 10.95 and 10.87%, respectively. (Fig. 12)

Subcutaneous and Visceral Fat Analysis

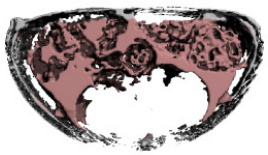

Figure 13. A representative microCT 3D reconstruction image of the visceral (red) and subcutaneous fat (white).

A representative microCT 3D reconstruction image shows the separation of the total fat into subcutaneous (white) and visceral (red) fat compartments using an automated script. From this, total and visceral fat values were determined and reported and subcutaneous fat content is calculated by subtracting the visceral fat volume from total fat volume. (Fig. 13)

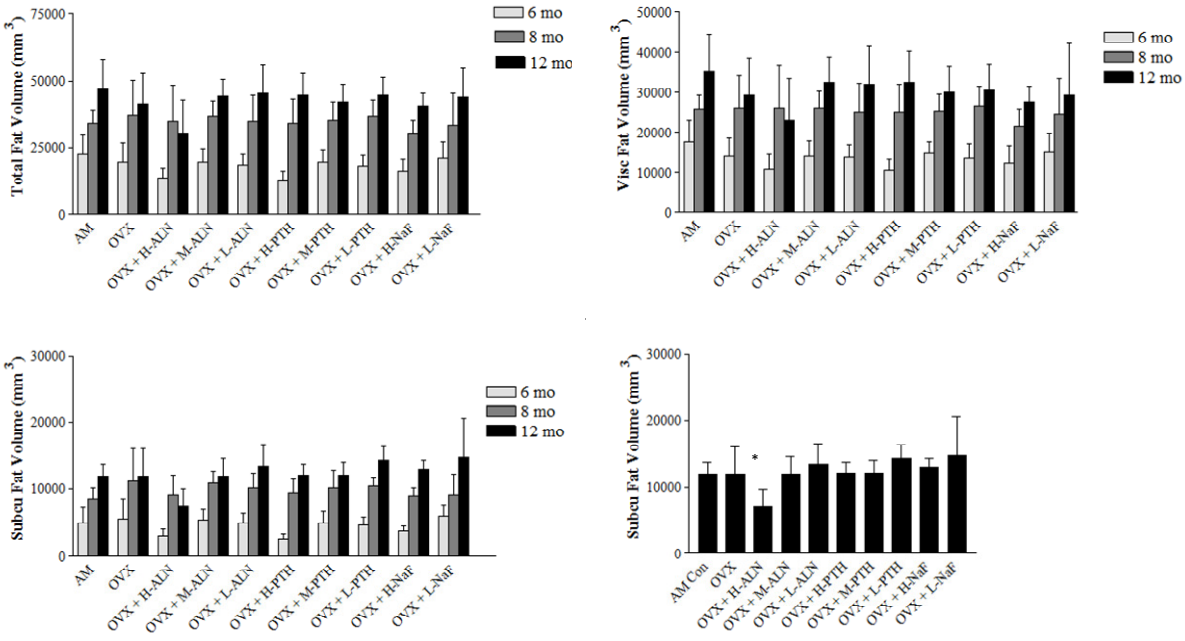

Figure 14. Animals were scanned at 6, 8 and 12 months with *in vivo* microCT. A.)Total fat volume, B.) visceral fat volume, C.) subcutaneous fat volume at 6, 8 and 12 months of age and D.) subcutaneous fat volume at 12 months. Data is represented as means + SD for age matched controls (AM), ovariectomy controls (OVX), OVX with high dose alendronate (ALN) treatment (OVX + H-ALN), OVX with medium ALN treatment (OVX + M-ALN), OVX with low ALN treatment (OVX + L-ALN), OVX with high parathyroid hormone (PTH) treatment (OVX + H-PTH), OVX with medium PTH treatment (OVX + M-PTH), OVX with low PTH treatment (OVX + L-PTH), OVX with high sodium fluoride (NaF) treatment (OVX + H-NaF) and OVX with low NaF treatment (OVX + L-NaF). (ANOVA) *p<0.01

Abdominal fat accumulation was strongly influenced by age, 59.7% of the variance in total fat, 50.8% of the variance in subcutaneous and 57.4% of the variance of visceral fat was accounted for by changes of age. (Two-Way ANOVA) ($p<0.001$) Differences in treatment only accounted for 3-5% of the variance seen in fat content. ($p<0.05$)

There were no differences between groups at 6 or 8 months of age. By 12 months of age, H-ALN treated animals had 35.4% less total fat than AM controls, ($p<0.01$) and 37.8 % less subcutaneous fat than OVX controls. ($p<0.01$) (Fig. 14)

Age Related Changes in Total Fat Content

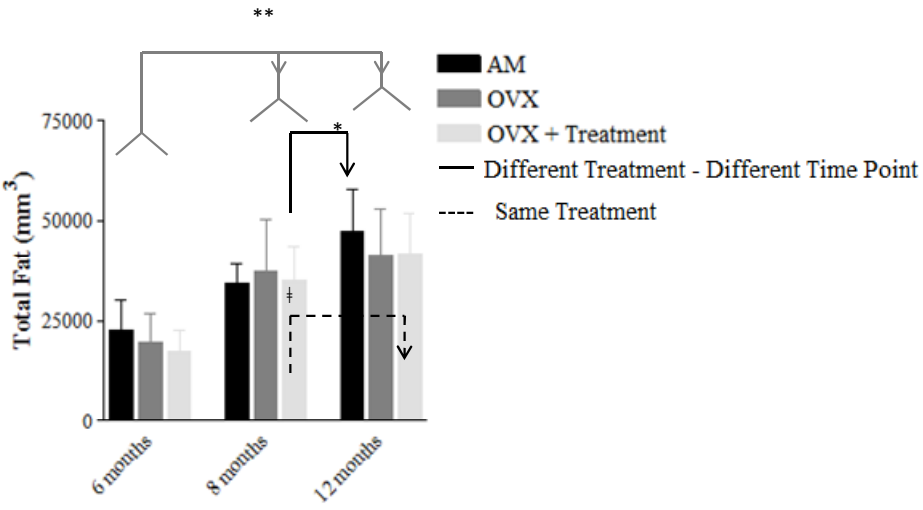

Figure 15. Fat volume at 6, 8 and 12 months for age matched controls (black-AM), ovariectomy controls (dark gray – OVX) and all high dose animals pooled (light gray – OVX + Treatment). Data is, represented as mean + SD. (ANOVA) *p<0.01,p<0.05**

Total fat volume increased as a function of age. At 6 months, all groups had 47.7% less fat than all groups at 8 months and 56.5% less fat than all groups at 12 months of age.($p<0.001$) The difference between fat volumes from 8 months to 12 months was 16.8%. ($p<0.01$) The treatment group had 35.8% less fat at 8 months compared to the total fat of AM controls at 12 months.($p<0.01$) (Fig. 15)

Ex vivo Vertebral Bone Analysis

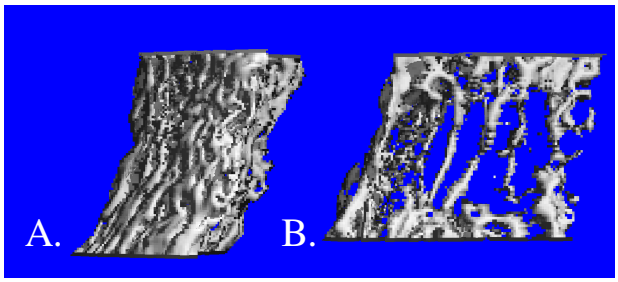

Figure 16. Representative bone images from *ex vivo* micro CT. A.) Healthy and B.) OVX rat trabecular bone from the L-4 vertebral body.

Changes in bone microarchitecture were determined through *ex vivo* microCT. This provided information on trabecular quantity, structure, and spatial distribution. Visual inspection of each 3-dimensional vertebral body analyzed by microCT demonstrates severe bone loss in the OVX rat compared to AM controls. (Fig. 16)

6 months

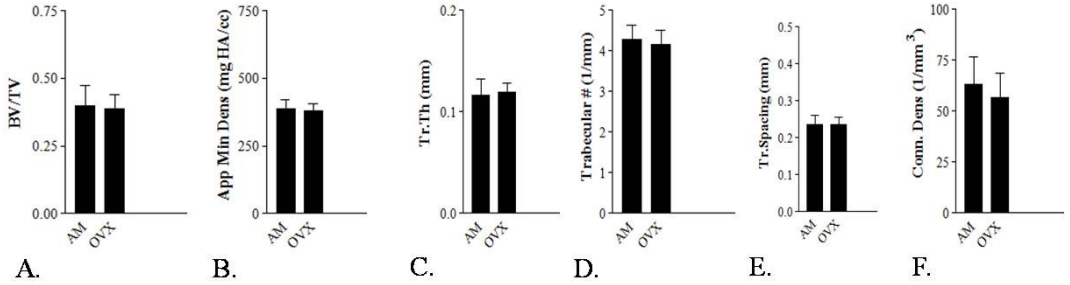

Figure 17. Micro architectural parameters of the L-4 vertebrae for animals at 6 months of age were determined via microCT. Microarchitecture is characterized by: A.) Bone volume fraction, B.) apparent mineral density C.) Trabecular thickness, D.) trabecular number, E.) trabecular spacing and F.) connectivity density. Data is represented as mean + S.D. for age matched (AM) and ovariectomy (OVX) control. (Student t-test)

At six months there were no differences in microarchitecture of bone tissue in baselines vs. ovariectomized rats. OVX showed slightly lower values in all parameters except trabecular spacing and trabecular thickness; however none of these differences were significant. This indicated that bone related drug affects shown in this study worked to prevent osteoporosis bone loss, as opposed to reversing the loss of bone which could have already occurred. (Fig. 17)

8 months

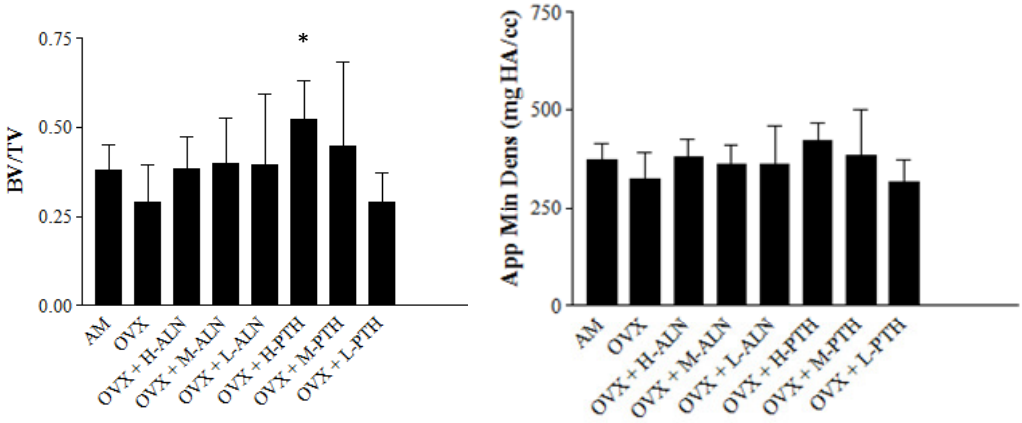

Figure 18. A.) Bone volume fraction and B.) apparent mineral density were determined for the trabecular region of the L-4 vertebral body at 8 months of age for age matched control (AM), ovariectomy control (OVX), OVX with high dose alendronate (ALN) treatment (OVX + H-ALN), OVX with medium ALN treatment (OVX + M-ALN), OVX with low ALN treatment (OVX + L-ALN), OVX with high parathyroid hormone (PTH) treatment (OVX + H-PTH), OVX with medium PTH treatment (OVX + M-PTH), OVX with low PTH treatment (OVX + L-PTH), OVX with high sodium fluoride (NaF) treatment (OVX + H-NaF) and OVX with low NaF treatment (OVX + L-NaF). (ANOVA) *p<0.01

At eight months of age, there were overall changes to bone volume fraction and apparent mineral density. OVX animals had lower bone volume fraction and density than all groups, except L-PTH. Trends suggest all treatments except low dose PTH were able to maintain bone volume fraction and bone mineral densities to values similar to age matched controls. OVX and L-PTH had reduced bone density and fraction at 8 months compared to age matched controls. H and M-PTH had slightly higher BV/TV values indicating the anabolic effects of these drugs. ALN groups were consistent to AM controls demonstrating the anti-catabolic effect of the drugs (Fig. 18)

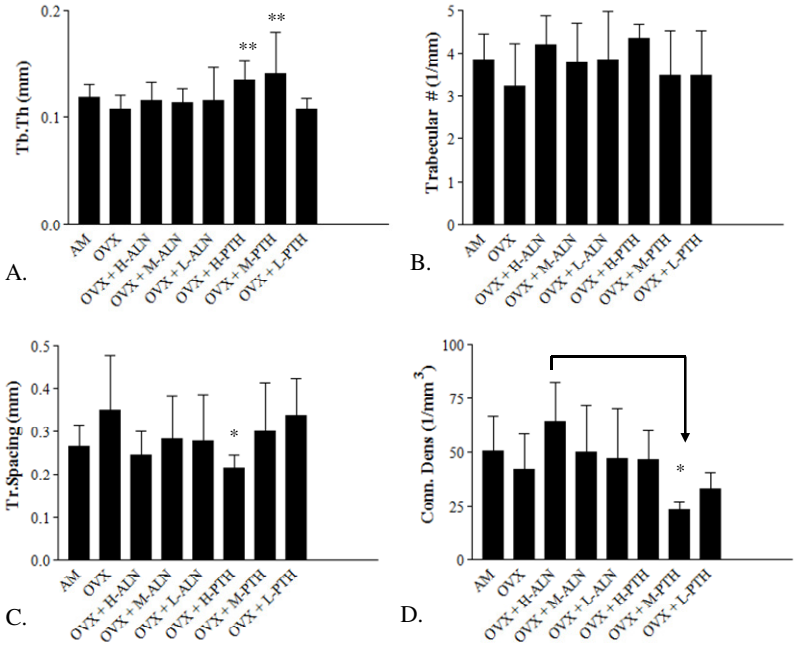

Figure 19. Microarchitectural parameters of the L-4 vertebrae for animals at 8 months of age were determined via microCT. Data is represented as group mean + SD. A.) Trabecular thickness, B.) trabecular number, C.) trabecular spacing and D.) connectivity density. Data is represented as age matched control (AM), ovariectomy control (OVX), OVX with high dose alendronate (ALN) treatment (OVX + H-ALN), OVX with medium ALN treatment (OVX + M-ALN), OVX with low ALN treatment (OVX + L-ALN), OVX with high parathyroid hormone (PTH) treatment (OVX + H-PTH), OVX with medium PTH treatment (OVX + M-PTH), OVX with low PTH treatment (OVX + L-PTH), OVX with high sodium fluoride (NaF) treatment (OVX + H-NaF) and OVX with low NaF treatment (OVX + L-NaF). (ANOVA) * p<0.001, **p<0.05

The microarchitecture of bone was maintained with osteoporosis treatments at 8 months. H and M-PTH treated rats had 31% and 25.3% thicker trabeculae than OVX controls. ($p<0.05$) H-PTH and H-ALN groups had the highest trabecular number indicating the dose dependent effect on trabecular architecture. Trabecular spacing was 23.8% greater in OVX animals compared to AM controls, but H-PTH had 38.2% greater

trabecular spacing than OVX controls. (p<0.01) Connectivity density was highest with H-ALN treatment was 63.4% higher than M-PTH treatment. (p<0.01) (Fig. 19)

12 months

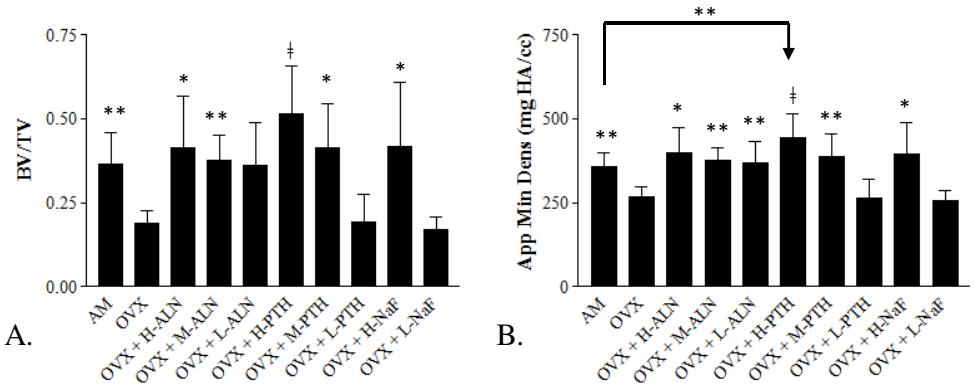

Figure 20. A.) Bone volume fraction and B.) apparent mineral density were determined for the trabecular region of the L-4 vertebral body at 12 months of age for age matched control (AM), ovariectomy control (OVX), OVX with high dose alendronate (ALN) treatment (OVX + H-ALN), OVX with medium ALN treatment (OVX + M-ALN), OVX with low ALN treatment (OVX + L-ALN), OVX with high parathyroid hormone (PTH) treatment (OVX + H-PTH), OVX with medium PTH treatment (OVX + M-PTH), OVX with low PTH treatment (OVX + L-PTH), OVX with high sodium fluoride (NaF) treatment (OVX + H-NaF) and OVX with low NaF treatment (OVX + L-NaF). (ANOVA) ǂp<0.001, *p<0.01, **p<0.05

By 12 months of age, bone volume fraction was reduced by 46.3% in OVX animals compared to AM controls. (p<0.05) L-PTH and L-NaF were unable to withstand the loss, with 45.8 and 52.2% less bone volume fraction than AM controls. (p<0.05) However, ALN, H and M-PTH and H-NaF was able to maintain or gain bone volume throughout 6 months of treatment. H-ALN, H-PTH and H-ALN had 54.5, 63.1 and 54.5% more bone than OVX controls. (p<0.01) There were no differences within ALN treatments, or within H and M PTH treatments.

Apparent mineral density was decreased by 34% in the OVX controls compared to AM controls. (p<0.05) Apparent mineral density was 49, 40.9 and 37.7% higher in H, M and L-ALN compared to OVX controls. (p<0.05) It was 66.1 and 45% higher with H and M-PTH and 47.9% higher with NaF treatment. (p<0.05) H-PTH had 24% greater apparent mineral density than AM controls. (p<0.05) (Fig. 20)

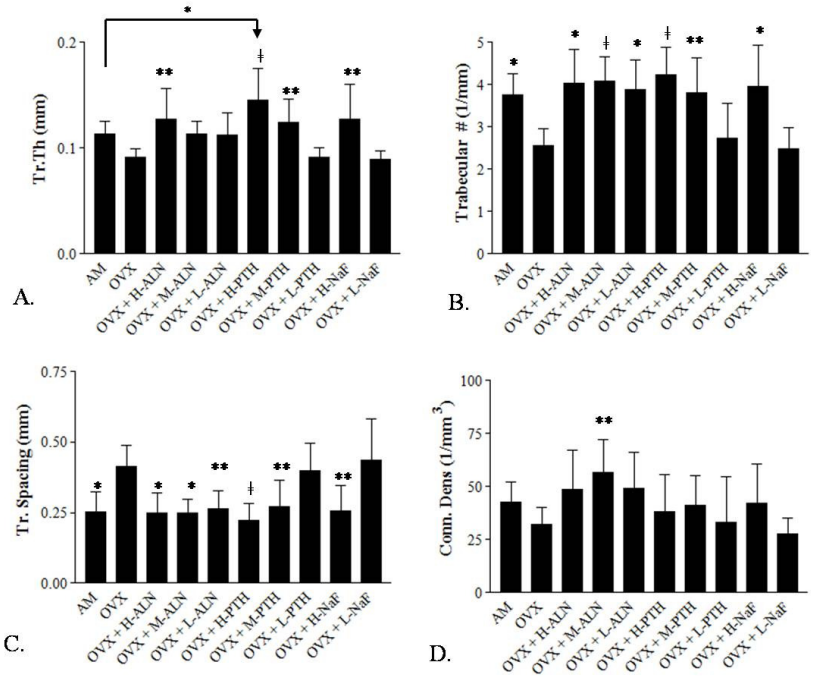

Figure 21. Microarchitectural parameters of the L-4 vertebrae for animals at 12 months of age were determined via microCT. Data is represented as group mean + SD. A.) Trabecular thickness, B.) trabecular number, C.) trabecular spacing and D.) connectivity density. Data is represented as age matched control (AM), ovariectomy control (OVX), OVX with high dose alendronate (ALN) treatment (OVX + H-ALN), OVX with medium ALN treatment (OVX + M-ALN), OVX with low ALN treatment (OVX + L-ALN), OVX with high parathyroid hormone (PTH) treatment (OVX + H-PTH), OVX with medium PTH treatment (OVX + M-PTH), OVX with low PTH treatment (OVX + L-PTH), OVX with high sodium fluoride (NaF) treatment (OVX + H-NaF) and OVX with low NaF treatment (OVX + L-NaF). (ANOVA) * p<0.001, *p<0.01, **p<0.05

Trabecular architecture was changed due to ovariectomy at 12 months of age. OVX resulted in a 46.9% decrease in trabecular number and a 38.5% increase in trabecular spacing compared to AM controls. ($p<0.01$) H-ALN, H-PTH and H-NaF had trabeculae 39.2, 59.4 and 39.9% thicker than to OVX controls. ($p<0.05$) Additionally, H-PTH trabeculae were 28.6% thicker than AM controls. ($p<0.01$) Trabecular number was higher in AM, H, M and L-ALN, H and M-PTH and H-NaF compared to OVX controls, ($p<0.05$) L-PTH and L-NaF were 27.1 and 34% lower than AM controls. ($p<0.05$) Trabecular spacing was increased in OVX, L-PTH and L-NaF groups.

Animals treated with anabolic drugs had the largest values for trabecular thickness; ALN treated animals had the greatest values for connectivity density. H, M and L-ALN were 51.5, 76.4 and 52.7% more connected than OVX controls, the difference between M-ALN and OVX was significant. ($p<0.05$) (Fig. 21)

Age Related Changes in Bone Parameters

Bone volume fraction did not decrease with age in healthy animals but it decreased in OVX. High dose treatment groups were pooled and compared as a function of age. 12 month OVX was significantly lower than all groups at all time points except 8 month OVX. But there is certainly a time dependent decrease shown in bone volume fraction during OVX. ($p<0.01$) All trabecular architecture data showed similar trends with differences between groups like those shown in BV/TV, indicating that microarchitecture does not deteriorate with age but does deteriorate after OVX when left untreated. This deterioration was prevented with osteoporosis drug intervention. (Fig. 22)

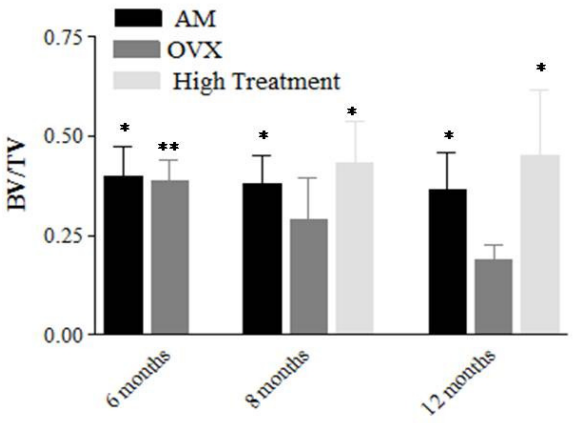

Figure 22. Bone volume fraction at 6, 8 and 12 months for age matched control (black-AM), ovariectomy control (dark gray – OVX) and all high dose treatments pooled (light gray – OVX + Treatment). Data is, represented as mean + SD. (ANOVA) *p<0.01,p<0.05**

There were no differences in tissue mineral density between groups at any time point. All animals of similar age were pooled and tissue mineral density was compared as a function of age. At 8 and 12 months of age, tissue samples were 3.9 and 4.5% more mineralized than at 6 months. ($p<0.01$, $p<0.001$) There was no significant increase in mineralization from 8 to 12 months. (Fig. 23)

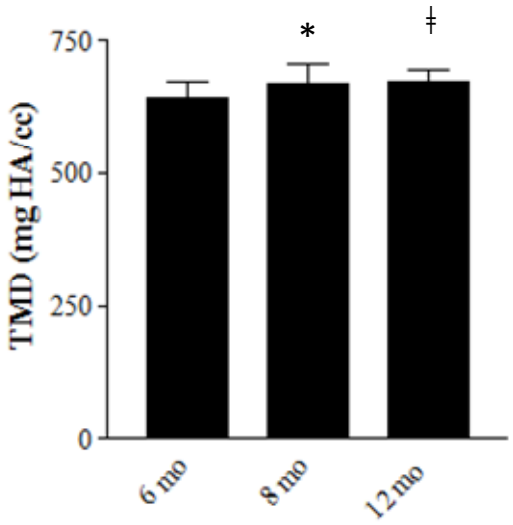

Figure 23. Tissue mineral density fraction at 6, 8 and 12 months for age for all data from each time point pooled. Data is, represented as age mean + SD. (ANOVA) ǂp<0.001,*p<0.01

2.5 DISCUSSION

Body composition is strongly affected by aging. It has been shown that body and fat mass increases as a function of age while lean tissue mass decreases (Kyle, 2001). Menopause related obesity is associated with increases in visceral fat accumulation, weight gain and deterioration of bone mass. Alendronate, parathyroid hormone and sodium fluoride are all methods of preventing post-menopausal bone loss but their effects on body composition and fat mass are largely unknown.

The time points chosen for age related analysis on body composition were not optimal for determining differences caused by treatment duration. At 8 months of age, differences between microarchitectural parameters were, in many instances, not significant. However, by 12 months of age, the desired affects were achieved and treatments proved to be effective at preventing the OVX related losses in bone. Extending the length of the study to 18 months of age for a total of 12 months of treatment would help to elucidate some of the important changes that occur with aging as well as due to dose, and treatment duration.

Age related changes in body composition were seen in this study such as weight gain, and fat accumulation. Ovariectomy increased body mass from 5 to 6 months of age compared to baseline controls. However, 6 months to 12 months of age, the AM controls had experienced larger weight gain due to aging than OVX controls. Similarly, increases in fat mass from 6 to 8 and from 8 to 12 months were greater in AM controls than in OVX controls. Osteoporosis drugs had slight effects on body mass and fat volume throughout the study; however, treatments did decrease the overall rate of weight and fat gain compared to OVX controls. The data suggest that there is a rapid change in body mass directly after ovariectomy, but natural aging from 6 to 12 months will induce increases in body mass and abdominal fat volume are inevitable regardless of ovariectomy. This idea can be supported by a study on the increase in weight gain seen in both male and female elderly populations demonstrating that the effects of aging are independent of estrogen withdrawal (Goodpaster, 2005).

The effects of OVX on visceral fat accumulation were less pronounced than previously shown in published literature. (Choi, 2009, Shinoda, 2002) Total fat mass, as observed through *in vivo* μCT, showed a decrease with H-ALN treatment at 12 months of

age, indicating that longer treatment duration could attenuate some of the changes that we might not see after only 6 months. Decreases in fat pad masses were not seen until 12 months, but data indicated that all treatments were able to decrease fat accumulation in the OVX rat.

Reduction in estrogen can result in severe decreases in bone quantity and quality. This leads to increased risk of skeletal fractures (Lemieux, 2003, Uusi-Rasi 2009). Drug treatments were able to prevent the loss in bone mass and microarchitecture in moderate to high doses. There were no differences in tissue mineral density after 6 months of treatment. We expected that alendronate treated animals would have an increase in tissue mineral density during extended treatment due to the prevention of bone turnover compared to age matched controls due to the prevention of resorption. Aged tissue has been shown to increase its mineralization. (Burr, 2003a) This could result in decreased tissue material properties that we might not be able to detect differences after only six months of treatment (Burr, 2003b). We can also expect to see degradation in material properties with sodium fluoride which would likely worsen with treatment duration (Sogaard, 1994, Riggs, 1980, 1982, Lindsay, 1990).

Bone volume, density and trabecular microarchitecture were all severely affected by ovariectomy. Osteoporosis drugs were able to prevent further bone loss and in most cases increase total bone volume. High dose treatments were most effective at increasing bone volume fraction, density and parameters of microarchitecture. Significant increases in trabecular thickness during H- and M-PTH treatment indicate their strong anabolic effect on bone formation. Connectivity density increased during ALN treatment indicating its effectiveness at decreasing bone resorption. These indices of bone morphology are evidence that treatments worked as intended. Similar changes in trabecular morphology were seen with μCT analysis during Teriparitide and alendronate treatments. (Benhamou, 2007)

L-PTH and L-NaF were unable to overpower the effects of estrogen withdrawal and could not prevent deterioration of bone tissue during six months of treatment, the effects were similar to those seen in OVX controls. *In vivo* analysis demonstrated that there was an overall decrease in apparent mineral density with H-NaF treatments. However the analysis of trabecular architecture, via *ex vivo* microCT showed apparent

mineral density increased during high dose NaF treatment. Sodium fluoride has been shown to be an excellent anabolic drug but produces tissue with reduced material properties. (Turner, Mosekilde) Others demonstrate the positive effects of sodium fluoride on trabecular architecture (Bonewald, 2008). The discrepancies seen between *in vivo* and *ex vivo* data can be attributed to a resolution issue from the *in vivo* microCT. Since the scans were conducted at 156um, it was unable to detect microarchitectural changes. Changes in mineralization could also be due to miscalculation of tissue surrounding the vertebral bodies, by including cartilage and other soft tissues, leading to a reduced apparent mineral density average value. The values reported from *ex vivo* μCT are more reliable because they represent changes specific to bone trabeculae.

Bone quantity and quality is reduced during osteoporosis. These deleterious changes can be improved through drug intervention to decrease the rate of resorption (alendronate) or increase the rate of formation (PTH and sodium fluoride). The effects of these drugs on body mass and abdominal fat volume were subtle but do represent some positive benefits osteoporosis drugs on adipogenic factors. Treatment response was dose and duration dependent. The greatest improvements in bone parameters were seen in high dose, long term treatments and improvements in body composition were strongly affected by treatment duration. Improving fat accumulation can help to alleviate the symptoms associated with bone loss and fat accumulation that occurs during and after menopause.

CHAPTER 3

OSTEOPOROSIS DRUGS NORMALIZE PARAMETERS OF FAT METABOLISM IN THE OVARIECTOMIZED RAT MODEL

3.1 ABSTRACT

Post-menopausal osteoporosis is associated with bone loss but menopause results in an increases tissue fat accumulation. Drugs such as alendronate (ALN), parathyroid hormone (PTH) or sodium fluoride (NaF) target bone loss but their effects on fat accumulation and metabolism are largely unknown. To this end, we subjected OVX rats to short-term (2 months) and long-term (6 months) treatments of different doses of ALN, PTH and NaF and analyzed abdominal fat pad weights, liver weight and brown fat weight as well as liver fatty acids, and serum leptin and IGF-I. Six-month old Sprague-Dawley rats were assigned to age-matched controls, untreated OVX, OVX treated with high (H), medium (M), or low (L) doses of hPTH (60, 15, or 0.3μg/kg/d), or OVX treated with H, M, or L-ALN (100, 10, or 1μg/kg/2xwk) or H or L-NaF (500ppm or 100ppm in drinking water). Rats were sacrificed at 6, 8, and 12mo of age (n=10/group/age).

At 8 months of age there were no differences between tissue weights, but by 12 months all treated animals had smaller fat pads than OVX controls, ($p<0.05$) and smaller livers, except H-PTH, than AM controls. ($p<0.01$) Liver esterfied free fatty acid (NEFA) concentrations were smaller at 8 months in H-PTH and L-ALN rats compared to OVX controls. ($p<0.05$) At 12 months, all groups except M-ALN and L-NaF had lower liver triglyceride (TG) and NEFA concentrations than OVX controls.($p<0.05$) Leptin serum concentrations increased with age and was higher in OVX with or without treatment compared to AM controls. Further, IGF-I serum concentrations were lower in H-ALN and H-PTH than in OVX controls at 12 months.($p<0.01$)

These data demonstrate that treatment with moderate to high doses of ALN and PTH can reduce tissue fat accumulation and normalize fat metabolism to those of normal age-matched controls but also indicates that high drug doses can suppress IGF-I levels.

3.2 INTRODUCTION

Fat accumulation is associated with menopause and can have devastating consequences on fat metabolism (Poehlman, 1995, Matthews, 1989,Gordon, Barret-

Conner, Kelley, 2000) During menopause the reduction in estrogen can cause an increase in body mass, visceral fat and tissue fat accumulation within organs. (Heilbronn, 2004)

Fat accumulation and metabolic disorders are more common in elderly women than in younger women (Zamboni, 1997), demonstrating the effects of age and menopause on metabolic function. There is a positive relationship between visceral fat content and indices of fat metabolism including triglycerides, leptin and free fatty acids. The levels of both fat and fat metabolism increase significantly in post-menopausal women, (Goodpaster, 2005) and is strongly associated with type 2 diabetes (Gastadelli, 2002).

Adipocytes produce estrogen which contributes to the protective mechanism that increased body weight plays against bone loss. Leptin, and other adipokines increase with age, as a function of fat mass and substantially increase in obese women. (Considine, 1996) However, the effects of menopause on indices of fat metabolism are complex and scientists have reported contradictory information. Sowers et. al reported that leptin concentrations increased in healthy weight women after the onset of menopause but obese women had higher initial levels of leptin and increase in levels after the onset menopause (Sowers, 2008) However, Rosenbaum showed leptin levels were decreased in post-menopausal women and showed how estrogen helps to modulate leptin concentrations (Rosenbaum, 1996).

A study done on the effects of Raloxofine in osteoporotic women showed that a selective estrogen receptor modulator were able to improve metabolic parameters with decreased triglyceride levels (Oktem, 2008) Others have shown that estrogen treatment can reverse the effects of food-induced and ovariectomy induced obesity in a mouse model (Zoth, 2010).

The interactions that alter fat metabolism are complex. Menopausal changes in hormones and fat accumulation only adds complexity to these interactions. Further research is needed to elucidate the effects of aging and menopause on changes in fat metabolism. Osteoporosis treatment effects on fat metabolism and fat accumulation could have important consequences for the aging population and needs to be studied further.

Using the ovariectomized rat model for osteoporosis, we hypothesized that alendronate, parathyroid hormone and sodium fluoride treatments would prevent the negative effects on fat metabolism (i.e. increased fat accumulation) caused by ovariectomy. Long term, high dose treatments would have the greatest effects on fat metabolism.

3.3 MATERIALS AND METHODS

Experimental Design

Adult (5 mo old) Sprague-Dawley rats were ovariectomized and randomized into healthy age matched controls, ovariectomized controls or ovariectomized drug treated groups (n=10 per group) for short term (2 mo) or long term (6 mo) treatment duration. Drug treatments included alendronate at three doses: high (2 mg/kg), medium (100 µg/kg) and low (10 µg/kg); parathyroid hormone at three doses: high (75 µg/kg), medium (15 µg/kg) and low (0.3 µg/kg); and sodium fluoride at two doses: high (500 ppm) and low (100 ppm). Treatment dose was determined based on previous literature for the clinically relevant dose (low), the maximum tolerable dose without known evidence of cytotoxicity (high) and a moderate dose that fell within the two limits (medium). Treatments began at six months of age. All rats were individually housed in standard cages and allowed free access to standard rodent chow and tap water. Weights for all animals were recorded weekly. All procedures were reviewed and approved by the Institutional Animals Care and Use Committee at the State University of New York at Stony Brook.

Ten healthy and ten ovariectomized animals were sacrificed at 6 months as baseline controls. Ten animals from each group were sacrificed at 8 and 12 months of age. The liver, fat pad associated with the fallopian tubes, and the soleus muscle of each animal was harvested at sacrifice and flash frozen in liquid nitrogen and stored at -80ºC. Blood was collected through cardiac puncture, spun at 4,000 rpm for ten minutes to separate serum. Serum was extracted and alliquoted into 200 µl aliquots and stored at -80ºC.

Tissue Mass at Sacrifice

During the sacrifice, the liver, gonadal fat pad and brown fat were weighed with a high-precision scale prior to storage. Masses were recorded; group averages and standard deviations were calculated.

Triglyceride Determination Assay

A triglyceride detection kit (Sigma-Aldrich) was used to determine TG content in the liver and the serum. For triglyceride content of the liver: approximately 200 mg of liver samples stored at -80º were extracted from the tissue and placed into 700 uL of phosphate buffered saline (PBS). The tissue was homogenized and 300 uL was pipetted into fresh centrifuge tubes. A 900 uL solution of a 3:1 chloroform: methanol solution was added and samples were vortexed for 1 minute. After samples settled into three phases, they were centrifuged at room temperature for 10 minutes at 4,000 rpm.

The bottom 400 uL layer (triglycerides in chloroform: methanol solution) from the three phase system was extracted and pipetted into fresh centrifuge tubes for each sample and allowed to evaporate over night.

Each sample was reconstituted with isopropanol and vortexed to create a uniform solution. Triglyceride free reagent (160uL) was added to each well of a standard 96 well plate and 10 uL of the sample was added in triplicate wells. A standard curve was created using glycerol reagent at 2.5 ug/uL and 40 uL of free glycerol reagent was added to each well. Plates were gently shaken for 30 minutes. All plates were read approximately 30 minutes after glycerol free reagent was added using a 96 well plate reader and K.C. Junior software.

Optical densities were determined and averaged for the triplicates and TG content was determined using the standard curve provided from the same plate. Average TG content for each group was determined. The same protocol was followed for triglyceride concentration in the Serum, except 20 uL of blood serum was added to each well without further processing.

Free Fatty Acid Determination Assay

An HR Series NEFA-HR(2) (Wako Diagnostics) assay was used to determine the free fatty acid content of the liver tissue. Approximately 200 mg of liver samples stored

at -80º were extracted from the tissue and placed into 700 uL of phosphate buffered saline (PBS). The tissue was homogenized and 300 uL was pipetted into fresh centrifuge tubes. 900 uL of a 3:1 chloroform: methanol solution was added and samples were vortexed for 1 minute. After samples naturally settled into three phases, they were centrifuged at room temperature for 10 minutes at 4,000 rpm.

The bottom of the 400 uL layer (triglycerides in chloroform: methanol solution), from the three phase system, was extracted and pipetted into fresh centrifuge tubes and allowed to evaporate over night.

Each sample was reconstituted with isopropanol and vortexed to create a uniform solution. 200 uL of Color Reagent A was added to each well followed by 10 uL of sample in duplicate wells. The plate was placed in an incubator at 37ºC for five minutes. The plates were read at 540 nm and 560 nm and values from each reading were averaged to provide sample blanks for each individual well. 100 uL of Color Reagent B was added to the wells and the plate was incubated for an additional 5 minutes. All plates were read at 540 nm and 560 nm and values from each reading were averaged. Samples were calculated by subtracting final optical density minus sample blank optical density. Concentrations were determined based on standard concentrations created by the standard curve.

Optical densities were determined and averaged for the duplicates and FFA content was determined using the standard curve provided from each plate. Average FFA content for each group was determined. The same protocol was followed for triglyceride concentration in the Serum, except 20 uL of blood serum was added to each well without further processing.

Leptin Determination Assay

Leptin determination was done on serum samples from 6 month, 8 month and 12 month animals. This analysis was conducted at University of Cincinnati by the Mouse Metabolic Phenotyping Center.

IGF-1 Determination Assay

IGF-1 determination was done on serum samples from 6 month, 8 month and 12 month animals. This analysis was conducted at University of Cincinnati by the Mouse Metabolic Phenotyping Center.

Statistical Analysis

All values are presented as mean + standard deviations. Statistical significance was computed by performing a One Way ANOVA. If there were significant differences, a Tukey post-hoc test was used to determine statistical differences between groups.

A Two-way ANOVA was conducted to determine effects caused by both age and treatment and the interaction between each parameter.

3.4 RESULTS

Tissue Mass

6 Months

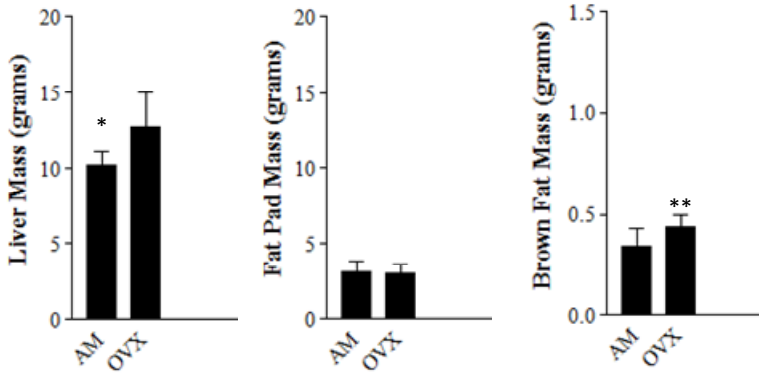

Figure 24. A.) Liver, B.) fat pad and C.) brown fat masses at sacrifice at 6 months of age in baseline controls (AM) and baseline OVX controls (OVX). Data is represented as group mean + S.D. (Student t-test) *p<0.01, **p<0.05

At six months of age, liver mass was 24.7% higher in the OVX animals compared to AM controls, ($p<0.01$) brown fat mass was 26.9% higher in the OVX animals compared to AM controls, ($p<0.05$) there were no differences in fat pad masses. (Fig. 24)

8 Months

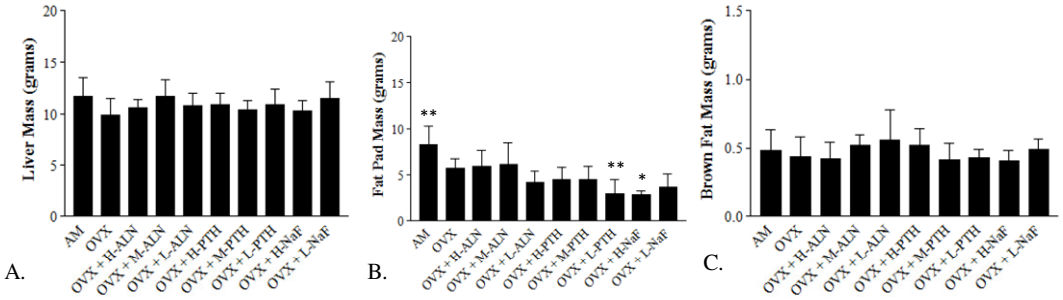

Figure 25. A.) Liver, B.) fat pad and C.) brown fat masses at 8 months of age for age matched control (AM), ovariectomy control (OVX), OVX with high dose alendronate (ALN) treatment (OVX + H-ALN), OVX with medium ALN treatment (OVX + M-ALN), OVX with low ALN treatment (OVX + L-ALN), OVX with high parathyroid hormone (PTH) treatment (OVX + H-PTH), OVX with medium PTH treatment (OVX + M-PTH), OVX with low PTH treatment (OVX + L-PTH), OVX with high sodium fluoride (NaF) treatment (OVX + H-NaF) and OVX with low NaF treatment (OVX + L-NaF). (ANOVA) * p<0.001, *p<0.01, **p<0.05

At 8 months of age, liver mass was similar in all animals. Fat pads were 30.3% larger in AM controls compared to OVX controls.($p<0.01$) Fat pads were 47.4% smaller in L-PTH and 49.3% smaller in H-NaF treated animals compared to OVX controls. ($p<0.05$) Brown fat mass was similar in all animals at 8 months of age. (Fig. 25)

12 Months

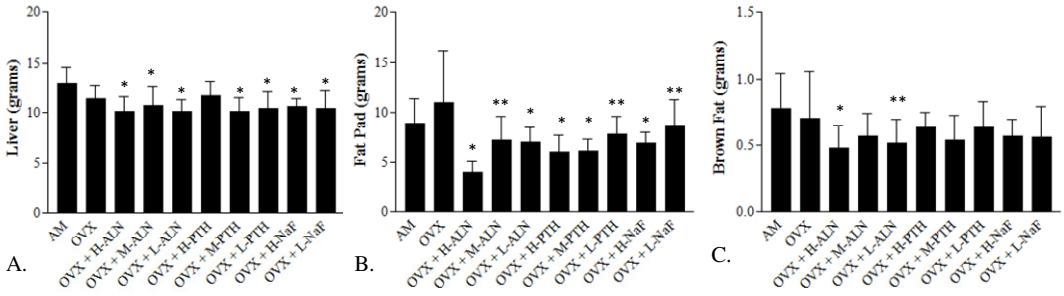

Figure 26. A.) Liver, B.) fat pad and C.) brown fat masses at sacrifice at 12 months of age for age matched control (AM), ovariectomy control (OVX), OVX with high dose alendronate (ALN) treatment (OVX + H-ALN), OVX with medium ALN treatment (OVX + M-ALN), OVX with low ALN treatment (OVX + L-ALN), OVX with high parathyroid hormone (PTH) treatment (OVX + H-PTH), OVX with medium PTH treatment (OVX + M-PTH), OVX with low PTH treatment (OVX + L-PTH), OVX with high sodium fluoride (NaF) treatment (OVX + H-NaF) and OVX with low NaF treatment (OVX + L-NaF). (ANOVA) * p<0.001, *p<0.01, **p<0.05

Liver mass was significantly decreased in all treated animals at 12 months of age compared to AM controls except H-PTH animals.($p<0.01$)

Fat pads were 51% smaller in H-ALN treated animals compared to OVX controls.($p<0.01$) Fat pads were 10.7 and 10.1% smaller in H and M-PTH treated animals compared to OVX controls. ($p<0.05$) Fat pad masses were slightly smaller in L-PTH and L-NaF treated groups. ($p<0.05$)

Brown fat mass was similar in AM controls and OVX controls at 12 months of age. There was less brown fat in each treatment group at all doses at 12 months of age. There was 47.5% less brown fat in H-ALN and 40.7% less in L-ALN treated animals than healthy age matched controls.($p<0.01$and $p<0.05$) (Fig. 26)

Triglyceride Liver Concentration

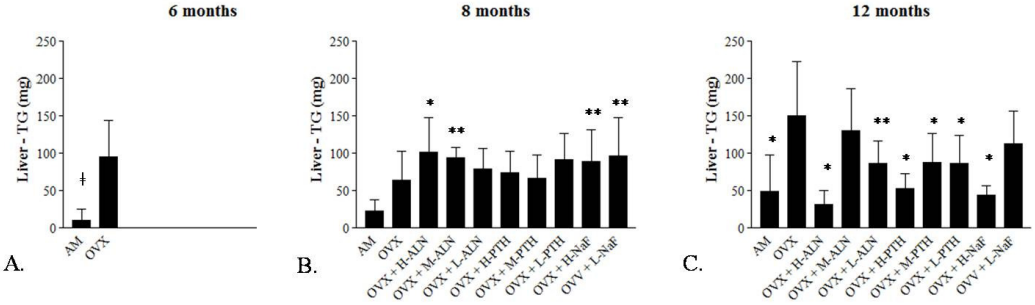

Figure 27. Triglyceride content of the liver for A.) 6 month, (Student t-test) B.) 8 month (ANOVA) and C.) 12 month old animals (ANOVA) . Data is represented as mean +S.D for age matched control (AM), ovariectomy control (OVX), OVX with high dose alendronate (ALN) treatment (OVX + H-ALN), OVX with medium ALN treatment (OVX + M-ALN), OVX with low ALN treatment (OVX + L-ALN), OVX with high parathyroid hormone (PTH) treatment (OVX + H-PTH), OVX with medium PTH treatment (OVX + M-PTH), OVX with low PTH treatment (OVX + L-PTH), OVX with high sodium fluoride (NaF) treatment (OVX + H-NaF) and OVX with low NaF treatment (OVX + L-NaF). (Student t-test, ANOVA) ǂ p<0.001, *p<0.01, **p<0.05

Liver triglyceride content was 89.5% higher in the OVX controls compared to AM controls at 6 months of age. ($p<0.001$) At 8 months of age, it was 63.7% higher in OVX compared to AM controls. H-ALN, M-ALN, H-NaF and L-NaF animals had higher TG levels than AM controls, but were statistically similar to OVX controls.

By 12 months of age, OVX controls had the highest TG liver content, 67.1% higher than AM controls. ($p<0.001$) H-ALN, H-PTH and H-NaF animals were 78.7, 64.4 and 70.5% lower than OVX controls. ($p<0.01$) L-ALN, M-PTH and L-PTH were also significantly lower than OVX controls. ($p<0.05$) (Fig. 27)

Triglyceride Serum Concentration

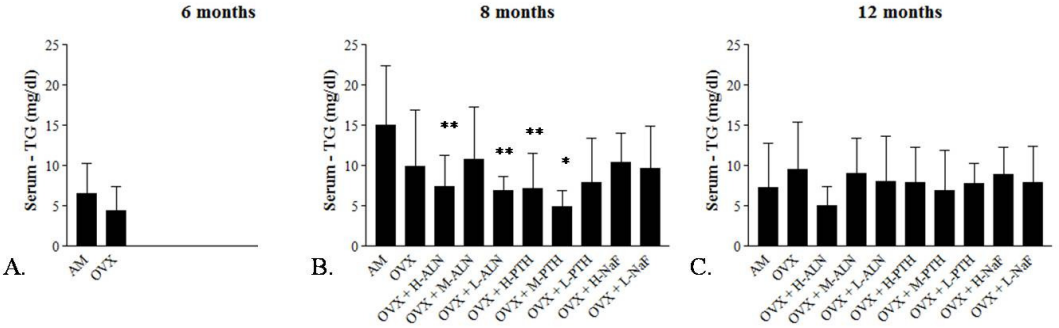

Figure 28. TG content of the serum for A.) 6 mo animals, B.) 8 mo animals and C.) 12 mo animals. Data is represented as group mean + SD for age matched control (AM), ovariectomy control (OVX), OVX with high dose alendronate (ALN) treatment (OVX + H-ALN), OVX with medium ALN treatment (OVX + M-ALN), OVX with low ALN treatment (OVX + L-ALN), OVX with high parathyroid hormone (PTH) treatment (OVX + H-PTH), OVX with medium PTH treatment (OVX + M-PTH), OVX with low PTH treatment (OVX + L-PTH), OVX with high sodium fluoride (NaF) treatment (OVX + H-NaF) and OVX with low NaF treatment (OVX + L-NaF). (Student t-test, ANOVA) ǂ p<0.001, *p<0.01, **p<0.05

Serum triglyceride concentrations were similar in AM controls and OVX controls at 6 months of age. At 8 months of age, serum triglyceride concentrations were lower in H and L-ALN treated animals as well as H and M-PTH treated animals compared to AM controls. ($p<0.05$) At 12 months, H-ALN, H-PTH and M-PTH animals had maintained lower levels of triglyceride concentrations which were 47, 17 and 28% lower than OVX controls but these differences were not significant. (Fig. 22)

Age Related Changes in Serum Triglyceride Concentration

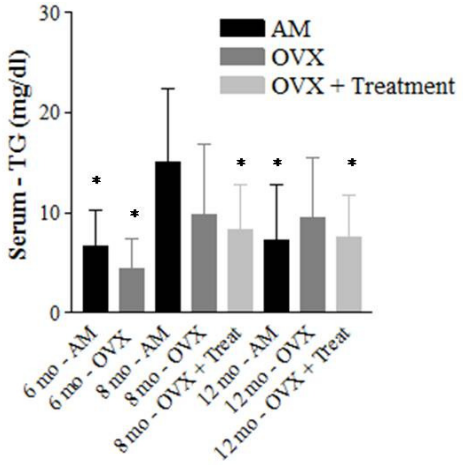

Figure 29. Serum triglyceride content at 6, 8 and 12 months of age for age matched controls (AM), ovariectomy controls (OVX) and ovariectomy controls that underwent treatment (OVX + Treat) (ANOVA) *p<0.01

All OVX treated animals were pooled and compared to AM controls and OVX controls at 6, 8 and 12 months. AM controls had significantly higher TG serum concentrations at 8 months compared to 6 month AM controls, all OVX treated animals and 12 month AM animals.($p<0.01$) However, OVX controls at 8 and 12 months of age were not significantly different than 8 month controls. (Fig. 29)

Free Fatty Acid Liver Concentration

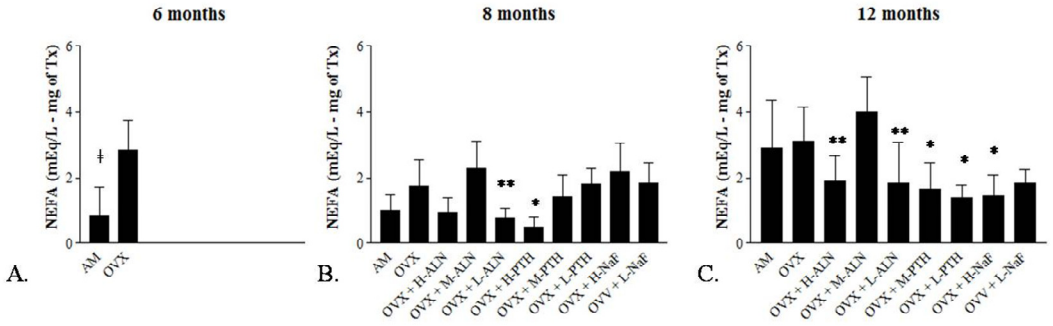

Figure 30. NEFA concentrations in the liver at A.) 6 months, B.) 8 months and C.) 12 months. Data is represented as mean + SD for age matched control (AM), ovariectomy control (OVX), OVX with high dose alendronate (ALN) treatment (OVX + H-ALN), OVX with medium ALN treatment (OVX + M-ALN), OVX with low ALN treatment (OVX + L-ALN), OVX with high parathyroid hormone (PTH) treatment (OVX + H-PTH), OVX with medium PTH treatment (OVX + M-PTH), OVX with low PTH treatment (OVX + L-PTH), OVX with high sodium fluoride (NaF) treatment (OVX + H-NaF) and OVX with low NaF treatment (OVX + L-NaF). (Student t-test, ANOVA) ǂ p<0.001,*p<0.01, **p<0.05

At 6 months, non-esterfied free fatty acid (NEFA) concentrations from liver tissue were 69.4% higher in OVX animals compared to AM controls.($p<0.001$) At 8 months, NEFA concentrations were 56.4 and 71.5% lower in L-ALN and H-PTH compared to OVX controls. ($p<0.05$) At 12 months of age all treatment groups were significantly lower than OVX controls except M-ALN and L-NaF. ($p<0.05$) (Fig. 30)

Free Fatty Acid Serum Concentration

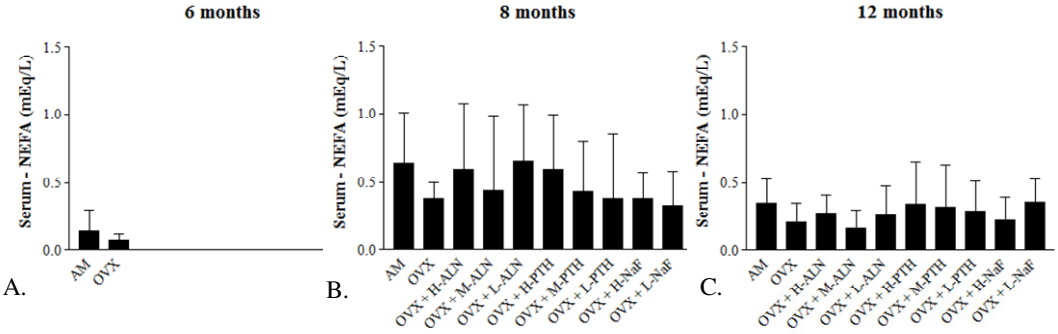

Figure 31. NEFA concentrations in the liver at A.) 6 months, B.) 8 months and C.) 12 months. Data is represented as mean + SD for age matched control (AM), ovariectomy control (OVX), OVX with high dose alendronate (ALN) treatment (OVX + H-ALN), OVX with medium ALN treatment (OVX + M-ALN), OVX with low ALN treatment (OVX + L-ALN), OVX with high parathyroid hormone (PTH) treatment (OVX + H-PTH), OVX with medium PTH treatment (OVX + M-PTH), OVX with low PTH treatment (OVX + L-PTH), OVX with high sodium fluoride (NaF) treatment (OVX + H-NaF) and OVX with low NaF treatment (OVX + L-NaF). (Student t-test, ANOVA)

High variability within groups resulted in no significant differences at each of the time points. (Fig. 31) There appeared to be age related increases in NEFA concentrations

so data for all treated animals were pooled and compared AM controls and OVX controls.

Age related Changes in Serum NEFA Concentrations:

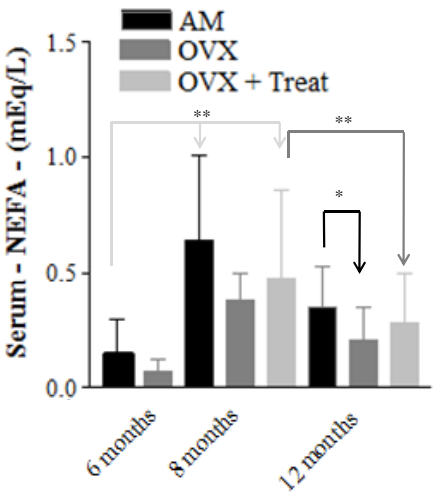

Figure 32. NEFA concentrations in the liver at 6, 8 and 12 months. Data is represented as mean + SD for age matched controls (AM - black), ovariectomy controls (OVX-dark gray) and the combined data set of all ovariectomy treated animals (OVX + Treatment - light gray) (ANOVA) ǂ p<0.001, **p<0.05

NEFA serum concentrations increased in AM by 76.8% and in OVX by 81.7% animals from 6 months to 8 months. ($p<0.05$) The OVX animals had 40.6% lower serum concentrations at 12 months than AM. ($p<0.01$) In all groups, NEFA concentrations were higher in 8 month animals compared to 12 month animals. NEFA levels were 83.5, 69.6and 85% lower in AM, OVX and OVX + treatment in 12 month animals compared to 8 month animals. This trend was similar to that seen in triglyceride serum data. (Fig. 32)

Leptin Serum Concentration

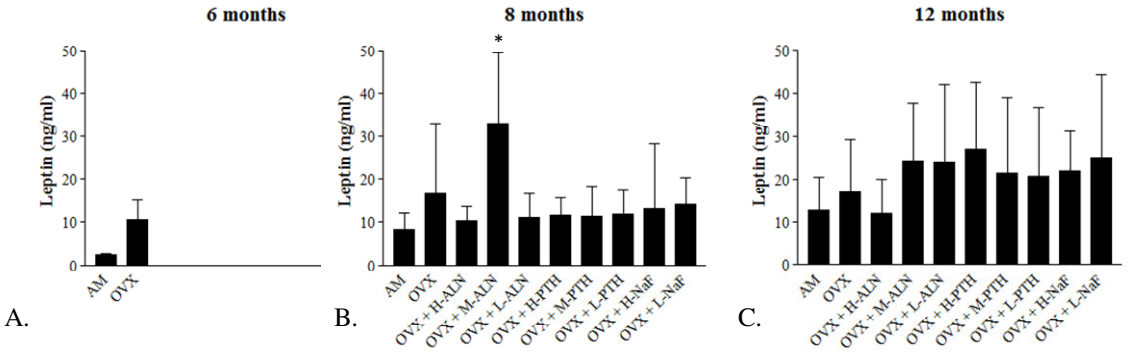

Figure 33. Leptin serum concentrations at A.) 6 months, B.) 8 months and C.) 12 months of age. Data is represented as mean + SD for age matched control (AM), ovariectomy control (OVX), OVX with high dose alendronate (ALN) treatment (OVX + H-ALN), OVX with medium ALN treatment (OVX + M-ALN), OVX with low ALN treatment (OVX + L-ALN), OVX with high parathyroid hormone (PTH) treatment (OVX + H-PTH), OVX with medium PTH treatment (OVX + M-PTH), OVX with low PTH treatment (OVX + L-PTH), OVX with high sodium fluoride (NaF) treatment (OVX + H-NaF) and OVX with low NaF treatment (OVX + L-NaF). (Student t-test, ANOVA) *p<0.01

Due to the variability in leptin serum concentrations within groups there were few significant differences between groups at each time point. There were no differences between AM and OVX at 6 months. At 8 months, M-ALN was significantly higher than all groups. ($p<0.01$) There were no differences at 12 months. (Fig. 33) Trends suggest that leptin increased as a function of age, and was highest in all OVX animals compared to AM controls, therefore all OVX groups were pooled and compared to AM controls to determine age related changes.

Age related Changes in Serum Leptin Concentrations

All OVX animals were pooled and compared to AM controls to determine differences in leptin as a function of age. Leptin was 70.5% higher in 8 month AM control animals compared to 6 month AM controls animals. Leptin was 34.5 % higher in 12 month AM controls than in 8 month controls. Leptin was 28.4% higher in 8 month OVX animals compared to 6 month OVX animals, and 31.63% higher in 12 month OVX animals than in 8 month OVX animals. AM controls had lower leptin concentrations compared to OVX animals at each time point. AM controls were 76.3% lower than OVX animals at 6 months, 42.5% lower at 8 months and 40% lower at 12 months. There was significantly more leptin in 8 month OVX animals, 12 month controls, and 12 month OVX animals compared to 6 month AM controls. ($p<0.05$) (Fig. 34)

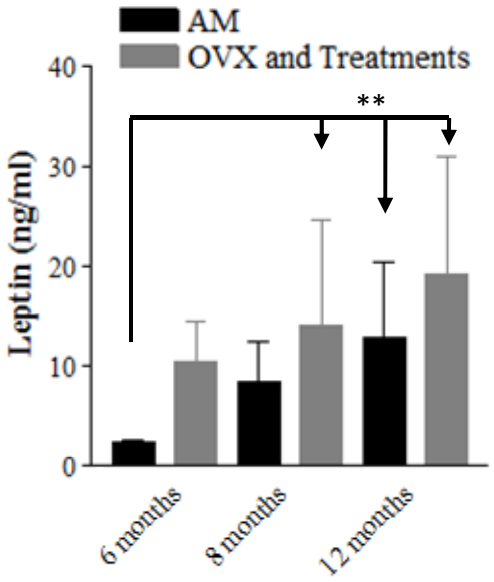

Figure 34. Leptin concentrations at 6, 8 and 12 months in age matched control (AM - black) and ovariectomy control (OVX - gray) animals. Leptin concentrations were lower in 6 month controls and 8 month OVX controls compared to 12 month controls. (ANOVA) **p<0.05

IGF-1 Serum Concentration

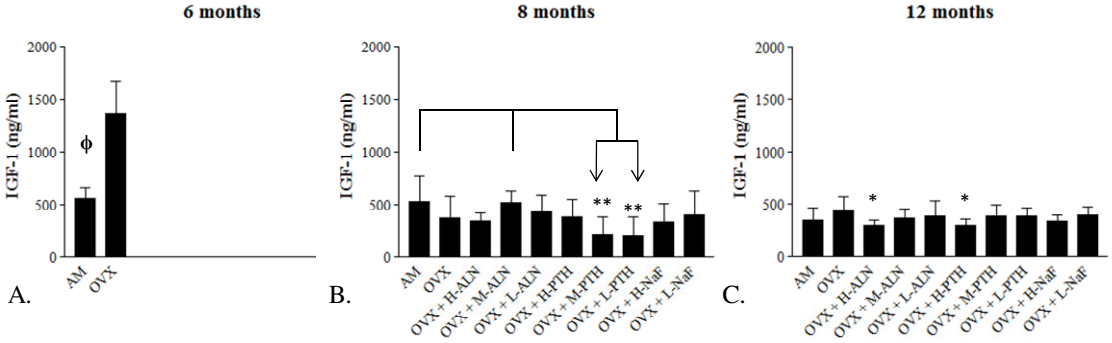

Figure 35. IGF-1 serum concentrations at A.) 6 months, B.) 8 months, C.) 12 months. Data is represented as means +SD for age matched control (AM), ovariectomy control (OVX), OVX with high dose alendronate (ALN) treatment (OVX + H-ALN), OVX with medium ALN treatment (OVX + M-ALN), OVX with low ALN treatment (OVX + L-ALN), OVX with high parathyroid hormone (PTH) treatment (OVX + H-PTH), OVX with medium PTH treatment (OVX + M-PTH), OVX with low PTH treatment (OVX + L-PTH), OVX with high sodium fluoride (NaF) treatment (OVX + H-NaF) and OVX with low NaF treatment (OVX + L-NaF (Student t-test, ANOVA) ϕ p<0.02 *p<0.01, **p<0.05

OVX animals at six months of age had IGF-1 serum concentrations 58.7% higher than AM controls. ($p<0.02$) There were no differences at 8 and 12 months between AM and OVX animals. At 8 months of age, M-PTH and L-PTH suppressed IGF-1 levels by 58.8 and 60.5% compared to AM controls. ($p<0.05$) At 12 months of age H-ALN and H-PTH animals were 32.3 and 11% lower than OVX controls. ($p<0.01$) (Fig. 35)

3.5 DISCUSSION

Fat accumulation associated with menopause can have devastating consequences on fat metabolism (Poehlman, 1995, Matthews, 1989,Gordon, Barret-Conner, Kelley, 2000) During menopause the reduction in estrogen causes an increase in body mass, visceral fat and tissue fat accumulation within organs. (Heilbronn, 2004) Fat accumulation and metabolic disorders are more common in elderly women than in younger women (Zamboni, 1997), demonstrating the effects of age and menopause on metabolic function.

Changes in adipogenic cellular mechanisms by osteoporosis drug treatment were not elucidated during this study. There is no information on interactions of the drug which caused the decrease in indices of fat metabolism and fat accumulation.

Increases in TG, NEFA and leptin levels were seen as a function of age. Ovariectomy increased serum and liver levels were elevated in OVX animals compared to AM controls. With osteoporosis treatment the increases in metabolic health that occurred due to OVX were minimized. These animals had lower metabolic indices which were similar to age matched controls.

There were several age related changes in the parameters of metabolic health. It appears that TG content was significantly decreased by long term drug use but there was little change after only two months indicating a benefit of long term treatment. The NEFA concentrations seemed to increase at 8 months but then decreased by 12 months indicating an immediate effect of OVX followed by a normalization. Leptin steadily increased with age and treatment had little effect on altering the ovariectomy related increase. However, H-ALN had slightly lowered leptin concentrations compared to all other treatment groups or OVX controls.

Leptin plays an important role in regulating bone formation. Leptin increased in all treatment groups from 8 to 12 months of age except H-ALN treated animals. This strong hormonal response to ovariectomy was also seen by Sowers et. al. However, H-ALN did not increase at 12 months which indicates the positive benefits of leptin on bone metabolism may have occurring all groups, but the increases in bone density and bone mass demonstrated during high dose ALN treatment occurred independently from leptin regulated bone metabolic effects. H-ALN animals had reduced fat pads, lower *in vivo* fat

volume and subsequent reduced leptin concentrations compared to other groups. They also had the lowest average body mass which did only slightly increased from 8 to 12 months with the lowest fat pad masses. Since fat mass regulates leptin concentrations, it explains why H-ALN leptin concentrations did not increase from 8 to 12 months.

IGF-1 is an indicator of bone formation. It was surprising to see such a large increase in IGF-1 levels at 6 months in the OVX control group. However, trabecular bone data indicated that OVX did not have an immediate deleterious effect on bone health, there were slight decreases in trabecular bone parameters but these differences were not significant. It is understood that resorption and formation are coupled processes (Eriksen, 1990, Canalis) so early osteoclast activity due to estrogen withdrawal could be simultaneously activating osteoblast activity causing subsequent formation. This hypothesis could explain increased IGF-1 levels as well as the minimal decreases in trabecular architecture in ovariectomy controls after one month. Another group found that IGF-1 is responsible for osteoclast recruitment, elevated levels of IGF-could be indicative of increased activity of osteoclasts in response to ovariectomy (Wang, 2006).

At 12 months IGF-1 levels were suppressed with both H-ALN and H-PTH treatments. This was surprising, but may be a sign of a secondary response to high dose treatment. The response could be negative, indicating a pathological complication or an indicator of an immune response due to the extreme dose.

Osteoporosis drugs reduced fat pad masses and improved metabolic health in the ovariectomized rat. Metabolic health worsened with ovariectomy, but the deterioration in indices of fat metabolism detected in both the serum and liver were improved, and sometimes normalized with moderate to high osteoporosis treatment. Treated animals had values that reflected those seen in healthy age matched animals. This indicates a positive secondary effect of osteoporosis drug use in addition to improving bone volume, density and structural parameters. If osteoporosis drugs can simultaneously reduce indices of fat metabolism while improving skeletal health, they could help to reduce the incidence of osteoporosis related obesity and other health problems that afflict post-menopausal women such as type 2 diabetes and cardiovascular disease.

CHAPTER 4

THE BONE-MASS RELATIONSHIP IS NORMALIZED DURING OSTEOPOROSIS DRUG TREATMENT, ALENDRONATE AND PARATHYROID HORMONE NEGATIVELY CORRELATE PARAMETERS OF BONE QUALITY AND FAT

4.1 ABSTRACT

Post-menopausal osteoporosis is associated with bone loss but menopause also increases body mass and abdominal adiposity, factors that can pose a secondary risk to skeletal health. Drugs such as alendronate (ALN), parathyroid hormone (PTH) or sodium fluoride (NaF) target bone loss but their effects on adiposity, metabolism, and the interrelationship between bone and fat are largely unknown. To this end, we subjected OVX rats to short-term (2 months) and long-term (6 months) treatments of different doses of ALN and PTH and analyzed vertebral bone, abdominal fat volume, liver fatty acids, and serum leptin and IGF-I. Six-month old Sprague-Dawley rats were assigned to age-matched controls, untreated OVX, OVX treated with high (H), medium (M), or low (L) doses of hPTH (60, 15, or 0.3μg/kg/d), or OVX treated with H, M, or L-ALN (100, 10, or 1μg/kg/2xwk) or OVX treated with H or L-NaF (500ppm or 100ppm in drinking water). Rats were sacrificed at 6, 8, and 12mo of age (n=10/group/age).

Body mass was positively correlated to bone volume and density for the combined dataset of age-matched controls and high dose treatment groups (r^2= 0.36, $p<0.01$), but was not correlated in the combined dataset of OVX controls and low dose treatments. Trabecular bone density was weakly correlated to body mass for the combined data set of all high dose treatments (r^2=0.13, $p<0.05$) as well as the combined data set of AM controls with M, L-ALN and M-PTH (r^2=0.12, $p<0.05$) but was not correlated in OVX pooled with L-PTH and NaF. Liver TG content was not correlated to apparent mineral density in OVX controls (r^2=0.001, $p<0.93$), but ALN, PTH and NaF treatment normalized this relationship to that of age-matched control rats.

ALN and PTH treatment had body fat to body mass relationships similar to the slope of age matched controls but with reduced elevations, indicating a reduction in total fat to body mass. OVX controls had no correlation between bone volume fraction and liver TG while AM controls pooled with NaF showed a positive relationship. All ALN

treatment groups pooled and all PTH treatment groups pooled showed negative correlations between bone density and liver TG content; the highest responders to treatment with greatest bone density also had lowest TG. These data demonstrate that treatment with ALN, PTH and NaF normalized bone morphology and indices of fat metabolism to those of normal age-matched controls. ALN and PTH treatment negatively correlated bone quality to fat showing animals that responded strongest to treatment also had the lowest tissue fat accumulation.

4.2 INTRODUCTION

The relationships between bone and fat are complex. They rely on a series of physical, chemical, genetic and metabolic factors (Luu, 2009). Body mass, fat pad mass and total fat volume all contribute to the mechanical forces acting on the skeletal system, higher mechanical forces leads to skeletal adaption and increased bone volume (Lanyon, 1996, Rubin, 1987). Therefore the differences in bone volume among individuals can in part be contributed to differences in their body composition.

In healthy individuals there is a positive relationship between body mass and bone volume (Reid, 1992, 2002). However, there is contradictory evidence on the impact of body mass on bone density. Some report body mass is strongly correlated to bone mineral density, (Ravn, 1999, Reid, 1992) others found that body mass was not at all correlated to bone mineral density. (Robbins, 2002)

Menopause is associated with increases in fat accumulation as well as increases in indices of fat metabolism including triglycerides, free fatty acids and leptin levels. (Rosenbaum, 1996, Sepe, 1995) There is a strong positive relationship between adipose tissue and fat metabolism. (Sowers,2008) Obesity is associated with decreased metabolic health indicated by elevated levels of leptin, trigylcerides, free fatty acids and cholesterol. (Gastaldelli, 2002) Increases in both fat content fat and metabolic parameters are indicators for cardiovascular risk, heart disease and type 2 diabetes. (Poehlman 1995, Matthews, 1989, Gorden) The positive relationship between body mass, fat mass to levels of metabolism is seen in both healthy and obese patients. (Petzel, 2007) Fat mass and leptin concentrations are both positively correlated to bone mineral density in post-menopausal women (Yamaguchi, 2009). Body mass and fat content significantly

influence parameters of bone mass and density and are important regulators of bone metabolism.

It has recently been shown that increases in fat can have detrimental effects on bone quality. In an obesity food induced mouse model, bone remodeling was affected by fat volume causing a reduction in trabecular architecture (Cao, 2010). Others have shown that men with metabolic syndrome have lower bone mineral density (Szulc, 2010). Obese post-menopausal women have also been shown to be at a greater risk of skeletal fracture than healthy weight post-menopausal women (Zhao, 2008). This demonstrates the importance of studying the relationship between fat accumulation and bone quality, and not just quantity. Treatments that can improve bone quality while reducing fat accumulation could have beneficial effects for osteoporosis as well as obesity and metabolic syndrome.

Using the ovariectomized rat model for osteoporosis, we hypothesized that alendronate, parathyroid hormone and sodium fluoride treatments would normalize the positive relationship between bone mass and body mass that is perturbed due to ovariectomy. We hypothesized that measures of bone quality would be negatively associated to fat content and osteoporosis treatments would strengthen this association.

4.3 MATERIALS AND METHODS

Data from chapters two and three were used to determine correlations between body composition, bone quantity, bone quality, fat content and parameters of metabolic health.

Statistical Analysis

Linear regressions were performed to determine relationships between bone and fat parameters as well as fat parameters and body weight. If the slope of the regression was significantly different than zero an ANCOVA was used to determine if groups had differences in slopes. The intercepts or elevations of regression lines were analyzed to determine differences between groups with similar slopes.

4.4 RESULTS

Body Mass Indicates Fat and Bone Volume

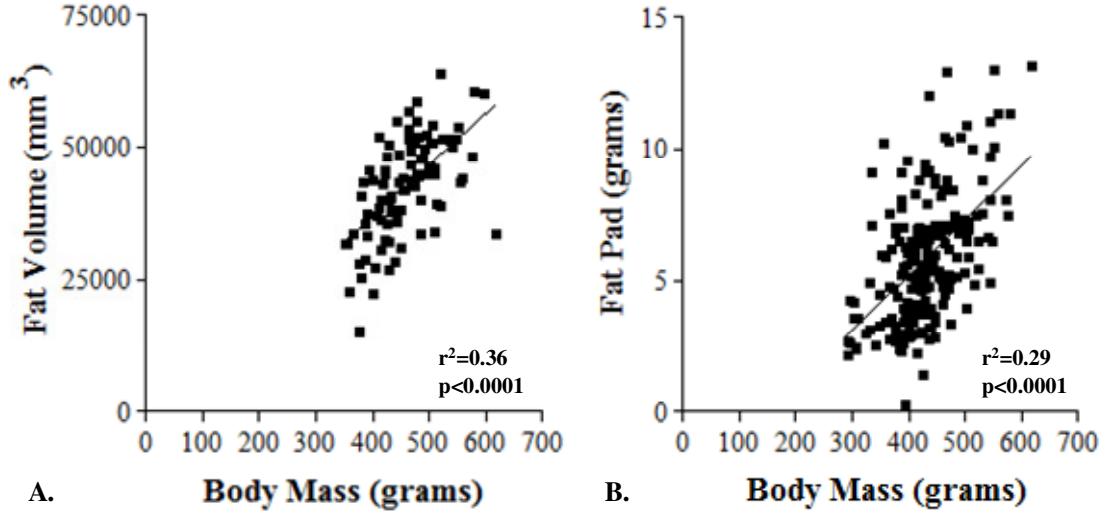

Figure 36. Body mass was positively correlated to A.) fat pad weights and B.) *in vivo* microCT fat volume. Data are represented as individual animals for all time points throughout the study. (Linear regression) (r^2=0.36, p<0.0001, r^2=0.29, p<0.0001)

Animal body mass was correlated to *in vivo* microCT fat volume. (r^2=0.36, p<0.0001) Animal body mass was also correlated to fat pad mass. (r^2=0.29, p<0.0001) (Fig. 36)

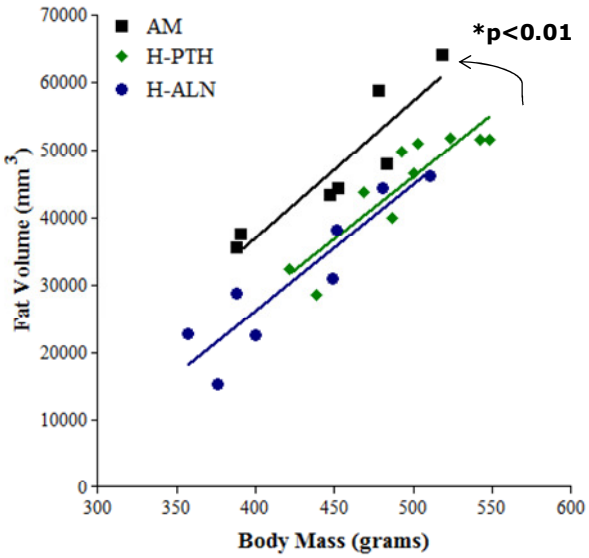

At 12 months of age, high dose ALN and PTH showed similar slopes as age matched controls for the regression of fat volume to body mass. (p=0.94, ANCOVA) However, H-ALN and H-PTH had significantly smaller intercepts compared to age matched controls indicating reduction in the fat volume to body mass ratio during treatment. (p<0.0001) (Fig. 37)

Figure 37. Body mass was positively correlated to fat volume at 12 months of age, in age matched control (AM), high dose alendronate (H-ALN) and high dose parathyroid hormone (H-PTH) groups. The slopes are similar but the treated animals have lower body mass to fat relationship. (Linear Regression, ANCOVA) p<0.0001

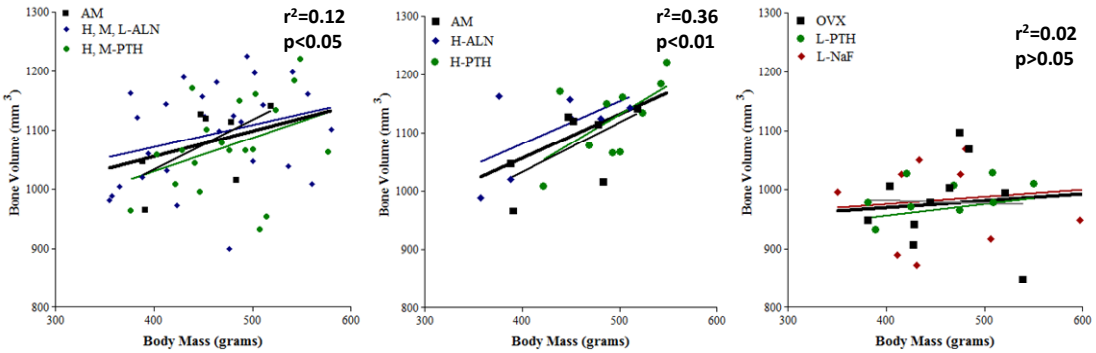

Figure 38. AM controls and high treatment groups were pooled and OVX controls and low treatment groups were pooled for all 12 month data. Body mass was positively correlated to bone volume in AM and treated animals and the correlation was strengthened with just AM, H-ALN and H-PTH groups . Body mass was not correlated to body weight in OVX and low dose treatment. (Linear Regression) (r^2=0.12, p<0.05) (r^2=0.36, p<0.01) (r^2=0.018, p>0.05)

Body mass was indicative of bone volume in healthy animals pooled with all treated animals except L-PTH and L-NaF. (r^2=0.12, p<0.05) The relationship was strengthened when only AM controls, H-ALN and H-PTH animals were included. (r^2=0.36, p<0.01) However, in OVX poled with low dose treated animals there was no correlation. (r^2=0.018, p=0.41) (Fig. 38)

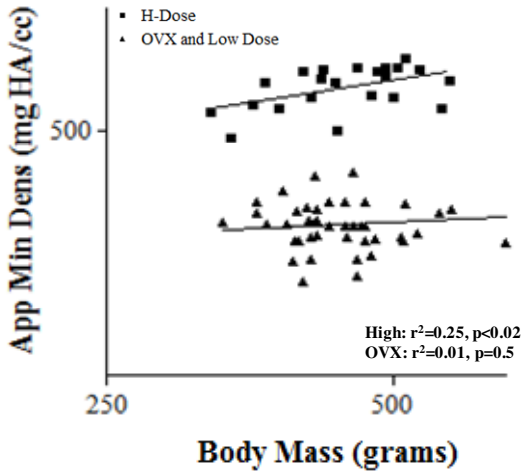

Figure 39. AM controls and high treatment groups were pooled, OVX controls and low treatment groups were pooled for all 12 month data. Body mass was positively correlated to *in vivo* apparent mineral density in AM and high dose treatment but was not correlated in OVX and low dose treatment. (Linear Regression) (r^2=0.25, p<0.02)(r^2=0.01, p=0.50)

In vivo apparent mineral density was correlated to body mass when H-ALN and H-PTH treated animals were pooled. (r^2=0.25, p<0.02) However this correlation was not true for the combined data set of OVX controls pooled with L-PTH and L-NaF treated animals. (r^2=0.01, p=0.5) There was no significant difference in slopes of the lines but the high dose animals had a significantly higher elevation than the OVX animals. (p<0.001) (Fig. 39)

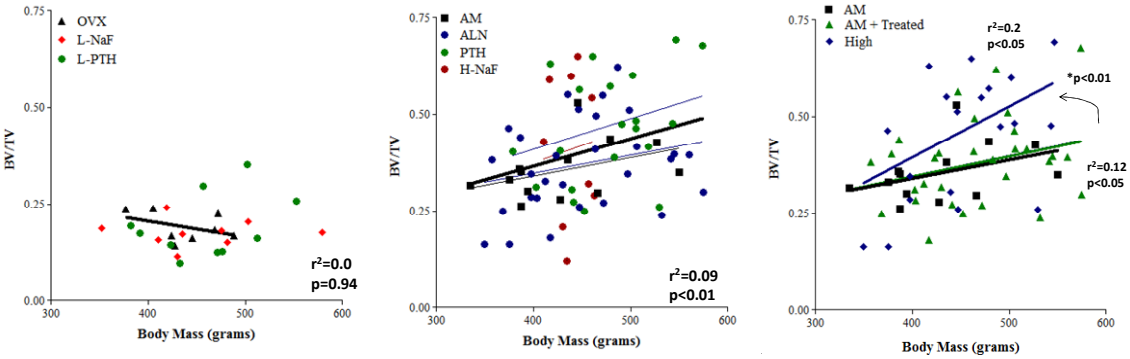

Figure 40. Body mass was not correlated to bone density at 12 months of age in the combined data set of OVX controls pooled with L-PTH and L-NaF. (Left) It was positively correlated in the combined data set of AM controls with ALN treatments and H and M-PTH and H-NaF. (Middle) The high dose treated animals had a higher slope than AM controls pooled with M and L-ALN and M-PTH. (Left) (Linear Regression, ANCOVA) p<0.01

There was a weak correlation between body mass and bone volume fraction of the trabecular bone from the L4 vertebral body in AM controls pooled with M and L-ALN and M-PTH at 12 months of age. (r^2=0.12, p<0.05) H-ALN, H-PTH and H-NaF were pooled and there was a positive relationship between bone volume fraction and body mass at 12 months of age. (r^2=0.13, p<0.05) In OVX animals pooled with L-PTH and L-NaF, bone volume fraction was not correlated to body weight at 12 months of age. (r^2=0, p=0.94)

There was no difference between the slope of the correlation in AM controls pooled with medium dose treated animals and the slope of high dose treated animals, (p=0.7) but high dose treatment had an increased elevation compared to AM controls. (p=0.01) (Fig. 40)

Fat Mass is Positively Correlated to Indices of Fat Metabolism

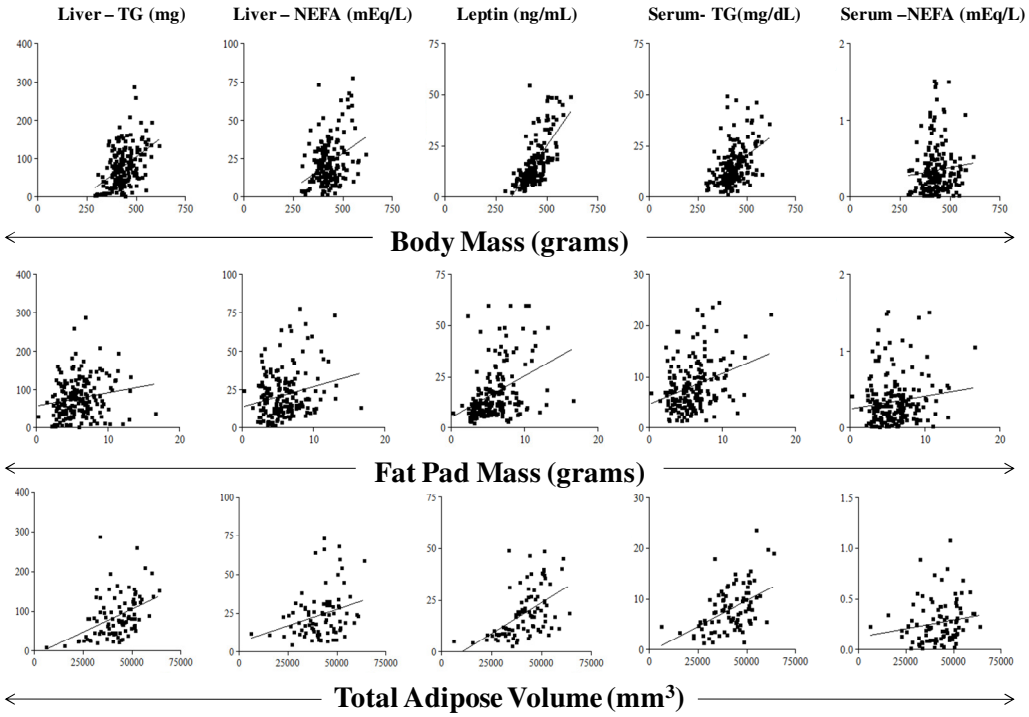

Figure 41. Metabolic parameters: liver triglyceride concentration (Liver –TG (mg)), liver non-esterfied free fatty acid concentration (Liver – NEFA (mEq/L)), serum leptin concentration (Leptin (ng/ml)), serum triglyceride concentration (Serum-TG (mg/dL)) and serum non-esterfied free fatty acid concentration (Serum – NEFA (mgEq/L)) were each correlated to body mass (top row), fat pad mass (middle row) and total adipose volume (from *in vivo* microCT) (bottom row). There was a significant positive relationship in all correlations except serum NEFA concentration to body mass, fat pad mass and total adipose tissue.

This analysis showed that there was a positive relationship between body mass, fat pad mass and total fat volume correlated to all indices of fat metabolism and tissue level fat content in the liver as well as in the serum. Data was significant for all analyses except serum NEFA concentrations. (Fig. 41)

Indices of Bone Quality are Negatively Correlated to Indices of Fat

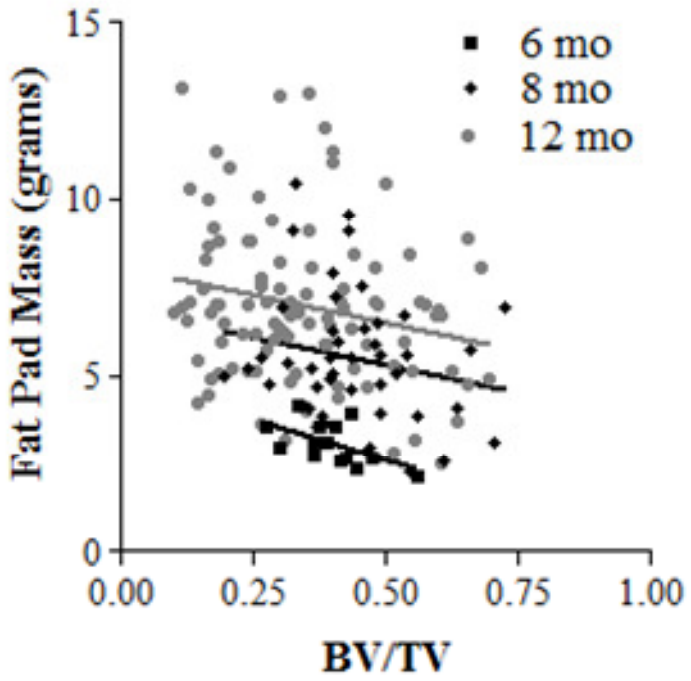

Figure 42. Fat pad mass was negatively correlated to bone volume fraction in all animals pooled for 6 (black -squares), 8 (black-diamonds), and 12 months (gray -circles). 12 month had a higher elevation than 8 months which was higher than 6 months. (ANCOVA) p<0.0001

There was a weak negative correlation between fat pad mass and bone volume fraction. (r^2=0.32, p<0.05) Slopes for 6, 8 and 12 months were identical, (p=0.98), but there were differences in elevations indicating age caused an upward shift in the relationship of fat pad mass to bone volume fraction.(p<0.001) This data demonstrated the negative relationship between fat and bone quality. (Fig. 42)

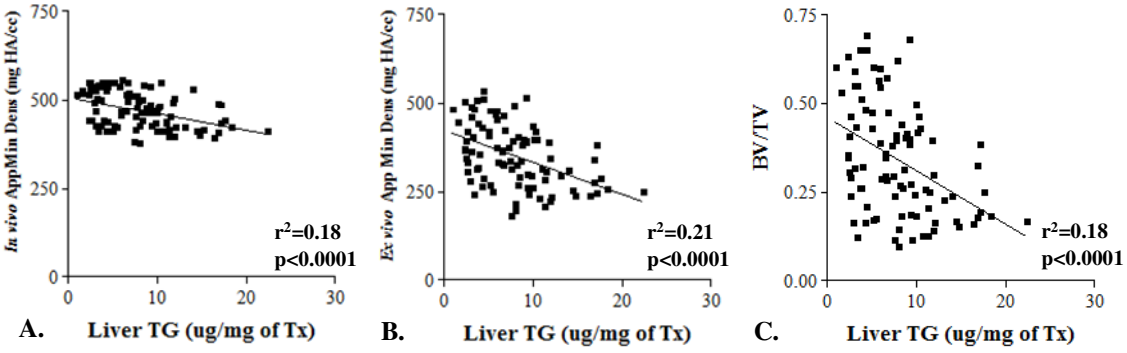

Figure 43. A) There was a negative correlation between liver TG content A.) *in vivo* apparent mineral density, B.) *ex vivo* apparent mineral density and C.) *ex vivo* BV/TV. (Linear regression) (r^2=0.18 or 0.21, p<0.0001)

There was a weak negative relationship between both bone volume fraction and apparent mineral density to liver TG content. This indicated that animals with higher

indices for trabecular microarchitecture subsequently had better metabolic health indices. (r^2=0.18, p<0.0001) (Fig. 43)

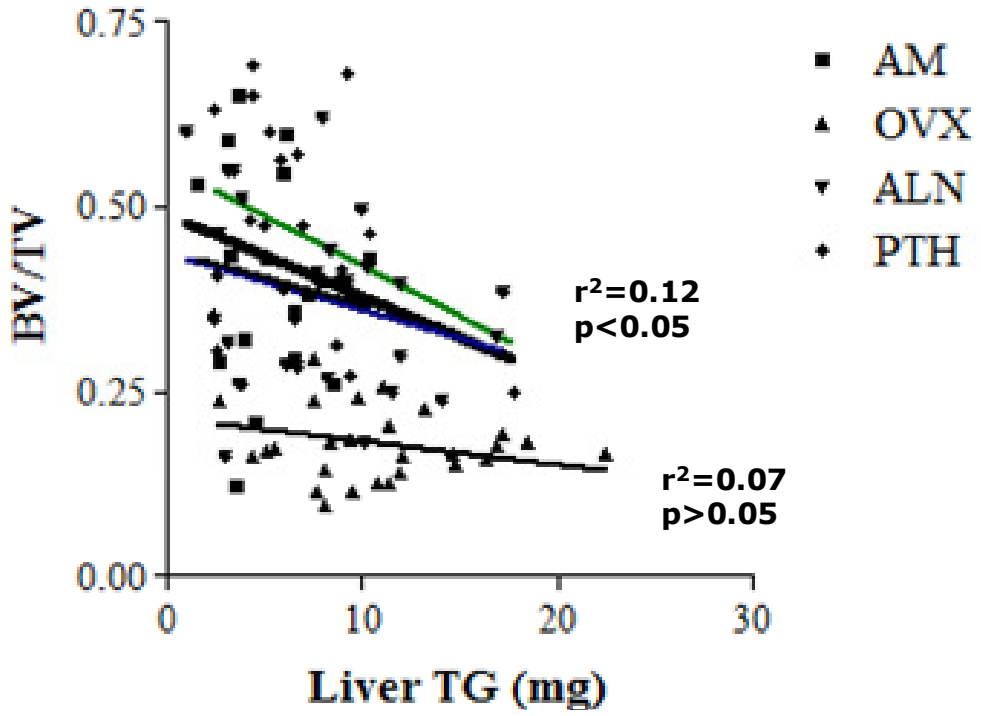

Figure 44. There was a negative relationship between BV/TV and Liver TG in AM Controls (Black squares, black line), ALN treated animals (Black –triangles, blue line) , PTH treated animals (black – diamonds, green line) or OVX pooled with L-PTH and L-NaF had low bone volume fraction with a large array of liver triglyceride content (Dark gray-diamonds, black line).

Bone volume fraction was negatively correlated to the triglyceride levels in the liver in AM controls (black line), PTH treated (green line) and ALN treated animals (blue line). When pooled there was a significant negative correlation. (r^2=0.12, p<0.05) There was no correlation in the combined dataset of OVX pooled with L-PTH and L-NaF. (r^2=0.07, p>0.05)

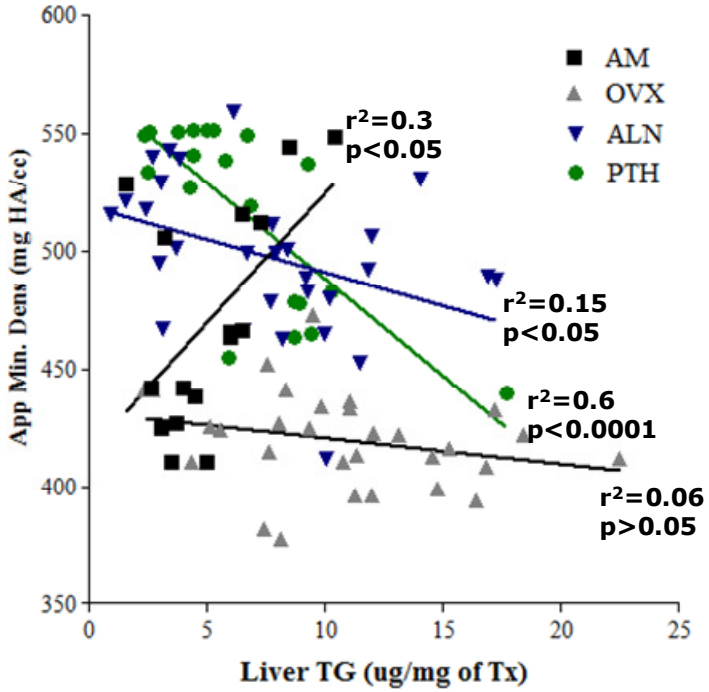

Figure 45. Apparent mineral density correlated to liver triglyceride content for all animals at 12 months of age. Animals were grouped as age matched controls pooled with high sodium fluoride (black - square), ovariectomy controls pooled with low sodium fluoride and low PTH (grey- triangle), H and M-PTH groups pooled (green - circle) and all alendronate treatments pooled (blue- triangle).

12 month AM controls pooled with H-NaF treated animals showed apparent mineral density was positively correlated to liver triglyceride content. (r^2=0.3, p=0.03) There was no relationship in OVX controls pooled with L-PTH and L-NaF groups. However, during H and M-PTH treatment, apparent mineral density was strongly and negatively correlated to triglyceride content. (r^2=0.57, p<0.001) H, M and L-ALN treatment also negatively correlated apparent mineral density with triglyceride content but the relationship was not as strong as that seen with PTH treatment. (r^2=0.15, p<0.05) PTH treatment had a significantly steeper negative slope than ALN treatment.(p=0.07) In both ALN and PTH treated animals, animals that responded the best to treatment, with the highest apparent mineral density had the lowest TG content in the liver. (Fig. 45)

4.5 DISCUSSION

Fat accumulation associated with menopause can have devastating consequences on fat metabolism and metabolic health (Poehlman, 1995). During menopause the reduction in estrogen causes an increase in body mass, visceral fat and tissue fat accumulation within organs (Heilbronn, 2004). Post-menopausal obesity is associated with reduced metabolic health and can result in reductions in bone mineral density and fracture (Nordin, 1992, Reid, 1992).

The effects of drug treatment on the cellular mechanisms responsible for adipogenesis were not elucidated during osteoporosis treatment. The data represented in this chapter can therefore not be assigned causation instead only represent associations between parameters of bone and fat and their interrelationship throughout osteoporosis drug treatment in the ovariectomized rat. Understanding the effects of drugs on the common progenitor of bone and fat cells, the mesenchymal stem cell would have been beneficial for understanding the effects of drugs on adipogenesis and will be considered during future work.

Body mass was positively correlated to fat pad mass as well as total fat volume. This indicates that larger animals had more fat than smaller animals. High doses of ALN and PTH had a similar relationship between body mass and fat volume but the amount of fat to body weight was reduced compared to AM controls at 12 months. This indicates that treatment affected the fat accumulation within individual animals, even if overall group differences in fat volume were not significantly reduced. In AM control animals, bone volume and bone density were positively correlated to body mass. Those with larger mass mechanically load their bones with higher mechanical forces and skeletal adaption increases the overall size of the skeleton to absorb these loads (Lanyon, 1996). Bone volume and bone density was severely affected by ovariectomy, which interrupted the healthy relationship between body mass and bone. OVX animals treated with high and medium dose osteoporosis drugs were successful at normalizing the relationship between body mass and bone volume as well as body mass and bone density; relationships were similar to those seen in healthy age matched controls. The relationship was strongest during high dose treatments.

The serum and liver metabolic levels were positively correlated to total fat volume and fat pad masses. This relationship was also seen in obesity studies and in patients with metabolic syndrome (Poehlman, 1995, Matthews, 1989). Body weight and fat content are good indicators for triglyceride, free fatty acids and leptin concentrations. Animals with higher fat content should have elevated levels of TG, NEFA and leptin demonstrating a reduction in metabolic health. This relationship between fat accumulation and TG, NEFA and leptin levels indicates the link between circulating concentrations and uptake and storage into adipose tissue. The body collects excess fatty acids, to prevent lipotoxicity, by sequestering free fatty acids by adipocytes and accumulate fat into adipose depots (Wu, 2007).

Increases in body weight, fat pad and total adipose tissue correlated to all parameters except serum NEFA concentrations. However this could be a result of hemolyzed samples used for NEFA determination or the use of heparin during blood collection which has been reported to interfere with the assay's enzymatic reaction. In general larger, fatter animals had higher metabolic parameters indicating the direct effect of weight gain, associated with post-menopausal osteoporosis as well as aging, on metabolic health.

Obesity has been shown to have detrimental effects on bone quality (Szulc, 2010, Luu, 2009). Indices of bone quality were determined through *ex vivo* μCT. The structural microarchitecture of trabecular bone was disrupted with ovariectomy, but was prevented with osteoporosis drug treatment. Apparent mineral density and bone volume fraction were both negatively correlated to parameters of tissue fat accumulation. Reid et. al, found that there is a positive relationship between total fat content and bone mineral density in pre-menopausal women, this correlation was independent of body mass or lean tissue mass. We saw similar results in bone volume fraction compared to triglyceride content in OVX with treatment as well as in AM controls.

Apparent mineral density was negatively correlated to fat content in both PTH and ALN treated animals. This indicates that treatment can directly improve bone health but also indirectly improve metabolic health. The animals that were affected the strongest, with the best bone mineral density and bone volume fraction also had the lowest metabolic numbers. This relationship does not determine causation, proposing that

decreasing triglyceride content would result in an increase in bone density would be incorrect. However, it does suggest that the treatments target increased osteogenic cellular processes and may indirectly decrease adipogenesis. It can be hypothesized that the common progenitor to both bone and fat cells, the mesenchymal stem cell, may be affected by ALN and PTH treatment. Ogita et. al found that PTH can differentiate periosteal osteoblast progenitor cells towards osteoblastic lineages. This indicates the implications of PTH on both bone and fat metabolism by modulation of the mesenchymal stem cell away from adipocyte lineage and towards osteogenic lineage (Ogita, 2008).

Long term osteoporosis drug use in the ovariectomized rat model improved indices of bone health but also reduced fat accumulation and prevented deterioration of metabolic health seen in ovariectomized control animals. Treatment normalized the relationship between bone and fat and created a negative association between indices of bone quality and fat content. The effects of osteoporosis drug treatment on post-menopausal bone loss and fat accumulation shows the benefits for osteoporosis as well as obesity. Drugs that can Increase bone quantity and quality while simultaneously decreasing tissue fat accumulation and improving fat metabolism would help in treatments for both osteoporosis and obesity and have therapeutic implications for millions of people.

CHAPTER 5

CONCLUSIONS

5.1 SUMMARY

Aging plays an important role in body mass and fat accumulation. Ovariectomy accelerates these changes and also decreases indices of bone quantity and quality. Alendronate, parathyroid hormone and sodium fluoride all worked at preventing losses to bone volume, density and microarchitecture. However, the drugs also influenced metabolic parameters and prevented fat accumulation throughout the body.

Current treatments of osteoporosis are commonly prescribed after bone loss has already occurred and fat mass has increased. By using these drugs as a preventative medicine, it may be possible to prevent the onset of bone loss related to estrogen withdrawal as well as to prevent fat accumulation. By using the drugs with the intention of targeting both bone and fat, treatments could help to reduce incidences of osteoporosis as well as obesity and type 2 diabetes. This type of prevention would be a promising therapeutic technique to help reduce health care costs and improve the overall health of an enormous population of people suffering from these diseases.

5.2 LIMITATIONS

The grant written for this study is focused on changes in bone quality as detected by changes in chemical composition as well as sub-micron-scale changes in microarchitecture through FTIR microscopy and nanoCT technologies. Since this research project attempts to understand how osteoporosis drugs affect metabolism and body composition there are several important pieces of information that would have been beneficial for a stronger understanding of the changes in bone quality and how quality relates to fat accumulation and metabolism.

Body weight parameters and *in vivo* microCT were used to determine changes in body composition throughout the study. However, there is no information on the metabolic activity during treatment. This information could have been collected by monitoring food intake to measure caloric intake during treatment duration. It is possible animals were heavier because of changes in metabolic indices and how food is processed, or simply because ovariectomized animals eat more food. Also, energy levels may be different in ovariectomy and ovariectomy with treatment. This could be measured

through calculating aerobic activity using metabolic cages with rat wheels to monitor exercise and activity levels. Ovariectomized rats may be more sedentary than healthy AM controls leading to increased body mass and decreased metabolic health.

A potential cause for reduced fat accumulation in treated animals is their exposure to daily or twice weekly injections. This could have caused an increase in metabolic activity. Injections were given during the day which is when rodents undergo their sleep cycle. The stress of the injection could have changed their activity levels, as well as introduced a period of exercise after receiving injections when animals are usually at rest. In order to determine whether this is the cause for reduced fat accumulation, a saline sham injection could have been given to all control animals, and all animals that did not receive injections. This way all animals would have received the same stimulus for the same number of days of the week. Because our low dose PTH treatment was ineffective at inducing bone formation it may be possible to elucidate the direct effects of injections on fat accumulation by considering this treatment dose as a saline control injection. Further analysis needs to be conducted to determine the overall implications of this missing control on the results of this study.

Indices of metabolic health could have been determined throughout the treatment period via blood draws to test for TG, NEFA and leptin in order to determine longitudinal changes throughout the study. One of the biggest limitations of this study is the comparison of metabolic parameters between time points. We did not have baseline readings for the individual animals, longitudinal differences would have given a more direct measurement of how concentrations changed throughout the course of treatment.

It would have been valuable to determine the effects of osteoporosis drugs on the stem cell population. This type of information would help to explain causation in some of the relationships we saw between bone and fat parameters. If the stem cell population was in fact affected by treatment, it would validate the hypotheses as to why there was a negative correlation between bone quality and triglyceride content during ALN and PTH treatment. Understanding the stem cell population would determine whether ALN and PTH are influencing mesenchymal stem cell differentiation through direct stimulation, during PTH treatment or perhaps indirectly through other cytokine signaling, during ALN treatment.

5.3 FUTURE DIRECTIONS

Bone quality and changes in fat metabolism are important concerns during extended long term osteoporosis pharmaceutical use. People need to consider the benefits as well as the risk of remaining on therapeutics to treat bone loss for long periods of time. A better understanding of long term drug use in the rat model will provide information for optimal recommendations of use in the clinical setting.

Bone quality was measured through trabecular architecture in this study. However, there are a variety of sources that provide a higher resolution of imaging as well as additional quantitative information. A study of different anatomical locations, including the femoral head, midshaft and diaphysis as well as the trabecular metaphysis will provide insight into site-specific drug related changes. Bone strength will be measured through a series of mechanical testing, from whole bone – to cortical bone samples – to nanoindentation.

Treatment induced changes in chemical composition in both cortical and trabecular bone will be conducted at Brookhaven National Labs (BNL) with the use of a Fourier Transfer Infrared Microscopy. This will provide valuable information on the potentially detrimental changes in bone's quality due to sodium fluoride treatment, as well as long term alendronate treatment. NanoCT conducted at BNL will provide changes in cortical architecture including differences between cortical pore size and number.

Bone's chemical, microarchitectural and mechanical properties during ovariectomy will provide insight into the role and affect that short and long term treatments play on bone quality. The data collected from this master's thesis has provided valuable information on fat accumulation and metabolic health of ovariectomized animals. With these data, it will be possible to draw conclusions on the interaction between bone quality and metabolic health in the ovariectomized rat model during osteoporosis treatment.

REFERENCES

Akerstrom G, Hellman P, Hessman O, Segersten U. Parathyroid glands in calcium regulation and human disease. Ann. N.Y. Acad. Sci. 2005. 1040: 53-58

Allan EH, Häusler KD, Wei T, Gooi JH, Quinn JM, Crimeen-Irwin B, Pompolo S, Sims NA, Gillespie MT, Onyia JE, Martin TJ. EphrinB2 regulation by PTH and PTHrP revealed by molecular profiling in differentiating osteoblasts. J Bone Miner Res. 2008. 23(8):1170-81.

Allen MR, Burr DB. Three years of Alendronate treatment results in similar levels of vertebral microdamage as after one year of treatment. JBMR. 2007. 22(11):1759-1765.

Allison DB, Gallagher D, Heo M, Pi-Sunyer FX, Heymsfield SB. Body mass index and all-cause mortality among people age 70 and over: the longitudinal study of aging. Int. J. of Obes. 1997. 21: 424-431.

Asiedu DK, Al-Shurbaji A, Rustan AC, Bjorkhem I, Berglund L, Berge RK. Hepatic fatty acid metabolism as a determinant of plasma and liver triaclycerol levels. Eur. J. Biochem. 1995. 227:715-722.

Aydin A, Sokal JE.Uptake of plasma free fatty acids by the isolated rat liver: effect of glucagon. 1962. 667-670.

Balena R, Toolan BC, Shea M, et al. The effects of 2-year treatment with the aminobisphosphonate alendronate on bone metabolism, bone histomorphometry, and bone strength in ovariectomized nonhuman primates. J Clin Invest. 1993. 92:2577-2586.

Benhamou C.L. Effects of osteoporosis medications on bone quality. Joint Bone Spine. 2007. 74:39-47.

Benjamin M, Hillen B. Mechanical influences on cells, tissues and organs - 'Mechanical Morphogenesis'. Eur J Morphol. 2003. 41(1):3-7.

Birnbaum RS, Bowsher RR, Wiren KM. Changes in IGF-I and –II expression and secretion during the proliferation and differentiation of normal rat osteoblasts. J Endocrinol. 1995. 144:251-259.

Bjornsson E. The natural history of drug-induced liver injury. Semin Liver Dis. 2009. 29: 357-363.

Black DM, Cummings SR, Karpf DB, Cauley JA, Thompson DE, Nevitt MC, Bauer DC, Genant HK, Haskell WL, Marcus R, Ott SM, Torner JC, Quandt SA, Reiss TF, EnsrudKE. Randomised trial of effect of alendronate on risk of fracture in women with existing vertebral fractures. Lancet. 1996. 348:1535–1541.

Black DM, Thompson DE, Bauer DC, Ensrud K, Musliner T, Hochberg MC, Nevitt MC, Suryawanshi S, Cummings SR, Fit RG. Fracture risk reduction with alendronate in women with osteoporosis: the Fracture Intervention Trial. J Clin Endocrinol Metab 2000. 85:4118–4124.
Bloomfield SA.Cellular and molecular mechanisms for the bone response to mechanical loading. Int J Sport Nutr Exerc Metab. 2000.11 Suppl: 128-136.

Bodenner D, Redman C, Riggs A. Teriparatide in the management of osteoporosis. Clin. Invest 2007. 2(4): 499-507.

Body JJ, Pfister P, Bauss F. Preclinical perspectives on bisphosphonate renal safety. The Oncologist 2005.10(1):3-7.

Bonewald LF, Johnson ML. Osteocytes, mechanosensing and Wnt signaling. Bone. 2008. 42(4):606-615.

Burger EH, Klein-Nulend J. Mechanotransduction in bone—role of the lacunocanalicular network. FASEB Journal 1999; S110 (13).

Burger E.H., Klein-Nulend J., Smit T.H. Strain-derived canalicular fluid flow regulates osteoclast activity in a remodeling osteon – a proposal. J. Biomech. 2003. 36(10): 1453-1459.

Burr D. Microdamage and bone strength. Osteoporosis Int. 2003a. 5(Suppl): 67-72.

Burr D, Miller L, Grynpas M, Li J, Boyde A, Mashiba T, et al. Tissue mineralization is increased following 1-year treatment with high doses of bisphosphonates in dogs. Bone. 2003b. 33:960-969.

Cao JJ, Sun L, Gao H.Diet-induced obesity alters bone remodeling leading to decreased femoral trabecular bone mass in mice. Ann N Y Acad Sci. 2010.1192(1):292-7.

Canalis E. The role of growth factors in skeletal remodeling. Endocrin. Metab. Clin. North Am. 1989. 18(4):903-918.

Canalis E. Insulin like growth factors and the local regulation of bone formation. Bone. 1993. 14:273-276.

Canalis E. Update in new anabolic therapies for osteoporosis. J Clin Endocrinol Metab. 2010. 95(4):1496-504.

Carmona R. The Obesity crisis in America, U.S. Surgeon General Testimony Before the Subcommittee on Education Reform Committee on Education and the Workforce. (Dept. of Health and Human Services, Washington D.C.) July 16, 2003.

Carter DR, Beaupré GS. Effects of fluoride treatment on bone strength. J Bone Miner Res. 1990. 5 Suppl 1:S177-84.

Casteilla L, Pénicaud L, Cousin B, Calise D.Choosing an adipose tissue depot for sampling: factors in selection and depot specificity. Methods Mol Biol. 2008. 456:23-38.

Centrella EM, Burch M, McCarthy TL. Insulin-like growth factor 1 mediates selective anabolic effects of parathyroid hormone in bone cultures. J. Clin Invest. 1989. 83: 60-65.

Choi JS, Song J. Effect of geistein on insulin resistance, renal lipid metabolism, and antioxidative activities in ovariectomized rats. Nutrition. 2009. 25:676-685.

Cifuentes M, Johnson MA, Leis RD, Heymsfield SB, Chowdhury HA, Modlesky CM. Bone turnover and body weight relationships differ in normal-weight compared with postmenopausal women. Osteo Int. 2004. 14(2):116-122.

Compston JE. Sex steroids and bone. Physiol Rev. 2001. 81:419-447.

Considine RV, Sinha MK, Leiman ML, Kriauciunas A, Stehpens TW, Nyce MR, Ohannesian JP, Marco CC, McKee LJ, Bauer TL, Caro JF. Serum immunoreactive-leptin concentrations in normal-weight and obese humans. New Eng. J. of Med. 1996. 334(5):292-296.

Constantz BR, Ison IC, Fulmer MT, Poser RD, Smith ST, VanWagoner M, Ross J, Goldstein SA, Jupiter JB, Rosenthal DI. Skeletal repair by in situ formation of the mineral phase of bone. Science. 1995. 267(5205):1796-9.

Cornish J, Costa JL, Naot D. The bone-fat mass relationship: laboratory studies. IBMS 2009; 6(9): 311-322.

Crannery A, Guyatt G, Griffith L, Wells G, Tugwell P, Rosen C, The osteoporosis group, and the osteoporosis research advisory group. Endocrine reviews 2002; 23(4):570-578.

Cummings SR, Black DM, Thompson DE, Applegate WB, Barrett-Connor E, Musliner TA, Palermo L, Prineas R, Rubin SM, Scott JC, Vogt T, Wallace R, Yates AJ, LaCroix AZ. Effect of alendronate on risk of fracture in women with low bone density but without vertebral fractures: results from the fracture intervention trial. JAMA. 280:2077–2082.

Cummings SR. How drugs decrease fracture risk: lessons from trials. J. Musculoskel Neuron Interact. 2002. 2(3):198-200.

Delmas P.D., Marin F., Marcus R., Misurski D.A., Mitlak B.H. Beyond hip: importance of other nonspinal fractures. Am. J. of Med. 2007. 120:381-387.

Dempster DW, Cosman F, Parisien M, Shen V, Lindsay R. Anabolic actions of parathyroid hormone on bone. Endocr Rev. 1993. 14: 690–709.

DeNino WF, Tchernof A, Dionne IJ, Toth MJ, Ades PA, Sites CK, Poehlman ET. Contribution of abdominal adiposity to age-related differences in insulin sensitivity and plasma lipids in healthy nonobese women. Diabetes Care. 2001. 24(5):925-32.

Deshaies Y, Dagnault A, Lalonde J, Richard D. Interaction of corticosterone and gonadal steroids on lipid deposition in the female rat. Am J Physiol Endocrinol Metab. 1997. 273:E355–62.

Diez JJ, Iglesias P. The role of the novel adipocyte-derived hormone adiponectin in human disease. Eur J of Endocrin. 2003. 148:293-300.

Dole VP. A relation between non-esterified fatty acids in plasma and the metabolism of glucose. 1955.150-154.

Duncan RL, Turner CH. Mechanotransduction and the functional response of bone to mechanical strain. Calcif Tissue Int. 1995. 57(5):344-58.

Egermann M, Goldhahn J, Schneider E. Animal models for fracture treatment in osteoporosis. Osteoporos Int. 2005.16(2):S129-S138.

Eriksen EF, Mosekilde L, Melsen F. Effect of sodium fluoride, calcium, phosphate and vitamin D on trabecular bone balance and remodeling in osteoporotics. Bone. 1985. 6:381–389.

Eriksen EF, Hodgson SF, Eastell R, Cedel SL, O'Fallon WM, Riggs BL. Cancellous bone remodeling in type 1 (postmenopausal) osteoporosis: quantitative assessment of rates of formation, resorption, and bone loss at tissue and cellular levels. J Bone Miner Res. 1990.5:311-319.

Fleisch H. Bisphosphonates: Mechanisms of action. Endocrine Reviews. 1998. 19(1): 80-100.

Folch J, Ascoli I, Lees M, Meath JA, LeBaron FN. Preparation of lipid extracts from brain tissue. J Biological Chem. 1951. 833-841.

Fox J, Miller MA, Newman MK, Metcalfe AF, Turner CH, Recker RR, Smith SY. Daily treatment of aged ovariectomized rats with human parathyroid hormone (1-84) for 12 months reverses bone loss and enhances trabecular and cortical bone strength. Calcif Tissue Int.. 2006. 79:262-272.

Friedl G, Turner RT, Evans GL, Dobnig H. Intermittent parathyroid hormone (PTH) treatment and age-dependent effects on rat cancellous bone and mineral metabolism. J Orth Res. 2007. 11:1454-1463.

Fuchs RK, Phipps RJ, Burr DB. Recovery of trabecular and cortical bone turnover after discontinuation of risedronate and alendronate therapy in ovariectomized rats. JBMR 2008. 23:1689-1697.

Gallagher JC, Goldgar D, Moy A. Total bone calcium in normal women: effect of age and menopause status. JBMR 1987. 2(6): 491-496.

Garnero P. Biochemical markers of bone turnover, endogenous hormones and the risk of fractures in postmenopausal women: the OFELY study. JBMR 2000. 15: 1526-1536.

Gastadelli A, Miyazaki Y, Pettiti M, Matsuda M, Mahankali S, Santani E, Defronzo RA, Ferrannini E. Metabolic Effects of Visceral Fat Accumulation in Type 2 Diabetes J of Clin Endocrin Metab 2002. 87(11):5098–5103.

Garthwaite SM, Cheng H, Bryan JE, Craig BW, Holloway JO. Ageing exercise and food restriction: effects on body composition. Mechanisms of aging and development. 1986. 36:187-196.

Gazzerro E, Canalis E. Skeletal actions of insulin-like growth factors. Expert Rev Endocrinol Metab. 2006. 1:47–56.

Gevers EF, Loveridge N, Robinson ICAF. Bone Marrow Adipocytes: A neglected target tissue for growth hormone. Endocrinology. 2002. 143(10):4065-4073.

Gimble JM, Zvonic S, Floyd ZE, Kassem M, Nuttall ME. Playing with bone and fat. J Cell Biochem. 2006. 98:251-266.

Gimble JM. The function of adipocytes in the bone marrow stroma: an update. Bone. 1996. 421-426.

Giustina A, Mazziotti G, Canalis E. Growth hormone, insulin-like growth factors, and the skeleton. Endocr Rev. 2008. 29:535–559.

Goodpaster BH, Krishnaswami S, Harris TB, Katsiaras A, Kritchevsky SB, Simonsick EM, Nevitt M, Holvoet P, Newman AB. Obesity, regional body fat distribution, and the metabolic syndrome in older men and women. Arch Intern Med. 2005. 165(7):777-83.

Gordon T, Kannel WB, Hjortland MC, McNamara PM. Menopause and coronary heart disease. The Framingham Study. Ann Intern Med. 1978;89:157-61.

Greenspan SL, Bone HG, Ettinger MP, Hanley DA, Lindsay R, Zanchetta JR, Blosch CM, Mathisen AL, Morris SA, Marriott TB. Effect of recombinant human parathyroid hormone (1-84) on vertebral fracture and bone mineral density in postmenopausal women with osteoporosis. Ann Intern Med. 2007. 146:326-339.

Grinspoon S, Baum H, Lee K, Anderson E, Herzog D, Klibanski A. Effects of short-term recombinant human insulin-like growth factor 1 administration on bone turnover in osteopenic women with anorexia nervosa. J Clin Engodcrin Metab. 1996. 81(11):3864-3870.

Guo W, Pirtskhalava T, Tchkonia T, Xie W, Thomou T, Han J, Wang T, Wong S, Cartwright A, Hegardt FG, Corkey BE, Kirkland JL: Aging results in paradoxical susceptibility of fat cell progenitors to lipotoxicity. Am J Physiol Endocrinol Metab. 2007. 292: 1041– 1051.

Haguenauer D, Welch V, Shea B. Fluoride for the treatment of postmenopausal osteoporotic fractures: a metaanalysis. Osteoporos Int. 2000. 11:727–738.

Heaney RP. Estrogen-calcium interactions in the postmenopause: a quantitative description. Bone Miner. 1990. 11(1):67-84.

Heilbronn L, Smith SR, Ravussin E. Failure of fat cell proliferation, mitochondrial function and fat oxidation results in ectopic fat storage, insulin resistance and type II diabetes mellitus. Int J Obes Relat Metab Disord. 2004. 28(Suppl 4):S12–S21.

Heindel J.J., Bates H.K, Price C.J., Marr M.C., Myers C.B. Schwetz B.A. Developmental toxicity evaluation of sodium fluoride administered to rats and rabbits in drinking water. Fund. and App. Tox. 1996. 30(2): 162-177.

Hewitt KN, Boon WC, Murata Y, Jones ME, Simpson ER. The Aromatase Knockout Mouse Presents with a Sexually Dimorphic Disruption to Cholesterol Homeostasis. Endocrin. 2003. 144(9):3895–3903.

Hill PA, Reynolds JJ, Meikle MC. Osteoblasts mediate insulin-like growth factor-I and –II stimulation of osteoclast formation and function. Endocrinol. 1995. 136:124-131.

Hock JM. Anabolic actions of PTH in the skeletons of animals. J Musculo Neuron Interact. 2001. 2(1): 33-47.

Hodsman AB, Hanley DA, Ettinger MP, Bolognese MA, Fox J, Metcalfe AJ, Lindsay R. Efficacy and safety of human parathyroid hormone-(1-84) in increasing bone mineral density in postmenopausal osteoporosis. J Clin Endocrinol Metab. 2003. 88:5212-5220.

Holloway PW. Desaturation of long-chain fatty acides by animal liver. Methods Enzymol 31:253-262.

Holloway WR, Collier FM, AitkenCJ, Myers DE, Hodge JM, Malakellis M, et al. Leptin inhibits osteoclast generation. JBMR 2002; 17:200-209.

Horowitz MJ, Tedesco MB, Gundberg C, Garcia-Ocana A, Stewart AF. Short-term, high-dose parathyroid hormone-related protein as a skeletal anabolic agent for the treatment of postmenopausal osteoporosis. J Clin Endocrinol Metab 2003; 88:569–575.

Hughes DE, Wright KR, Uy HL, Sasaki A, Yoneda T, Roodman GD, Mundy GR, Boyce BF. Biphosphonates promote apoptosis in murine osteoclasts in vitro and in vivo. JBMR. 1995. 10(10): 1478 – 1487.

Hughes DE, Dai A, Tiffee JC, Li HH, Mundy GR, Boyce BF. Estrogen promotes apoptosis of murine osteoclasts mediated by TGF-beta. Nat Med. 1996. 2(10):1132-6.

Hughes VA, Roubenoff R, Wood M, Frontera WR, Evans WJ, Fiatarone Singh MA. Anthropometric assessment of 10-y changes in body composition in the elderly. Am J Clin Nutr 2004. 80(2):475-82.

Iwaniec U.T. Trevisiol C.H., Maddalozzo G.F., Rosen C.J., Turner.H. Effects of low-dose parathyroid hormone on bone mass, turnover, and ectopic osteoinduction in a rat model for chronic alcohol abuse. Bone. 2008. 42: 695–701

Iwata K, Li J, Follet H, Phipps RJ, Burr DB Bisphosphonates suppress periosteal osteoblast activity independently of resorption in rat femur and tibia. Bone 2006. 39:1053-1058.

Jiang Y. Zhao J.J., Mitlak B.H., Wang O., Genant H.K. Eriksen E.F. Recombinant human parathyroid hormone (1-34) [Teriparatide] improves both cortical and cancellous bone structure. JBMR. 2003. 18(11): 1932-1941.

Jilka RL 2007 Molecular and cellular mechanisms of the anabolic effect of intermittent PTH. Bone 40:1434–1446

Judex S., Luu K., Ozcivici E., Adler B., Lublinski S., Rubin C. Analysis of visceral and subcutaneous adiposity via micro-computer tomography. Scanco medical application note.

Kalu DN. The ovariectomized rat model of postmenopausal bone loss. Bone Miner. 1991. 15(3):175-91.

Kanazawa I. Yamuguchi T., Yammamoto M. Yamauchi M. Yano S., Toshitsugu S. Serum osteocalcin/bone-specific alkaline phosphatase ratio is predictor for the presence of vertebral fractures in men with type 2 diabetes. Calcif. Tiss. Int. 2009. 85: 228-234.

Karim R, Mack WJ, Hodis HN, Roy S, Stanczyk FZ. Influence of age and obesity on serum estradiol, estrone, and sex hormone binding globulin concentrations following oral estrogen administration in postmenopausal women. J Clin Endocrinol Metab. 2009 . 94(11):4136-43.

Ke H.Z., Chen H.K., Simmons H.A., Qi H., Crawford D.T., Pirie C.M., Chidsey-Frink K.L., Ma Y.F., Jee W.S.S., Thompson D.D. Comparative effects of Droloxifene, Tamoxifen, and Estrogen on bone, serum cholesterol, and uterine histology in the ovariectomized rat model. Bone 1997. 20(1):31-39.

Kelley DE, Thaete FL, Troost F, Huwe T,Goodpaster BH: Subdivisions of subcutaneous abdominal adipose tissue and insulin resistance. Am J Physiol Endocrinol Metab 2000; 278:941–948.

Khosla S, Atkinson EJ, Riggs BL, Melton LJ III. Relationship between body composition and bone mass in women. J Bone Miner Res. 1996. 11:857–863.

Kim C.H., Takai E., Zhao J., Stechow D.V., Muller R., Dempster D.W., Guo X.E. Trabecular bone response to mechanical and parathyroid stimulation. The role of the mechanical microenvironment. JBMR. 2003. 18(12): 2116-2125.

Kneissel M., Boyde A., Gasser J.A. Bone tissue and its mineralization in aged estrogen-depleted rats after long-term intermittent treatment with parathyroid hormone (PTH) analog SDZ PTH 893 or human PTH(1-34). Bone. 2001. 28(3): 237-250.

Kopelman P. Symposium 1: Overnutrition: consequences and solutions: Foresight Report: the obesity challenge ahead. Proc Nutr Soc. 2010 Feb;69(1):80-5.

Kulkarni NH, Wei T, Kumar A, Dow ER, Stewart TR, Shou J, N'cho M, Sterchi DL, Gitter BD, Higgs RE, Halladay DL, Engler TA, Martin TJ, Bryant HU, Ma YL, Onyia JE. Changes in osteoblast, chondrocyte, and adipocyte lineages mediate the bone anabolic actions of PTH and small molecule GSK-3 inhibitor. J Cell Biochem. 2007. 102(6):1504-18.

Kyle U.G., Hans D., Karsegard L. Slosman D.O. Pichard C. Age-related differences in fat-free mass, skeletal muscle, body cell mass and fat mass between 18 and 94 years. Eur. J. Clin. Nutrition. 2001. 55:663-672.

Kyung TW, Lee JE, Phan TV, Yu R, Choi HS. Osteoclastogenesis by bone marrow-derived macrophages is enhanced in obese mice. J. Nutr 2009. 139:502-506.

Laet C De.., J.A. Kanis A. Ode´n H. Johanson O. Johnell P. Delmas J.A. Eisman H. Kroger S. Fujiwara P. Garnero E.V. McCloskey D. Mellstrom L.J. Melton 3rd P.J. Meunier H.A.P. Pols J. Reeve A. Silman A. Tenenhouse. Body mass index as a predictor of fracture risk: A meta-analysis. Osteoporos Int. 2005. 16: 1330–1338

Lanyon, L. E. 1996 Using functional loading to influence bone mass and architecture: Objectives, mechanisms, and relationship with estrogen of the mechanically adaptive process in bone. Bone. 1996. 18:37S-43S.

Lafage M.., Balena R., Battle M.A., Shea M., Seedor J.G., Klein H., Hayes W.C., Rodan G.A. Comparison of alendronate and sodium fluoride effects on cancellous and cortical bone in minipigs. J. Clin. Invest. 1995. 95: 2127-2133.

Lelovas PP, Xanthos TT, Thoma SE, Lyritis GP, Dontas IA. The laboratory rat as an animal model for osteroporosis research. Comparative Med. 2008. 58(5): 424-430.

Lemieux C., Picard F., Labrie F., Richard D., Deshaies Y. The estrogen antagonist EM-652 and dehydroepiandrosterone prevent diet- and ovariectomy- induced obesity. Obesity Research. 2003. 11:477-490.

Lewis J.R., Mohanty S.R. Nonalcoholic fatty liver disease: A review and update. Dig Dis Sci. 2010. 55: 560-578.

Lindsay R. Fluoride and bone--quantity versus quality. N Engl J Med. 1990. 22;322(12):845-6.

Lindsay R., Nieves J., Formica C., Henneman E., Woelfert RN, Shen V., Dempster D, Cosman F. Randomised controlled study of effect of parathyroid hormone on vertebral-bone mass and fracture incidence among postmenopausal women on oestrogen with osteoporosis. 2000.

Loveridge N. Bone: more than a stick. J Anim Sci. 1999. 77(2):190-6.

Lublinski S., Luu Y.K., Rubin C.T., Judex S. Automated Seperation of visceral and subcutaneouse adiposity in In vivo microcomputed topographies of mice. J. Dig. Imaging 2009. 22(3):222-231.

Lublinski S., Ozcivici E., Judex S. An automated algorithm to detect the trabecular-cortical bone interface in micro-computed tomographic images. Calcif Tissue Int. 2007.

Luu Y.K., Capilla E., Rosen C.K., Gilsanz V., Pessin J.E., Judex S., Rubin C.T. Mechanical stimulation of mesenchymal stem cell proliferation and differentiation promotes osteogenesis while preventing dietary-induced obesity. JBMR. 2009. 24(1): 50-61.

Malaval L. Modrowski D., Gupta A.K., Aubin J.E. Cellular expression of bone-related proteins during in vitro osteogenesis in rat bone marrow stromal cell cultures. J. Cell. Physiol. 1994. 158:555-572.

Manolagas S.C., Jilka R.L. Bone marrow, cytokynes, and bone remodeling. Emerging insights in the pathophysiology of osteoporosis. NEJM. 1995. Vol 332(5): 305-311.

Manson JE, Martin KA, Postmenopausal hormone-replacement therapy. N Engl J Med. 2001. 345:34-40.

Mantzoros CS. The role of leptin in human obesity and disease: areview of current evidence. Annals of Internal Medicine. 1999. 130: 651–657.

Marcus R, Greendale G, Blunt BA, Bush TL, Sherman S, Sherwin R, Wahner H, Wells B Correlates of bone mineral density in the postmenopausal estrogen/progestin interventions trial. J Bone Miner Res. 1994. 9:1467–1476.

Marshall D, Johnell O, Wedel H. Meta-analysis of how well measures of bone mineral density predict occurrence of osteoporotic fractures. BMJ. 1996. 312(7041):1254-9.
Martin RB, Zissimos SL Relationships between marrow fat and bone turnover in ovariectomized and intact rats. Bone. 1991. 12:123–131

Matthews KA, Meilahn E, Kuller LH, Kelsey SF, Caggiula AW, Wing RR. Menopause and risk factors for coronary heart disease. N Engl J Med. 1989;321:641-6.

Mazariegos M, Wang ZM, Gallagher D, Baumgartner RN, Allison DB, Wang J, Pierson RN Jr, Heymsfield SB.Differences between young and old females in the five levels of body composition and their relevance to the two-compartment chemical model. J Gerontol. 1994. 49(5):M201-8.

Mazess RB, Barden HS, Ettinger M, Johnston C, Dawson- Hughes B, Baran D, Powell M, Notelovitz M 1987 Spine and femur density using dual-photon absorptiometry in US white women. Bone Miner 2:211–219.

Messinis IE, Milingos SD, Alexandris E, Kariotis I, Kollios G, Seferiadis K. Leptin concentrations in normal women following bilateral ovariectomy. Hum Reprod 1999. 14:913–18.

Meunier P, Aaron J, Edouard C, Vignon G. Osteoporosis and the replacement of cell populations of the marrow by adipose tissue. A quantitative study of 84 iliac bone biopsies. Clin Orthop 1971. 80:147-154

Mochizuki H, Hakeda Y, Wakatsuki N, Usui N, Akashi S, Sato T, Tanaka K, Kumegawa M Insulin-like growth factor-I supports formation and activation of osteoclasts. Endocrinology 1992. 131:1075–1080

Mori S., Burr D.B. Increased Intracortical remodeling following fatigue damage. Bone. 1993. 14(2):103-109.

Mosekilde L, Thomsen JS, Mackey MS, Phipps RJ 2000 Treatment with risedronate or alendronate prevents hind-limb immobilization-induced loss of bone density and strength in adult female rats. Bone27:639-645.

Mudali S., Dobs A.S. Effects of testosterone on body composition of the aging male. Mech. Of aging and Devel. 2004. 124:297-304.

Mulgund M, Beattie KA, Wong AKO, Papaioannou A, Adachi JD. Assessing adherence to teriparatide therapy, causes of nonadherence and effect of adherence on bone mineral density measurements in osteoporotic patients at high risk for fracture. Therapeutic Advances in Musculoskeletal Disease 2009; 1:5-11.

Nancollas GH, Tang R, Phipps RJ, Henneman Z, Gulde S, Wu W, Mangood A, Russell RG, Ebetino FH. Novel insights into actions of bisphosphonates on bone: differences in interactions with hydroxyapatite. Bone. 2006. 38(5):617-27.

National Center for Health Statistics. 2004. Survey.
www.cdc.gov/nchs/products/pubd/hestats/obese/obse99.htm. Accessed April 2010

National Toxicology Program. NTP Toxicology and Carcinogenesis Studies of Sodium Fluoride (CAS No. 7681-49-4)in F344/N Rats and B6C3F1 Mice (Drinking Water Studies). Natl Toxicol Program Tech Rep Ser. 1990 Dec;393:1-448.

Neer RM, Arnaud CD, Zanchetta JR, Prince R, Gaich GA, Reginster JY, Hodsman AB, Eriksen EF, Ish-Shalom S, Genant HK, Wang O, Mitlak BH Effect of parathyroid hormone (1-34) on fractures and bone mineral density in postmenopausal women with osteoporosis. N Engl J Med 2001. 344:1434-1441.

Nepokroeff C.M., Lakshmanan M.R., Porter J.W. Fatty-acid synthase from rat liver. Methods Enzymol. 1975. 6:37-44.

NIAMS: National Institutes of Health, Osteoporosis and Related Bone Diseases. Osteoporosis Overview. May 2009.

Noble, B. S., H. Stevens, N. Loveridge, and J. Reeve.. Identification of apoptotic changes in osteocytes in normal and pathological human bone. Bone. 1997. 20:273-282.

Nordin C. Need A.G., Bridges A., Horowitz M. Relative contributions of years since menopause, age and weight to vertebral density in postmenopausal women. J. Clin. Endo. And metab. 1992. 74(1): 20-23.

Nuttall ME, Gimble JM Is there a therapeutic opportunity to either prevent or treat osteopenic disorders by inhibiting marrow adipogenesis? Bone 2000. 27:177–184

Ogita M, Rached MT, Dworakowski E, Bilezikian JP, Kousteni S. Differentiation and proliferation of periosteal osteoblast progenitors are differentially regulated by estrogens and intermittent parathyroid hormone administration. Endocrinology. 2008. 149(11):5713-23.

Oktem M., Atar I., Zeyneloglu H.B., Yildirir A., Kuscu E., Muderrisoglu H. Raloxifene has favorable effects on metabolic parameters but has no effect on left ventricular function in postmenopausal women. Pharm. Research. 2008. (57) 364-368.

O'Sullivan AJ, Martin A, Brown MA. Efficient fat storage in premenopausal women and in early pregnancy: a role for estrogen. J Clin Endocrinol Metab 2001. 86:4951-4956

Ott S. Long-term safety of bisphosphonates. J Clin Endocrinol Metab 2005. 90:1897-9

Paula de F.J.A., Rosen C.J. Back to the future: revisiting parathyroid hormone and calcitonin control of bone remodeling. Horm. Metab. Res. 2010.

Parfitt AM. Bone-forming cells in clinical conditions. In: Hall BK, ed. The osteoblast and osteocyte. Vol. 1 of Bone. Boca Raton, Fla.: Telford Press/ CRC Press, 1990. 351-429.

Parfitt AM. Osteonal and hemi-osteonal remodeling: the spatial and temporal framework for signal traffic in adult human bone. J Cell Biochem 1994. 55:273-286

Parfitt AM The bone remodeling compartment: a circulatory function for bone lining cells. J Bone Miner Res. 2001. 16:1583–1585

Peter C, Rodan GA. Preclinical safety profile of alendronate. Int J Clin Pract. 1999. Suppl 101:3-8.

Petzel M. Action of leptin on bone and its relationship to menopause. Biomed Pap Med Fac. 2007. 151(2):195-199.

Poehlman ET, Toth MJ, Gardner AW. Changes in energy balance and body composition at menopause: a controlled longitudinal study. Ann Intern Med. 1995. 123(9):673-5.

Pols HA, Felsenberg D, Hanley DA, Stepa´n J, Mun˜ oz-Torres M, Wilkin TJ, Qin-sheng G, Galich AM, Vandormael K, Yates AJ, Stych B, for the Fosamax International Trial Study Group Multinational, placebo-controlled, randomized trial of the effects of alendronate on bone density and fracture risk in postmenopausal women with low bone mass: results of the FOSIT study. Osteoporos Int. 1999. 9:461–468

Price E.A. Aging and erythropoiesis: Current state of knowledge Blood Cells, Molecules, and Diseases 2008. 41:158–165

Qu H, Wie M. The effect of fluoride contents in fluoridated hydroxyapatite on osteoblast behavior. Acta Biomater. 2006. 2:113–119

Ravn P, Cizza G, Bjarnason NH, Thompson D, Daley M, Wasnich RD, McClung M, Hosking D, Yates AJ, Christiansen C Low body mass index is an important risk factor for low bone mass and increased bone loss in early postmenopausal women. Early Postmenopausal Intervention Cohort (EPIC) study group. J Bone Miner. 1999. Res 14:1622–1627.

Recker R, Lappe J, Davies KM, Heaney R Bone remodeling increases substantially in the years after menopause and remains increased in older osteoporosis patients. J Bone Miner Res. 2004. 19: 1628–1633

Recker R, Masarachia P, Santora A, Howard T, Chavassieux P, Arlot M. Trabecular bone microarchitecture after alendronate treatment of osteoporotic women. Curr Med Res Opin 2005. 21:185-194.

Reid I.R.. Relationships between fat and bone. Osteoporos Int 2008. 19:595-606.

Reid IR, Ames R, Evans MC, Sharpe S, Gamble G, France JT, Lim TM, Cundy TF Determinants of total body and regional bone mineral density in normal postmenopausal women—a key role for fat mass. J Clin Endocrinol Metab. 1992. 75:45–51.

Reid IR, Plank LD, Evans MC. Fat mass is an important determinant of whole body bone density in premenopausal women but not in men. J Clin Endocrinol Metab. 1992 Sep;75(3):779-82.

Richard D. Effects of ovarian hormones on energy balance and brown adipose tissue thermogenesis. Am J Physiol Regul Integrative Comp Physiol. 1986. 250:R245–9.

Rickard DJ, Wang FL, Rodriguez-Rojas AM, Wu Z, Trice WJ, Hoffman SJ, Votta B, Stroup GB, Kumar S, Nuttall ME. Intermittent treatment with parathyroid hormone (PTH) as well as a non-

peptide small molecule agonist of the PTH1 receptor inhibits adipocyte differentiation in human bone marrow stromal cells. Bone. 2006. 39(6):1361-72.

Riggs BL, Hodgson SF, Hoffman DL, Kelly PJ, Johnson KA, Taves D. Treatment of primary osteoporosis with fluoride and calcium. Clinical tolerance and fracture occurrence. JAMA. 1980 1;243(5):446-9.

Riggs BL, Seeman E, Hodgson SF, Taves DR, O'Fallon WM. Effect of the fluoride/calcium regimen on vertebral fracture occurrence in postmenopausal osteoporosis. Comparison with conventional therapy. N Engl J Med. 1982. 306(8):446-50.

Riggs BL, Hodgson SF, O'Fallon WM, Chao EY, Wahner HW, Muhs JM, Cedel SL, Melton LJ Effect of fluoride treatment on the fracture rate in postmenopausal women with osteoporosis. N Engl J Med. 1990.322:802-809.

Rodan G.A. The effects of 2-year treatment with the aminobisphosphonate alendronate on bone metabolism, bone histomorphometry, and bone strength in ovariectomized nonhuman primates. J Clin. Invest. 1993. 92: 2577-2586.

Rosen C.J., Donahue LR, Hunter SJ. Insulin-like growth hormone and bone: the osteoporosis connection. Proc Soc Exp Biol Med 1994. 206:83-102

Rosen C.J. What's new with PTH in osteoporosis: where are we and where are we headed? Trends Endocrinol Metab. 2004. 15:229-233.

Rosen C.J., Bouxsein M.L., Mechanism of disease: is osteoporosis the obesity of bone? Nature Clinical Prac. 2006. 2(1): 35-43.

Rosenbaum M., Nicolson M, Hirsch J, Heymsfield SB,Gallagher D, Chu F, Leibel RL. Effects of gender, body composition, and menopause on plasma concentrations leptin. J Clin Endocrinol Metab. 1996;81:3424–3427.

Rubin C.T., Turner AS, Muller R, Mittra E, McLeod K, Lin W, Qin YX Quantity and quality of trabecular bone in the femur are enhanced by a strongly anabolic, noninvasive mechanical intervention. J Bone Miner Res 17. 2002. 349-357

Rubin C.T. Lanyon L.E. Kappa delta award paper. Osteoregulatory nature of mechanical stimuli: function as a determinant for adaptive remodeling in bone. J. Orthop. Res. 1987. 5(2): 300-310.

Rubin C.T., Capilla E., Luu Y.K., Busa B., Crawford H., Nolan D.J., Mittal V., Rosen C.J., Pessin J.E., Judex S. Adipogenesis is inhibited by brief, daily exposure to high-frequency, extremely low-magnitude mechanical signals. PNAS. 2007. 104: 17879-17884.

Saag KG, Zanchetta JR, Devogelaer JP, Adler RA, Eastell R, See K, Krege JH, Krohn K, WarnerMR. Effects of teriparatide versus alendronate for treating glucocorticoid-induced osteoporosis: thirtysix- month results of a randomized, double-blind, controlled trial. Arthritis Rheum 2009. 60:3346–3355

Sama AA, Khan SN, Myers ER, Huang RC, Cammisa FP, Jr., Sandhu HS, Lane JM High-dose alendronate uncouples osteoclast and osteoblast function: a study in a rat spine pseudarthrosis model. Clin Orthop Relat Res. 2004. 135-142.

Sebastian J. Schambach A., Simona Bag A, Lothar Schilling B, Christoph Groden, Marc A. Brockmann. Application of micro-CT in small animal imaging. Methods. 2010. 50: 2–13

Seeman E, Delmas PD, Hanley DA, Sellmeyer D, Cheung AM, Shane E, Kearns A, Thomas T, Boyd SK, Boutroy S, Bogado C, Majumdar S, Fan M, Libanati C, Zanchetta J. Microarchitectural deterioration of cortical and trabecular bone: Differing effects of denosumab and alendronate. J Bone Miner Res. 2010.

Sepe A. Tchkonia T., Thomou. Zamboni M. Aging and regional differences in fat cell progenitors – a mini review. Gerentology. 2010.

Shapses S.A., Bone turnover and body weight relationships differ in normal-weight compared with heavier postmenopausal women. Osteoporos. Int. 2003. 14:116-22.

Shapses S.A., Riedt C.S. Bone, body weight, and weight reduction: What are the concerns? J. Nutrition 2006.1453-1456.

Shinoda M., Latour M.G., Lavoie J.M. Effects of physical training on body composition and organ weights in ovariectomized and hyperestrogenic rats.Int. J. of Obesity 2002. 26:335-343.

Skerry TM, Bitensky L, Chayen J, Lanyon LE. Early strain-related changes in enzyme activity in osteocytes following bone loading in vivo. J Bone Miner Res. 1989. 4(5):783-8.

Sogaard CH, Mosekilde L, Thomsen JS, Richards A, McOsker JE A comparison of the effects of two anabolic agents (fluoride and PTH) on ash density and bone strength assessed in an osteopenic rat model. Bone. 1997. 20:439-449.

Sogaard CH, Richards A, Mosekilde L. Marked decrease in trabecular bone quality after five years of sodium fluoride therapy - assessed by biomechanical testing of iliac crest bone biopsies in osteoporotic patients. Bone. 1994.15:393–399.

Sorensen MB, Rosenfalck AM, Hojgaard L, Ottesesn B. Obesity and sarcopenia after menopause are reversed by sex-hormone therapy. Obes Res. 2001. 9:622-626.

Sowers M.R., Wildman R.P., Mancuso P., Eyvazzadeh A.D., Karvonen-Gutierrez C.A., Rillamas-Sun E., Jannausch M.L. Change in adipocytokines and ghrelin with menopause. Maturitas. 2008. 59: 149-157.

Stepan JJ, Burr DB, Pavo I, Sipos A, Michalska D, Li J, Fahrleitner-Pammer A, Petto H, Westmore M, Michalsky D, Sato M, Dobnig H. Low bone mineral density is associated with bone microdamage accumulation in postmenopausal women with osteoporosis. Bone. 2004. 41(3):378-85.

Suda T. Takahashi N., Martin T.J. T. Modulation of Osteoclast Differentiation Endocrine Reviews. 1992. 13(1):69-80.

Suda T. Takahashi N. Udagawa N., Jimi E., Gillespie M.T., Martin J.T. Modulation of Osteoclast Differentiation and Functionby the New Members of the Tumor Necrosis Factor Receptor and Ligand Families. Endocrine Reviews 20(3): 345–357

Szulc P., Vaennes A., Delmas P.D., Goudable J., Chapuriat R., Men with metabolic syndrome have lower bone mineral density but lower fracture risk – the MINOS study. JBMR. 2010. 13.

Tchernof A, Poehlman ET, Despres JP. Body fat distribution, the menopause transition, and hormone replacement therapy. Diabetes Metab. 2000;26:12–20.

Tchkonia T, Corkey BE, Kirkland JL: Current views of the fat cell as an endocrine cell:lipotoxicity. Endocrine Updates 2006; 26: 105–118

Thomas T, Gori F, Khosla S, Jensen MD, Burguera B, Riggs BL. Leptin acts on human marrow stromal cells to enhance differentiation to osteoblasts and to inhibit differentiation to adipocytes. Endocrinology 1999; 140:1630-1638.

Thomsen J.S. Mosekilde L.I. Gasser J.A. Long-term therapy of ovariectomy-induced osteopenia with Parathyroid Hormone analog SDZ PTS 893 and bone maintenance in retired breeder rats. Bone 1999. 25(4):561-569.

Tiniakos DG, Vos MB, Brunt EM.Nonalcoholic fatty liver disease: pathology and pathogenesis. Annu Rev Pathol. 2010;5:145-71. Review.

Tomkinson A, Gevers EF, Wit JM, Reeve J, Noble BS. The role of estrogen in the control of rat osteocyte apoptosis. J Bone Miner Res. 1998. (8):1243-50.

Tomkinson A, Reeve J, Shaw RW, Noble BS. The death of osteocytes via apoptosis accompanies estrogen withdrawal in human bone. J Clin Endocrinol Metab. 1997. 82(9):3128-35.

Tommasini SM, Nasser P, Schaffler MB, Jepsen KJ. Relationship between bone morphology and bone quality in male tibias. J Bone Miner. Res. 2005;20:1372e80.

Travison T.G., Araugo A.B., Esch G.R. The relationship between body composition and bone mineral content: threshold effects in a racially and ethnically diverse group of men. Osteop. Int. 2008. 19:29-38.

Trayhurn P & Beattie JH. Physiological role of adipose tissue: white adipose tissue as an endocrine and secretory organ. Proceedings of the Nutrition Society 2001. 60 329–339.

Turner CH. Biomechanics of bone: determinants of skeletal fragility and bone quality. Osteoporosis Int. 2002;13:97e104.

Uusi-Rasi K., Sievanen H., Kannus P., Pasanen M., Kukkonen-Harjula K., Fogelholm M. Influence of weight reduction on muscle performance and bone mass, structure and metabolism in obese premenopausal women. J Musculoskelet Neuronal Interact. 2009. 9(2):72-80.

Vahle J.L. Sato M., Long G.G., Young J.K., Francis P.C., Engelhardt J.A., Westmore M.S., Ma Y.L, Nold J.B. Skeletal changes in rats given daily subcutaneous injections of recombinant human parathyroid hormone (1-34) for 2 years and relevance to human safety. Toxicologic Path. 2002. 3(3): 312-321.

Vesterby A, Gundersen HJG, Melsen F, Mosekilde L Marrow space star volume in iliac crest decreases in osteoporotic patients after continuous treatment with fluoride, calcium and vitamin. Bone. 1991. 12:33–37.

Vestergaard P., Jorgensen N.R., Schwarz P., Mosekilde L. Effects of treatment with fluoride on bone mineral density and fracture risk – a meta-analysis. Osteoporos. Int. 2008. 19:257-268.

Wade GN, Gray JM, Bartness TJ. Gonadal influences on adiposity. Int J Obes Relat Metab Disord. 1985;9:83–92.

Wang Y, Nishida S, Elalieh HZ, Long RK, Halloran BP, Bikle DD Role of IGF-I signaling in regulating osteoclastogenesis. J Bone Miner Res. 200. 621:1350–1358

Wajchenberg BL Subcutaneous and visceral adipose tissue: their relation to the metabolic syndrome. 2000. Endocr Rev 21:697–738

Watts N.B., Diab D.L. Long-term use of bisphosphonates in osteoporosis. J. Clin. Endocrin. Metab. 2010. 95(4).

Whitfield JF. Leptin: brains and bones. Exp Opin Invest Drugs. 2001;10:1617–1622.

Winer J.P. Janmey P.A., McCormick M.E., Funaki M. Bone Marrow-Derived Human Mesenchymal Stem Cells become quiescent on soft substrates but remain responsive to mechanical stimuli. Tiss Engineering. 2009. 15(1): 147-154

Wolf AM. What is the economic case for treating obesity? Obes Res. 1998 Apr;6 Suppl 1:2S-7S.

Wu D, Ren Z, Pae M, Guo W, Cui X, Merrill AH, Meydani SN: Aging up-regulates expression of inflammatory mediators in mouse adipose tissue. J Immunol 2007. 179: 4829–4839.

Yamaguchi T, Kanazawa I, Yamamoto M, Kurioka S, Yamauchi M, Yano S, Sugimoto T. Associations between components of the metabolic syndrome versus bone mineral density and vertebral fractures in patients with type 2 diabetes. Bone. 2009 Aug;45(2):174-9.

Yao W, Hadi T, Jiang Y, Lotz J, Wronski TJ, Lane NE Basic fibroblast growth factor improves trabecular bone connectivity and bone strength in the lumbar vertebral body of osteopenic rats. Osteoporos Int. 200516:1939-1947.

Yakar S., Rosen C.J., Beamer W.G., Ackert-Bicknell C.L., Wu Y., Liu J.L, Setser J., Frystyk J., Boisclair Y.R., LeRoith D. Circulating levels of IGF-1 directly regulate bone growth and density.J. Clin. Investig. 2002. 110(6):771-781.

Yasari S., Dufresne E., Prud'homme D., Lavoi J.M. Effect of the detraining status on high-fat diet induced fat accumulation in the adipose tissue and liver in female rats. Phys. And Behav. 2007. 91:281-289.

Zamboni M, Armellini F, Harris T, Turcato E, Micciolo R, Bergamo-Andreis IA, Bosello O. Effects of age on body fat distribution and cardiovascular risk factors in women. Am J Clin Nutr. 1997. 66(1):111-5.

Zhang M., Xuan S., Bouxsein M.L. von Sthechow D., Akeno N. Faugere M.C. Malluche H., Zhao G., Rosen C.J., Efstratiadis A., Clemens T.L. Osteoblast-specific knockout of the insulin-like growth factor (IGF) receptor gene reveals an essential role of IGF signaling in bone matrix mineralization. J. Bio Chem. 2002. 277: 44005-44012.

Zhao G., Monier-Faugere M.C. Langub M.C., Geng Z., Nakayama T., Pike J.W., Chernausek S.D., Rosen C.J., Donahue L.R., Malluche H.H., Fagin J.A., Clemens T.L. Targeted overexpression of insulin-like growth factor 1 to osteoblasts of transgenic mice: increased trabecular bone volume without increased osteoblastic proliferation. Edoncrinology. 2000. 141: 2674-2782.

Zhao L.J., Papasian C.J.Maulik D., Drees B., Hamilton J., Deng H.W., Correlation of obesity and osteoporosis: effect of fat mass on the determination of osteoporosis. JBMR. 2008. 23(1): 17-29.

Zierath JR, Livingston JN, Thorne A, Bolinder J, Reynisdottir S, Lonnqvist F, Arner P. Regional difference in insulin inhibition of non-esterified fatty acid release from human adipocytes: relation to insulin receptor phosphorylation and intracellular signaling through the insulin receptor substrate-1 pathway. Diabetologia 1998. 41:1343-1354

Zoth N, Weigt C, Laudenbach-Leschowski U, Diel P. Physical activity and estrogen treatment reduce visceral body fat and serum levels of leptin in an additive manner in a diet induced animal model of obesity. J Steroid Biochem Mol Biol. 2010.

Books:

Carter D.R. Beaupre G.S. Skeletal Function and Form: Mechanobiology of Skeletal Development, Aging and Regeneration. Cambridge Univ. Press 2001.

Martin R.B., Burr D.B. Sharkey N.A. Skeletal Tissue Mechanics. Springer 1998.

Glantz S.A. Primer of Biostatistics. Fifth EditionMcGraw Hill Publishing. 2002.